



Department of Physics

Model independent constraints on geometrical extended theories of gravity

María Ortiz Baños

Supervisors:
Dr. Ruth Lazkoz Sáez
Dr. Vincenzo Salzano

A thesis submitted for the degree of
Doctor of Physics

2016-2020

Acknowledgements

I arrived in Bilbao in 2016 and now, almost five years later, I look back over these past years and remember all the people that have helped me all along this way. First of all, I would like to acknowledge my supervisors, Ruth Lazkoz and Vincenzo Salzano. Thank you for your guidance during this thesis and for teaching me the tools to work together and get through such an interesting field as Cosmology.

Of course, I am also grateful to all the people of the Department of Theoretical Physics and History of Science: Alex Feinstein, David Brizuela, Jon Urrestilla, José Juan Blanco Pillado, José M. Senovilla, Juan M. Aguirregabiria, Ivan De Martino, Igor Bandos, Manuel Ángel Valle, Géza Tóth, Lianao Wu, Michele Modugno, Thomas Broadhurst and Jesus Ibáñez. Thanks also to Íñigo Egusquiza, for helping me with the bureaucracy and, of course, thanks to Raül, the master of computers, who has been always available to make my computer work. Finally, I do not want to forget Montse, who has helped me to solve many problems related with university procedures.

Regarding financial support, this thesis has been possible thanks to the FPI fellowship contract from the Spanish Ministry of Economy and Competitiveness (BES-2015-071489) linked to the research project FIS2014-57956-P and also thanks to the Basque Government through research project No. GIC17/116-IT956-16. Besides, some research stays have been possible thanks to the fundings coming from the COST Action CA15117 (CANTATA).

During these years, I have done some collaborations and many visits and stays, all of them enriching and profitable. Firstly, I want to express my gratitude to Mariam Bouhmadi López. I have learnt a lot from our time together. Secondly, I want to acknowledge the team from the Cosmology Group of the University of Szczecin. I have always felt very welcome there. I will always remember Szczecin as the coldest and the most special trip of my PhD, where I took Enzo's first lessons. Finally, I want to thank all the team from the Institute of Astrophysics and Space Sciences of the University of Lisbon. Specially, I want to thank Noemi Frusciante, who, even if we could not keep on the project we started, gave me very useful lessons. And, of course, I have to thank Francisco S.N. Lobo for inviting me to Lisbon. It was a great

experience to work with you, not only from a scientific perspective but also from a personal one. I really enjoyed my time there.

To end up, I want to thank my teachers in Murcia, in Zaragoza and in Marseille, specially Christian Marinoni, who made me fall in love with Cosmology; and also my favourite physics teacher at high school, Tomás Rupérez, as the one who lighted the spark which made me study physics.

Estos años me he cruzado con personas maravillosas en muchas conferencias, en Euskal Herria, en Bilbo y, en concreto, en la universidad. A veces hemos estado más cerca y otras más lejos, pero siempre es un placer compartir con vosotras.

Lehenik eta behin, eskerrak eman nahi dizkiet nire bulegokideei: Pablo, Joao, Asier, Mikel, Fran eta Dani. Asko gozatu dut zuekin egoteaz. Jarraitzeko, Ikerri, nire neba-akademikoa, eskerrik asko nire zalantzak erantzuteko beti hurbil egoteagatik. Laguntza handi bat izan zara niretzat. Borja eta Iñaki, milesker zure adiskidetasunagatik. Ailegatu nintzenetik, oso erraza izan da zuekin hitz egitea eta ez dakizue zenbat lagundu didazuen.

Como el camino es largo, no me puedo olvidar de las personas que, nada más llegar, me acogieron con los brazos abiertos, así como de las que se han ido añadiendo en el camino en Bilbo, en Lisboa y en Szczecin: Laura, Aitziber, Naiara, Santi, Nastassja, Olatz, Charlotte, Giuseppe, Adrián, Iagoba, Joanes, Iñigo, Iraultza, Jeremy, Mark, Julen, Kepa, Mattin, Peio, Xiao-Hang, Airam, Álvaro, Asier, Sara, Jose, Marco, Isma, Hussain, Manuel, Federico y alguna persona más que seguro que se me escapa.

Quiero agradecer también a mis pisukides Laura, Vir, Silvia, Raulet y Enrique. Por soportarme, porque el roce hace el cariño y porque a partir de ahí ya no hay vuelta atrás.

Gracias a mi gente murciana, en especial a Esmeralda y a Pablo. Habéis sido el chorríco de limón que mi tesis necesitaba. Y, por supuesto, gracias a mis valencianas de pega, Cynthia y Arantxa, por vuestro abrazo constante.

Eskerrik asko Maialen, etapa hau askoz errazagoa izan da zugaz konpartitzeagatik. Zure pazientzia, maitasuna eta alaitasuna funtsezkoak izan dira.

Por último, quiero agradecer a mi madre, Isabel, y a mi padre, Tomás, por estar siempre al pie del cañón, por aguantarme, aconsejarme y animarme. Por enterarse más o menos de lo que hago y ser capaces de decírselo a la gente. En estos momentos no dejo de pensar en toda mi familia, los que están y las que no, desde Murcia hasta Barcelona. A todas vosotras: ¡Mirad lo que habéis conseguido!

Resumen

Desde los primeros estudios sobre el uso de Supernovas Tipo Ia a modo de candelas estándar, sabemos que el universo se expande aceleradamente. La descripción físico-matemática de este fenómeno puede abordarse desde perspectivas muy diferentes. Por un lado, si se quiere mantener un universo descrito por la teoría de la Relatividad General de Einstein, es necesario acudir a la idea de que un tipo de fluido diferente de la materia bariónica debe estar presente. Dentro de este escenario, una posibilidad es incluir la denominada constante cosmológica, que puede interpretarse como un fluido con ecuación de estado constante. De hecho, este modelo es el que actualmente está más aceptado y es considerado el modelo estándar de la Cosmología. Otra opción bastante más general es considerar un fluido dinámico, lo que normalmente se conoce como energía oscura. Por último, una tercera perspectiva que puede adoptarse, conlleva dejar de lado el contexto de la Relatividad General y establecer otro marco teórico partiendo de una definición diferente de la acción. Dentro de este grupo se encuentran las teorías de gravedad modificada.

Un ingrediente crucial a la hora de describir de qué manera ocurren las interacciones en el universo y cómo se forman las estructuras es la densidad de energía presente en él. Por un lado, tenemos la materia bariónica, la radiación y los neutrinos (cuya naturaleza es conocida hoy día). Por otro lado, hemos de tener en cuenta que las observaciones cosmológicas y astrofísicas del entramado que forma la estructura del universo señalan la presencia de otro componente más, generalmente conocido como materia oscura. Por último, el fenómeno de la expansión del universo, al menos desde una perspectiva conservadora, exige la presencia de otro componente de naturaleza desconocida, la energía oscura. No obstante, en el marco de la gravedad modificada, donde la descripción de las interacciones cambia completamente, esta energía oscura es completamente prescindible y de hecho, es una de las motivaciones para estudiar alternativas a la Relatividad General de Einstein.

Otra alternativa ampliamente estudiada dentro del marco de la Relatividad General es la denominada energía oscura unificada. Dado que la presencia de energía oscura y de materia oscura en el universo es aproximadamente del mismo orden, y teniendo en cuenta que desconocemos la naturaleza de ambas, parece lógico considerar un fluido capaz de describir el comportamiento de ambos componentes.

En esta tesis analizamos cada una de las perspectivas expuestas en lo anterior.

En el primer Capítulo 1, hacemos una breve introducción a la cosmología moderna desde un punto de vista histórico y explicamos los pilares fundamentales sobre los que se sustenta. Presentamos un esquema general sobre la energía oscura y la gravedad modificada y, finalmente, describimos en detalle los datos observacionales que hemos usado, así como la base de la estadística Bayesiana, haciendo énfasis en los métodos de Monte Carlo Markov Chain, una pieza fundamental en nuestro trabajo.

En el Capítulo 2, estudiamos las teorías $f(R)$ desde un enfoque “observational tester friendly”, y para ello utilizamos el redshift. Los resultados de este estudio han sido publicados en:

- “ $f(R)$ modifications: from the action to the data”, R. Lazkoz, M. O-B, V. Salzano, *Eur. Phys. J. C* (2018) 78: 213.

En el Capítulo 3, aplicamos el procedimiento anterior a una clase diferente de teorías de gravedad modificada menos explotadas. En concreto, trabajamos con la “no-metricidad”, Q , explorando un método similar al aplicado para las teorías $f(R)$ (que consiste en una generalización del Lagrangiano), pero incluyendo objetos geométricos completamente diferentes, dando lugar a las teorías $f(Q)$. Este tipo de teorías ofrece una nueva perspectiva por investigar que servirá para estudiar diferentes fenómenos cosmológicos para los que aún no existe una explicación consensuada. El análisis realizado en torno a este tema ha ido publicado en:

- “Observational constraints on $f(Q)$ gravity”, R. Lazkoz, F. S. N.Lobo, M. O-B, V. Salzano, *Phys. Rev. D* 100, 104027 (2019).

En el Capítulo 4, siguiendo con el tema de las teorías de gravedad modificada, analizamos una alternativa que forma parte de las teorías $f(R)$ que incluyen un acoplo no-mínimo entre la geometría y la materia. Este tipo de teorías permite sustituir el componente de energía oscura por un acoplo cuyo valor puede modular el efecto de un componente repulsivo que produce la presente expansión acelerada del universo. Este trabajo ha sido enviado como:

- “ Λ CDM suitably embedded in $f(R)$ with a non-minimal coupling to matter, M. O-B, V. Salzano, M. Bouhmadi-López, R. Lazkoz, *Submitted to Phys. Rev. D*.

Finalmente, en el Capítulo 5, estudiamos un “fluido oscuro” dentro del contexto de la Relatividad General descrito por las ecuaciones de Einstein-Hilbert usuales, pero exhibiendo una ecuación de estado dinámica no-lineal y cuyo parámetro característico

no es fácilmente reducible a una simple expresión analítica. Este modelo puede ser adscrito a la familia de los Chaplygin generalizados, y de ahí el nombre *umami* Chaplygin: tiene más parámetros libres que el Chaplygin original pero organizados de una manera que hace posible la unificación entre materia oscura y energía oscura. Este estudio ha sido publicado en:

- “*The umami Chaplygin model*”, R. Lazkoz, M. O-B, V. Salzano, *Phys.Dark Univ.* 24 (2019) 100279.

Abstract

Since the late 90's, when it was discovered that Type Ia Supernovae could be used as standard candles and their first batch-mode surveys were planned and completed, we know that our universe is expanding in an accelerated way.

This observational evidence can be addressed from many different perspectives. In the context of Einstein's General Relativity, it was soon realized that some "exotic" extra fluid, other than the usual baryonic matter, was needed to counterbalance the pull of gravity and eventually overcome it, in order to account for this phenomenon. One possibility in this sense is to include the so-called cosmological constant. This is, in fact, the most accepted approach and it establishes the basis of what is nowadays better known as the "standard consensus model of cosmology". However, as an alternative, one could also consider a more general fluid, generally called dark energy, characterized by a dynamical behaviour that would make it responsible of this expansion.

As a drastically different approach one could instead even abandon the framework of General Relativity and try to consider and develop a totally new theory of gravity, starting from a proper re-definition of the action. Theories of modified gravity lie within this kind of description.

The energy-density components which are present in the universe have a crucial role in the way interactions occur and structures get formed. Among these elements, firstly we have to mention those whose nature is well-known nowadays: radiation, neutrinos and baryonic matter (which is the matter we are made of). In addition to them, we also know that astrophysical and cosmological observations related to the internal dynamics of all the gravitational structure which make the cosmic web, their formation and evolution, make unavoidable to include in this cosmic inventory a new kind of non-baryonic matter of unknown nature, the dark matter. As a plus which we have already anticipated, to explain the accelerated expansion of the universe we need, at least, conservatively speaking, the presence of another "dark" energy-density ingredient; unless one decides to take a completely different path and change the theoretical scheme which defines interactions at the gravitational level, in which case we would be talking about modified gravity approaches, as we have mentioned.

Each of these two options of course provides a very distinct theoretical panorama; whether phenomenological or fully backed up by a theoretical idea, observations are the main and only tool we have to discriminate between them. Given the present knowledge we have about the energy-matter content of our universe, dark matter and dark energy account for most of the energy-density of the universe. However, their origin is still unknown. On the one hand, dark matter neither emits nor absorbs light so, although several proposals have been studied (WIMPS, axions, etc. . .) we still do not know what it is. On the other hand, the extensive list of dark energy and modified gravity candidates gets larger without arriving at a consensus on which mechanism should be driving such late speed up of the universe. Thus, the uncertain nature of dark matter and dark energy and the fact that nowadays they are present in similar proportions, make it interesting to consider the possibility that these two components could be, indeed, the same and unique fluid whose behavior gets modified with time. This is an intriguing framework which also can be considered.

In this thesis we address the three approaches we have mentioned, i.e. dark energy, modified gravity and unified dark fluids, to study the phenomenon of the accelerated expansion of the universe. On the one hand, we explore some cosmological setups belonging to the $f(R)$ and $f(Q)$ scenarios, and on the other hand, we study a unified dark energy model within the Chaplygin-type theories. We perform a theoretical and phenomenological analysis of each model and end up implementing an observational analysis examining the physical quantities which concern what happens at the background level of the universe. We show the power of prediction of the statistical methods we have developed by using a quite complete combination of observational data sets to test our theories and compare them with the standard model of cosmology. We have divided this thesis into different chapters and we will detail below the content of each one.

In Chapter 1, we start by introducing modern cosmology both from a historical point of view and explaining the fundamental mathematical pillars on which it rests. We provide a general overview on dark energy and modified gravity and finally, we explain in detail the observational probes we have used as well as the basis of Bayesian statistics, focusing on Monte Carlo Markov Chain methods, a fundamental point in our work.

In Chapter 2, we study the widely-known $f(R)$ theories but implementing an observational tester friendly approach using the redshift in order to facilitate observational tests. The results of this work have been published in:

- “ $f(R)$ modifications: from the action to the data”, R. Lazkoz, M. O-B, V. Salzano, *Eur. Phys. J. C* (2018) 78: 213.

In Chapter 3, we apply this same approach to a more drastic modification of gravity. More specifically, we work with the non-metricity, Q , exploring an approach which is similar to $f(R)$ for what concerns the methodology (a generalization of the Lagrangian), but involves completely different geometrical objects in it, thus leading to $f(Q)$ theories. This approach offers a brand new perspective which may open many possibilities to study unexplained cosmological phenomena. The analysis done has been published in:

- “*Observational constraints on $f(Q)$ gravity*”, R. Lazkoz, F. S. N. Lobo, M. O-B, V. Salzano, *Phys. Rev. D* 100, 104027 (2019).

In Chapter 4, always within the topic of modified theories of gravity, we analyze an alternative belonging to the $f(R)$ class of theories which includes a non-minimal coupling between geometry and matter. This kind of theories allows to replace the dark energy component by a coupling whose strength can modulate the effect of a “repulsive” component which is driving the present accelerated expansion. This work has been submitted as:

- “ *Λ CDM suitably embedded in $f(R)$ with a non-minimal coupling to matter*”, M. O-B, V. Salzano, M. Bouhmadi-López, R. Lazkoz, *Submitted to Phys. Rev. D*.

Finally, in Chapter 5, we study a dark fluid which lies within the General Relativity framework described by the usual Einstein-Hilbert action but exhibiting a dynamical equation of state highly non-linear and whose characteristic parameter is not easily reducible to any simple and standard analytical expression. The model can be ascribed to the generalized Chaplygin-like family, which is the reason for its name, *umami* Chaplygin model: it has more free parameters than the original Chaplygin model but arranged in such a way to allow and model a possible unification of dark matter and dark energy. This study has been published in:

- “*The umami Chaplygin model*”, R. Lazkoz, M. O-B, V. Salzano, *Phys. Dark Univ.* 24 (2019) 100279.

List of publications:

- “*f(R) modifications: from the action to the data*”, R. Lazkoz, M. O-B, V. Salzano, *Eur. Phys. J. C* (2018) 78: 213.
- “*The umami Chaplygin model*”, R. Lazkoz, M. O-B, V. Salzano, *Phys.Dark Univ. 24* (2019) 100279.
- “*Observational constraints on f(Q) gravity*”, R. Lazkoz, F. S. N. Lobo, M. O-B, V. Salzano, *Phys. Rev. D* 100, 104027 (2019).

Submissions:

- “ *Λ CDM suitably embedded in f(R) with a non-minimal coupling to matter*”, M. O-B, V. Salzano, M. Bouhmadi-López, R. Lazkoz, *Submitted to Phys. Rev. D* (2020).

Communications:

- “*f(R) gravity: from the action to the data*”, Seminar at the University of Szczecin, Szczecin (2017).
- “*f(R) gravity: from the action to the data*”, Future Gravitational Alternatives Meeting (FUGA), Valencia (2018).
- “*The umami Chaplygin model*”, 22nd International Conference on General Relativity and Gravitation - Edoardo Amaldi Conference on Gravitational Waves, Valencia (2019).

Contents

1	Introduction	1
1.1	Modern cosmology	1
1.2	Accelerated expansion of the Universe	7
1.2.1	General Relativity	7
1.2.2	Geometric ingredients	9
1.2.3	Energy-density content and Friedmann equations	13
1.2.4	Standard Model: Λ CDM	15
1.3	Dark energy	20
1.4	Modified gravity	25
1.4.1	$f(R)$ theories	30
1.4.2	$f(Q)$ theories	34
1.5	Observational data	37
1.5.1	Type Ia Supernovae	37
1.5.2	Cosmic Microwave Background radiation	41
1.5.3	Baryon Acoustic Oscillations	45
1.5.4	Hubble data	51
1.5.5	Quasars	52
1.5.6	Gamma Ray Bursts	53
1.6	Statistical Analysis	54
1.6.1	Monte Carlo Markov Chain (MCMC)	61
1.6.2	Model selection	62
2	$f(R)$ gravity	65
2.1	From $f(R)$ to $f(z)$	67
2.1.1	Requirements for $f(z)$ proposals	68
2.1.2	Final proposals	72
2.2	Observational test	74
2.2.1	Model 1: Λ CDM	74

2.2.2	Models 2-4	76
2.2.3	Models 5-8	77
2.2.4	Bayesian Evidence	77
2.3	Lessons from $f(R)$ vs. $f(z)$	77
3	$f(Q)$ gravity	80
3.1	Setting the stage: $f(Q)$ gravity	81
3.2	The $f(z)$ approach	82
3.2.1	Cosmology	82
3.2.2	Specific $f(z)$ proposals	83
3.2.3	Models considered	84
3.3	Results of the observational tests	85
3.3.1	Model 1: Λ CDM	85
3.3.2	Models 2-3	86
3.3.3	Models 4-7	86
3.4	Lessons from $f(Q)$ vs. $f(z)$	87
4	Non-minimal $f(R)$ gravity	89
4.1	Non-minimally coupled $f(R)$	90
4.1.1	Field equations	90
4.1.2	Dynamics of a homogeneous and isotropic Universe	90
4.2	A Λ CDM geometry within non-minimally coupled $f(R)$ gravity	91
4.2.1	An arbitrary f_1 with $f_2 = R$	92
4.2.1.1	Dust: $\rho = \rho_m$	93
4.2.1.2	Perfect fluid with constant EoS parameter: $\rho = \rho_w$	93
4.2.2	An arbitrary f_2 with $f_1 = R - 2\kappa^2\Lambda$	94
4.2.2.1	Dust: $\rho = \rho_m$	95
4.2.2.2	Perfect fluid with constant EoS parameter: $\rho = \rho_w$	95
4.3	Cosmography within non-minimally coupled $f(R)$ gravity	97
4.3.1	An arbitrary f_1 with $f_2 = R$	97
4.3.2	An arbitrary f_2 with $f_1 = R - 2\kappa^2\Lambda$	99
4.4	Lessons from non-minimally coupled $f(R)$ gravity	100
5	Umami Chaplygin model	103
5.1	Model	104
5.1.1	Results	106
5.2	Lessons from the <i>umami</i> Chaplygin fluid	110

6 Conclusions	112
Bibliography	115

List of Figures

1.1	Introducing comoving coordinates.	10
1.2	Evolution of a fiducial Λ CDM cosmological model.	18
1.3	Visual representatin of curvature, torsion and nonmetricity.	35
1.4	Final <i>Planck</i> temperature power spectrum.	46
1.5	BAO modes.	48
1.6	Burn-in and stabilization of the MCMC chain.	63
4.1	Non-minimal $f(R)$ model: dimensionless derivaties with respect to R	101
5.1	Evolution of the pressure with the scale factor for the <i>Umami</i> Chap- lygin models.	109
5.2	Energy density, pressure and energy conditions for the <i>Umami</i> Chap- lygin models.	110

List of Tables

2.1	Results at $z = 10$ for the different $f(z)$ models proposed in Chapter 2 within the $f(R)$ formalism.	75
2.2	Results at $z = 100$ for the different $f(z)$ models proposed in Chapter 2 within the $f(R)$ formalism.	75
3.1	Results for the different $f(z)$ models proposed in Chapter 3 within the $f(Q)$ formalism.	86
5.1	Results for the three <i>umami</i> Chaplygin models considered in Chapter 5 within the unified dark energy formalism.	106
5.2	Comparison of the baryonic and dark matter background parameters and of the Hubble parameter H_0 from our <i>umami</i> models with those derived from <i>Planck</i> 2018 data.	108

Chapter 1

Introduction

1.1 Modern cosmology

The term “cosmology” comes from the ancient Greek and literally means “study of the cosmos”, where the term “cosmos” actually had for the ancient Greeks connotations slightly different with respect to the present days. In fact, it was used to indicate the world (or Universe) as an orderly, harmonious system [1].

Nowadays “cosmology” is a well established branch of the natural sciences which deals with the study of the evolution of the Universe and its components all the way from the past to the future. It is interesting to notice how the question ancient people asked, “what is happening around me?”, has now lost locality and has become: “how does the Universe work?”. This is closely related to the core point of cosmology: it does not focus on every single particle which surrounds us but on the Universe as a whole. This ambitious and broad perspective shows the strength that this branch of science has, as well as the potent tools it requires in order to be brought forward.

Modern cosmology is considered to have begun in the early twentieth century, an incredibly fruitful period for research in both observational and theoretical aspects of the study of the Universe. It was during this period that Einstein gave birth to his best known theory, the General Relativity (GR) [2], an essential building block for the development of modern cosmology, a revolutionary re-definition of gravity as the manifestation of a (more or less complicated) interplay between space and time (the geometry of the Universe) with any kind of matter and energy which can be found in the Universe. In the same years, in parallel to theoretical advances, important discoveries were taking place in the observational field, although theoretical work has been for a very long time ahead of observational results, the latter one being constrained mainly by technological limits. One remarkable result was obtained in 1908, when the astronomer Henrietta Swan Leavitt discovered a relation between the

period of variability and the luminosity of a class of pulsating stars, the Cepheids [3]. Among the many important astrophysical contributions that have been based on this relation, one should mention the work by Helen Sawyer Hogg, who used it to enhance the understanding of our galaxy, the Milky Way, by studying its size, age and structure [4]. But Leavitt's discovery has been also crucial for cosmology itself, because it has provided astronomers with the first standard candle which might be used to measure distances of very distant objects. It was a decisive tool to address a problem that was in the spotlight of the scientific community at that time: while Einstein was developing GR, the vast majority of astronomers was still thinking that the Milky Way really contained all the stars present in the Universe and that beyond its limits there was just a great cosmic void. In 1916, some years after Leavitt's discovery, Vesto Slipher helped to throw some light onto this issue: he measured galactic spectral shifts and computed the velocities of the (then) so-called "nebulas" (i.e., nowadays, galaxies) finding that the majority of them were moving away from us [5]. Later on, in 1926, the ground sown with Leavitt's and Slipher's measurements gave Edwin Hubble the perfect impulse to unravel the extragalactic nature of the Cepheids he had observed in one of these "nebulas", which later turned out to be the Andromeda galaxy [6].

Some years after the discovery of extragalactic stars, in 1929, Hubble discovered another astonishing phenomenon: the Universe was expanding [7, 8]. More exactly, he found that the faster a galaxy was moving, the fainter it was (or, equivalently, the faster it was moving, the farther it was). From the theoretical point of view, it has to be said that such observational discovery could be well accommodated into a theoretical model which Alexander Friedmann had already formulated in 1922, when he had found an expanding Universe solution to Einstein's field equations [9].

Five years later Georges Lemaître also found independently the same kind of solutions [10] and was also the first to propose a cosmological model for the early-time Universe, which some years later started to be known as the Big Bang theory [11]. In the Big Bang scenario the entire known Universe was concentrated in a very-initial singularity from whose expansion everything we know today has derived. The model states that, at the beginning, all the matter in the Universe was compressed in a primordial state of extremely high density and temperature. Later on, its rapid expansion would have resulted in a significant decrease in density and temperature. While a detailed description of this model is out of the goals of this thesis, we will remind here only some of its main points. The huge amount of radiation in the early Universe environment ensured that any atom or nucleus formed would be immediately

destroyed by a high energy photon. At that time the Universe was very close to being homogeneous and was certainly strongly radiation dominated. As the Universe was cooling down, the light elements such as hydrogen, helium and lithium isotopes began to form, starting a process known as “nucleosynthesis”. The history of Big Bang nucleosynthesis began with the calculations of Ralph Alpher in the 1940s, and was finally stated in its definitive version by a joint work among Alpher, Hans Bethe and George Gamow, who published the famous $\alpha\beta\gamma$ paper that outlined the theory of light-element production in the early Universe [12]. While studying the process of the nucleosynthesis of light elements at very early times in the Universe, Gamow, Alpher and Herman realized that, in order to have the nuclei of these elements synthesized, the early Universe needed to have been not only extremely hot and much smaller, but also, the leftover radiation from that epoch should still be present in the Universe and be detectable, nowadays, as a cosmic microwave background (CMB) radiation [13, 14, 15, 16]. After the nucleosynthesis period, the Universe continued cooling, till reaching energy levels low enough for photons, electrons and nuclei to be able to combine into atoms (mostly hydrogen). This epoch is known as recombination (we will describe it in more detail in subsequent sections). The drop in density and energy also made light no longer interacting and being scattered off by free electrons, and instead it started to travel freely through the Universe in the form of that relic radiation which is CMB. As time passed, some marginally denser regions (whose origin we will describe later in this chapter) of the almost uniformly distributed matter grew gravitationally and became denser and denser, forming stars, galaxies and the rest of the astronomical structures that are currently observed.

The expansion of the Universe is considered as one of the main discoveries within modern cosmology. However, before the discovery of Hubble, the possibility of a dynamical Universe was widely rejected. More interestingly, in the early days of GR, Einstein thought about a possible solution to his equations by introducing a constant term - nowadays called Λ - of geometric nature. In his ideas it should have contrasted the action of gravity eventually leading to a static Universe, as it was clear that something more, and very different from standard matter, was needed to get this type of Universe. This was the mainstream idea about its dynamics, at that time, to which Einstein himself adhered to, in absence of any confuting observational probe. But, contrarily to his thoughts, he soon realized that such a Λ -term could give rise to an accelerated Universe. That is why he initially rejected this possibility. However, he came back to it when Hubble made his crucial discovery about the accelerated

Universe (leading him to spell his famous sentence about *“his greatest blunder”*, when referring to his initial doubts concerning the dynamical Universe).

It would be in 1998 when, using Type Ia Supernovae as standard candles, it was found that, indeed, the Universe was expanding in a very specific way: it was accelerating. This measurement was made independently by two different teams, the Supernova Cosmology Project (headed by Saul Perlmutter) and the High-Z Supernova Search Team (headed by Brian Schmidt and Adam Riess) [17, 18] who were both awarded the Nobel Prize in Physics in 2011 for such a discovery, which constitutes one of the main pillars on which modern cosmology is based. Due to it, the possible existence of a “dark” (unknown) energy component which should drive the acceleration of the Universe entered the scene, initially in its simple form of a constant (the cosmological constant) originally introduced by Einstein.

We have to remark that the idea of an accelerated expansion of the Universe has also an important role in the early stages of its evolution. Motivated by trying to find a solution to the problems of the standard Big Bang model (as the flatness problem, the monopoles, or the origin of the gravitational structures which we see today), Willem de Sitter, Alan Guth, Alexei Starobinsky, Andrei Linde and Paul Steinhardt tackled them starting from the context of field theory, by predicting a possible accelerated expansion phase of the early Universe, which was soon called “cosmological inflation”, and which should have taken place right after the initial singularity of the Big Bang [19, 20, 21, 22, 23, 24, 25, 26]. However, it is important to stress that such early-time acceleration is deeply different from the late-time one, for what concerns its origin, duration and velocity, as we will explain in the following pages.

Besides, in the sixties of the past century, the existence of another dark component started to be considered. The astronomer Vera Rubin, together with Kent Ford, measured and analyzed the rotation velocities of stars in spiral galaxies in terms of their distances from the center [27] and how the gas in the disks was moving. Until that moment it was thought that the mass distribution in spiral galaxies should follow the light distribution emitted by its stars: given that the brightness decreases as moving far from the center, the center should contain more mass and, thus, the rotation velocity of the stars was expected to be higher in the center and decreasing for large distances. However, by analyzing different objects, they found that the velocity curve tended to flatten as the distance from the center increased. To interpret this, they retrieved the work by Fritz Zwicky in 1930, who proposed that some non-visible “missing” mass (what he would call “dark” matter) was needed in order to explain the dynamics of hot gas in the Coma galaxy cluster [28, 29]. Actually, the gas was too

hot for being gravitationally bounded in a limited region by the only visible mass, and a quite larger amount of additional mass was needed in order to fit it within clusters' scales.

Another decisive discovery which drastically affected the paradigm of modern cosmology was, in fact, accidentally done by Arno Allan Penzias and Robert Woodrow Wilson in 1965 [30]. While working on the calibration of a satellite communications antenna, they found the Earth submerged in a highly uniform bath of microwave radiation. As we have mentioned, the existence of such cosmic microwave background (CMB) had been postulated on theoretical grounds some years before, in the late 1940s. When Penzias and Wilson (who were awarded the Nobel Prize in 1978 for it) detected this signal, they approached Peebles and his team asking for advice, and they realized they had detected the theorised relic background radiation. After that, Peebles' team would give a deeper physical interpretation to these results [31, 32], for which he obtained the Nobel Prize of Physics in 2019. Indeed, Peebles recognised that the CMB was a rich source of information concerning the formation of large structures as galaxies and the primordial conditions of the Universe. This is the reason why the CMB is much more used in cosmology nowadays. While we will describe it in more detail in the next sections, we will just state here briefly that this discovery was the key evidence in support of the Big Bang model. And it was crucial not only for this reason: the extreme large-scale uniformity of CMB was a clear evidence against any centrality of our "local environment" (in a cosmological sense) in our Universe. Already in 1952, Baade had already discovered spiral galaxies as the Milky Way were "typical" galaxies, very numerous in our Universe, thus stepping aside from the idea that we are in a privileged position, leading to an experimental confirmation of the Copernican principle on very large scales. Isotropy and homogeneity are nowadays the mainstream pillars of the most used cosmological models and these two features together precisely constitute the so-called Cosmological principle, the main principle of modern cosmology.

Closing this fast and far-from-exhaustive summary of the main historical steps and achievements in modern cosmology, we cannot forget to mention one of the main keys for its advancement. In fact, while theoretical ideas have been for a long time forward observations, in the latest 30 years we have seen a fast rise in the technological progress employed in observational cosmology. At the beginning, astronomers could just rely on the visible part of the spectrum to study the Universe but one of the great successes of the 20th century has been the full exploitation of the whole electromagnetic spectrum through both ground and satellite based telescopes. Among all the experiments which

have been performed with (also) a cosmological purpose, we want to remind here some of them, for their crucial achievements. We can begin by mentioning the Hubble Space Telescope (HST), which was launched in the 90's and has helped to walk through many problems in cosmology, from showing that black holes are probably common to the centers of all galaxies [33, 34] to measuring the Hubble constant [35], finding a value of $H_0 = 72 \pm 8 \text{ km s}^{-1} \text{ Mpc}^{-1}$. A decade after, the Sloan Digital Sky Survey (SDSS) took place, detected for the first time Baryon Acoustic Oscillations (BAO) in galaxy clustering [36] and mapped the Large Scale Structure (LSS) of the Universe [37] (we will discuss them in next sections). For what concerns the study of the CMB, the very first results were obtained by the COBE satellite, launched in 1989, which observed the almost perfect black-body spectrum of CMB radiation, and gave the first hints for its fainter anisotropies which are now so crucial for cosmology [38]. Such anisotropies were the main goal of the following more advanced spacecrafts: both the Wilkinson Microwave Anisotropy Probe (WMAP) [39], launched in 2001, and *Planck* [40, 41], in 2009, centered their activity on measuring the temperature differences across the sky in the CMB. On one side, WMAP's measurements played a key role in establishing the current standard model of Cosmology, providing a more precise value of $H_0 = 70.0 \pm 2.2 \text{ km s}^{-1} \text{ Mpc}^{-1}$, and finding also, for the first time in 2008, indirect evidence for the existence of a cosmic neutrino background with an effective number of neutrino species of 3.26 ± 0.35 . On the other side, *Planck*, although being a shorter mission, was more precise and confirmed the Universe having approximately 26% content of dark matter, 68% of dark energy, as well as validating the simplest models of inflation.

We must mention here the latest exceptional experiment which has recently opened a new window within observational cosmology: the Laser Interferometer Gravitational Wave Observatory (LIGO). Born in 2002, it was designed to confirm the existence of the gravitational waves (GW) predicted in GR and to explore their properties [42]. GWs are produced in cosmic massive phenomena, as galaxy impacts, supernovae explosions, black holes and neutron stars formation from binary systems. The first direct observation of GW was in september of 2015 [43], and from that time until today, many more detections have been found, the most recent one being [44] and the Nobel Prize in Physics 2017 has been awarded for such results.

Last but not least, we have to remind the exceptional times which are ahead of us, with a lot of future missions which are going to take place in the following years, and will drive us directly in the fully-exploited precision cosmology era: *Euclid*¹, planned

¹<https://www.euclid-ec.org/>

to be launched in 2022 to investigate dark matter and dark energy [45]; the Wide Field Infrared Survey Telescope (WFIRST), recently renamed Nancy Grace Roman Space Telescope², scheduled for mid-2020s and designed to settle essential questions in the areas of dark energy, exoplanets, and infrared astrophysics [46] or the Square Kilometre Array (SKA), a project to build a radio telescope whose construction is likely to begin in 2021. This will become the world’s largest scientific instrument and its wide scientific goals spread from studying the formation and evolution of the first stars and galaxies to unveil the nature of the “dark” components of the Universe³.

1.2 Accelerated expansion of the Universe

One of the main problems in Cosmology today is to understand the nature of accelerated expansion of our Universe, and this will be the main topic to be tackled in the present work. In the previous section, we have carried out an historical journey through the different theoretical and experimental achievements which have let us arrive at the current setting of Cosmology. In the present section, we will explicitly describe the theoretical framework that encompasses the evolution of the Universe, which also serves as a quantitative and qualitative tool to make predictions and weigh the constraining power of the available observational data.

1.2.1 General Relativity

As we have already mentioned, the mainstream theory which is used in Cosmology is GR. This theory is based on two main principles: the equivalence principle, which states that the laws of physics in a curved spacetime must reduce to those ones corresponding to special relativity in a flat space-time; the principle of general covariance, which asserts that the form of the laws of physics must have to be the same in every inertial and accelerating frame. This is achieved by using a tensorial description through the introduction of covariant derivatives (which replace the usual partial derivatives) [47].

This theory is eventually fully expressed as a set of second order differential equations, the Einstein’s field equations, which describe how the geometry of the space-time and the energy content of the Universe are related. In other words, the energy content affects the curvature, and the geometry influences the way particles move (in a wide sense). Such equations are obtained by applying the variational principle to

²<https://roman.gsfc.nasa.gov/>

³<https://www.skatelescope.org/>

the Einstein-Hilbert action [48]. Considering a cosmological constant and minimally coupled matter fields, the action reads

$$\mathcal{S} = \frac{1}{2\kappa^2} \int \sqrt{-g}(R - 2\Lambda + \mathcal{L}_m(g_{\mu\nu}, \Psi))d^4x, \quad (1.1)$$

where: $\kappa^2 = 8\pi G$ with G the gravitational constant; $g_{\mu\nu}$ is the metric tensor (the mathematical object which captures the geometric and causal structure of spacetime); g is the determinant of the metric; Λ is the cosmological constant; \mathcal{L}_m is the matter Lagrangian, describing the matter/energy content of the Universe (by the matter fields Ψ); and R is the Ricci scalar defined by $R = g^{\mu\nu} R_{\mu\nu}$, where the Ricci tensor $R_{\mu\nu}$ is the contraction of the Riemann tensor and can be written as

$$R_{\mu\nu} = R^\rho{}_{\mu\rho\nu} = \partial_\rho \Gamma^\rho{}_{\nu\mu} - \partial_\nu \Gamma^\rho{}_{\rho\mu} + \Gamma^\rho{}_{\rho\lambda} \Gamma^\lambda{}_{\nu\mu} - \Gamma^\rho{}_{\nu\lambda} \Gamma^\lambda{}_{\rho\mu}. \quad (1.2)$$

Here $\Gamma^\alpha{}_{\beta\gamma}$ is a geometrical object with indexes technically called a connection, which in spite of its non-tensorial nature makes the covariant derivative a true tensor. In the simplest case, i.e. the torsionless metric formalism, the connection corresponds to the Levi-Civita one, described by the usual Christoffel symbols defined in terms of the metric tensor $g_{\mu\nu}$,

$$\Gamma^\rho{}_{\alpha\beta} = \frac{1}{2} g^{\rho\gamma} \left(\frac{\partial g_{\gamma\alpha}}{\partial x^\beta} + \frac{\partial g_{\gamma\beta}}{\partial x^\alpha} - \frac{\partial g_{\alpha\beta}}{\partial x^\gamma} \right) = \frac{1}{2} g^{\rho\gamma} (g_{\gamma\alpha,\beta} + g_{\gamma\beta,\alpha} - g_{\alpha\beta,\gamma}), \quad (1.3)$$

which follows from the metricity relation $\nabla_\lambda g_{\mu\nu} = 0$. If this quantity happens to be different from zero, one defines the non-metricity tensor, given by $Q_{\alpha\mu\nu} = \nabla_\lambda g_{\mu\nu}$. Then, if torsion or non-metricity are present in the theory, consequences are highly non trivial. Although we will discuss them in more details in Sec. 1.4.2, let us keep in mind what they mean qualitatively. On the one hand, if there is torsion, when two vectors are transported along each other, the parallelogram formed does not get closed. On the other hand, if there is non-metricity, the length of a vector varies when it is transported.

Finally, the variation of Eq. (1.1) with respect to the metric brings as a result the Einstein's field equations (EFE), which are usually written as

$$G_{\mu\nu} + g_{\mu\nu}\Lambda = \frac{8\pi G}{c^4} T_{\mu\nu}. \quad (1.4)$$

As both sides of the equation are symmetric two-index tensors, we would have a set of ten equations. Nevertheless, Bianchi identities, i.e. $\nabla^\mu G_{\mu\nu} = 0$, represent four constrains on $R_{\mu\nu}$, letting us with just six equations which are truly independent.

Bianchi identities are very important, as they represent the local conservation of the energy-momentum tensor. Here we have defined

$$G_{\mu\nu} \equiv R_{\mu\nu} - \frac{1}{2}g_{\mu\nu}R, \quad (1.5)$$

$$T_{\mu\nu} \equiv -\frac{2}{\sqrt{-g}} \frac{\delta\sqrt{-g}\mathcal{L}_m}{\delta g^{\mu\nu}}, \quad (1.6)$$

where $G_{\mu\nu}$ is the Einstein's tensor and $T_{\mu\nu}$ is the energy-momentum tensor, which must account covariantly for all the species that contribute to the budget of matter and energy. Actually, we must point out that, in contrast with the first attempts, nowadays in cosmology it is usual to consider the cosmological constant as another component in the energy-density budget, and not as a geometric term, so that it is included in $T_{\mu\nu}$.

1.2.2 Geometric ingredients

Coming back to what has been said in the introduction, and keeping in mind the importance of the mathematical corpus of the theory driving the gravitational interactions, we can now be more explicit about the family of exact solutions of Einstein's field equations which was found independently by Alexander Friedmann, Georges Lemaître, Howard P. Robertson and Arthur Geoffrey Walker in the decades of the 1920's and 1930's. The constraints set by the cosmological principle translate into a description of the Universe given by the Friedmann Lemaître Robertson Walker (FLRW) line element,

$$ds^2 = -c^2 dt^2 + a(t)^2 [dr^2 + S_k^2(d\theta^2 + \sin^2\theta d\phi^2)], \quad (1.7)$$

with c , the speed of light in vacuum; r , θ and ϕ , the three spatial coordinates; $a(t)$, the scale factor and $S_k(r)$, a function depending on the spatial curvature, k ,

$$S_k(r) = \begin{cases} \sin r/\sqrt{k} & k > 0 \text{ (closed Universe)} \\ r & k = 0 \text{ (flat Universe)} \\ \sinh r/\sqrt{|k|} & k < 0 \text{ (open Universe)} \end{cases} \quad (1.8)$$

Special attention must be paid to the scale factor. This quantity is introduced to take into account the effects of the expansion of the Universe and it sets the scale of the geometry of space, i.e. it tells us about the relative size of the Universe at a specific time with respect to its size today, when it is usually assumed to be $a(t = t_0) = 1$. It is also crucial for the measurement of distances in an expanding Universe. While in the next pages we will provide a more rigorous definition of all the distances used

in cosmology, here we just want to introduce the two basic notions which will help us to understand the role of the scale factor. On one hand, we have the *physical distance*, the *only* real and not measurable distance, which gets larger and larger as the Universe expands. On the other hand, we have the *comoving distance*, which factors out the expansion of the Universe and provides the relative distance on a grid which does not change with time due to the expansion. In Fig. 1.1 we try to provide a more clear visual realization of the meaning of $a(t)$. A priori, no prediction about the explicit time evolution of the scale factor is possible if no assumption is made about the matter-energy content in the Universe. In fact, even if one specifies the matter content, one still has to be able to solve the dynamical equations, which in most of the cases is not possible analytically. But this is not a problem to understand the meaning and difference between physical and comoving coordinates.

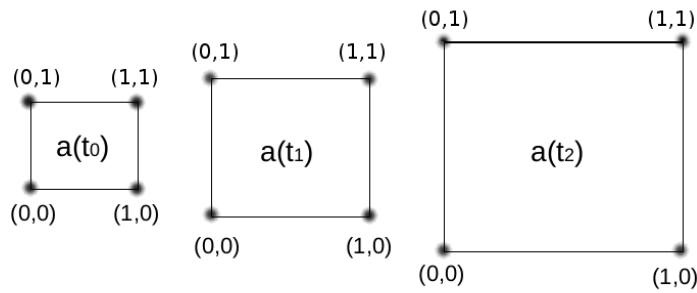


Figure 1.1: Assuming that the points in the vertices are galaxies, we note that as long as the Universe expands, the physical distance among them (the side length of the squares) gets larger because of the Universe expansion, and this corresponds to a larger scale factor. However, the comoving distance namely, the distance between grid points (the numbers in the vertices) is by definition constant no matter the rate of expansion of the Universe. Thus, the scale factor drives the relation of proportionality between the physical and the comoving distances.

One of the main fundamental quantities in observational cosmology which can be related directly to the scale factor is the Hubble parameter, defined as

$$H(t) = \frac{\dot{a}(t)}{a(t)}. \quad (1.9)$$

Clearly this quantity measures the rate of expansion of the Universe and, as we will see, it is somehow related to many other properties of the Universe.

The most important information about the expansion of the Universe, i.e. $a(t)$, comes from the measurements of the shifts in the wavelength of the light emitted by

distant sources. By considering Eq. (1.7) for an electromagnetic wave one arrives to the following relation [49]

$$\frac{\lambda_0}{\lambda_1} = \frac{a(t_0)}{a(t_1)}, \quad (1.10)$$

with λ_0 being the wavelength measured today by us and λ_1 the wavelength as emitted by the distant source. The previous relation is usually written in terms of the cosmological redshift, defined as

$$z = \frac{\lambda_0 - \lambda_1}{\lambda_1}, \quad (1.11)$$

which, in terms of the scale factor, and generalizing for any instant of time t , gives

$$z(t) = \frac{a(t_0)}{a(t)} - 1. \quad (1.12)$$

Cosmological distances in an expanding Universe

Some definitions of cosmological distances are now needed for a better understanding of how we can describe our Universe. When studying objects in an expanding Universe, one has to be specially careful at measuring distances. As we have previously introduced, on the one side, one has the physical distance, which grows with expansion and on the other, the comoving one, which remains fixed. The fundamental distance measurement, from which all the others may be calculated, is the distance in the comoving frame. We can then compute the total *comoving distance* which light could have traveled since $t = 0$ in the absence of interactions. Starting from Eq. (1.7), one can find that in a time dt , light travels a comoving distance $dr = c dt/a$, so that the total comoving distance the light could have traveled is

$$\eta = \int_0^t \frac{c dt'}{a(t')}, \quad (1.13)$$

Regions separated by a distance greater than η are not causally connected because it is not possible for information to propagate further than η . This is why this quantity is commonly named as the *comoving horizon*. We can generalize this definition to any time interval, so that the comoving distance can correspond to the distance between an emitter located at a scale factor a and us, which are generally located at scale factor $a(t_0) = 1$, and is given by [50]

$$D_C = \int_{t(a)}^{t_0} \frac{c dt'}{a(t')} = D_H \int_0^z \frac{dz'}{E(z')}, \quad (1.14)$$

where $D_H \equiv c/H_0$. We have used the definition of H given Eq. (1.9) and have rearranged it as $H(z) = H_0 E(z)$, where H_0 is Hubble constant (i.e. expansion rate at the present time) and $E(z)$ is the dimensionless Hubble parameter, carrying the cosmological dynamical behaviour of our Universe (as we will see in Eq. (1.32)).

Even if we have now operational definitions for the cosmological distances, we must point out that we cannot measure neither the comoving nor the physical one. Actually, in astronomy, we use to define different types of measurable distances which are then connected to those former ones.

One possible measure is the comoving distance between two events at the same redshift but separated on the sky by some angle θ , which is $D_M \theta$, where D_M is called the *transverse comoving distance*. It is related to the comoving distance D_C as

$$D_M = \begin{cases} \frac{1}{\sqrt{k}} \sinh(\sqrt{k} D_C) & k > 0 \text{ (closed Universe)} \\ D_C & k = 0 \text{ (flat Universe)} \\ \frac{1}{\sqrt{|k|}} \sin(\sqrt{|k|} D_C) & k < 0 \text{ (open Universe)} \end{cases} \quad (1.15)$$

Another method consists on determining the angular size θ subtended by an object of *known* transverse physical size l . With this quantities one can compute the *angular diameter distance*

$$d_A = \frac{l}{\theta}. \quad (1.16)$$

As the comoving size of the object is l/a , the angle subtended is $\theta = (l/a)/D_C$. Then, in a spatially-flat expanding Universe one gets

$$d_A = \frac{D_C}{1+z}. \quad (1.17)$$

For any spatial curvature, one can write the angular diameter distance in terms of the transverse comoving distance:

$$d_A = \frac{D_M}{1+z}. \quad (1.18)$$

It is also possible to infer distances measuring the flux F from an object of *known* luminosity L . The flux we observe in an expanding Universe is given by

$$F = \frac{L a^2}{4\pi D_C^2} = \frac{L}{4\pi D_L^2}, \quad (1.19)$$

where we have defined $D_L \equiv D_C/a$ as the *luminosity distance*. If we want to generalize this expression to any spatial curvature we can write it in terms of transverse comoving distance as

$$D_L = (1+z)D_M. \quad (1.20)$$

From the luminosity distance one generally defines and works with the *distance modulus*, which is a way to express distance on a logarithmic scale because we actually do not measure directly the luminosity of objects but magnitudes. It is defined as

$$\mu \equiv m - M = 5 \log \left(\frac{D_L}{10 \text{ pc}} \right), \quad (1.21)$$

because it is the magnitude difference between an object's observed total flux and what it would be if it were at 10 pc (this was once thought to be the distance to Vega). Here m is the apparent magnitude⁴, being related to the observed flux of the object, and M is the absolute magnitude, which depends on the intrinsic luminosity of the object.

1.2.3 Energy-density content and Friedmann equations

The energy-momentum tensor, given by the definition in Eq. (1.6), provides covariant information about the density and flux of energy and momentum within the space-time. As matter produces curvature, it is a source of gravitational field in Einstein's field equations. For theoretical completeness, we want to note that having a non-vanishing $T_{\mu\nu}$ is not the only way to guarantee a gravitational field. In empty space, Eq. (1.4) reduces to $R_{\mu\nu} = 0$. But it can be shown that while in two or three dimensions the field equations in empty space effectively ensure that the curvature tensor vanishes [49], in the case of four dimensions, instead, it is possible to satisfy the field equations in empty space with a non-vanishing curvature tensor, which implies the existence of gravitational fields in empty space.

Generally, in an isotropic and homogeneous Universe⁵ (as it is the case that concerns this work), the energy density content is described in the form of a perfect fluid, whose behaviour is given by

$$T^{\mu\nu} = \left(\rho + \frac{p}{c^2} \right) u^\mu u^\nu + p g^{\mu\nu}, \quad (1.22)$$

where ρ is the density of every fluid which may be present in the Universe, p is its pressure and u^μ is its four velocity.

At this point, we can find the dynamics of the Universe and study its evolution with time solving the EFE for the FLRW line element. We end up with the Friedmann

⁴The apparent magnitude of an astronomical source in a photometric bandpass is defined as the ratio of the apparent flux of that source to the apparent flux of the bright star Vega, through that bandpass.

⁵In fact, here we can interpret that the Universe can be foliated into spacelike slices so that each of the slices is homogeneous and isotropic [47].

and Raychaudhuri equations, i.e.

$$H^2 = \frac{8\pi G}{3}\rho + \frac{\Lambda c^2}{3} - \frac{kc^2}{a^2}, \quad (1.23)$$

$$H^2 + \dot{H} = -\frac{4\pi G}{3}\left(\rho + \frac{3p}{c^2}\right) + \frac{\Lambda c^2}{3}. \quad (1.24)$$

In addition to this set of equations we consider the so called *conservation equation*, which can be obtained by replacing Eq. (1.23) and its derivative into Eq. (1.24). If we assume that all the fluids are not interacting among each other, we can separate each of them and every component will have to satisfy this equation independently, eventually leading to

$$\dot{\rho} + 3H\left(\rho + \frac{p}{c^2}\right) = 0. \quad (1.25)$$

We also introduce the equation of state (EoS) parameter of a barotropic fluid, $w = p/(\rho c^2)$, which is dimensionless. As long as w is constant, the integration of Eq. (1.25) gives $\rho \propto a^{-3(1+w)}$, from which one can compute the evolution of each energy-density component ρ_i with respect to the scale factor. For cold matter (dark and baryonic), with $w = 0$, one finds $\rho_m \propto a^{-3}$; for radiation, with $w = 1/3$, one finds $\rho_r \propto a^{-4}$. Moreover, the quantity H allows to redescribe the density components into dimensionless parameters called as *reduced density parameters*,

$$\Omega_i(a) = \frac{8\pi G\rho_i(a)}{3H^2}, \quad (1.26)$$

where the subindex i corresponds to each energy-density content considered.

Then, one can write the first Friedmann equation as

$$\sum_i \Omega_i(a) + \frac{kc^2}{(aH)^2} = 1, \quad (1.27)$$

where one can define

$$\Omega_k(a) = \frac{kc^2}{(aH)^2}, \quad (1.28)$$

which accounts for an *effective density* content associated to the spatial curvature.

By assuming some matter-energy content in the Universe one can introduce the solution of Eq. (1.25) in Eq. (1.27) in order to compute an explicit function of $a(t)$. For example, for a matter dominated era one obtains $a \propto t^{2/3}$ and for a radiation dominated one, $a \propto t^{1/2}$. We can notice that in Eq. (1.27), the energy content and the geometry are related. Let us note that the parameter k is decisive on describing the spatial geometry of the Universe, as we have seen in the definition of the distances in the previous subsection. In fact, a very recent and controversial result concerning

the value of Ω_k has been published in [51]. Although its value has been strongly constrained by *Planck* to a value very close to zero (which indicates a spatially-flat Universe) [41], in [51] the authors claim about a possible statistical evidence for a closed Universe, showing that a positive curvature could provide an explanation for the enhancement in the lensing amplitude in the CMB power spectra detected by *Planck* with respect to the predicted signal within a standard Λ CDM model.

1.2.4 Standard Model: Λ CDM

A cosmological model based on a Universe with radiation and matter dominated epochs can be well described within the framework of GR. However, we now know that the Universe has undergone two phases of cosmic acceleration, which cannot be explained by the presence of only radiation and standard matter.

The first one is inflation. The theoretical motivation of this phase has to do with several problems related with the Big Bang theory, among them the well known flatness and the horizon problem. The flatness problem arises from realizing that some of the initial conditions which are supposed to be applied to the very first stages of the Universe history, appear to be fine-tuned to very special values, and that any small deviations from them would have extreme effects on the appearance of the Universe at the current time and would be in conflict with current observations, in particular, with the CMB-based nearly flat spatial curvature. The horizon problem, instead, arises from the difficulty to explain the observed homogeneity detected by CMB among regions of the space which should be instead, in the standard Big Bang scenario, causally disconnected. Without going into the details, which can be found in dedicated reviews like [52, 53], the most accepted inflation theories are thought to have taken place prior to the radiation domination epoch, and are driven by some scalar field ϕ , generally named inflaton, whose potential is sufficiently flat for sufficient time, i.e. there is an inflationary phase when the field rolls very slowly down its related potential if compared to the rate of expansion of the Universe. This is a period of very fast expansion, where the temperature drops very quickly to a very low value which is maintained during the whole phase. When it ends, temperature returns to the pre-inflationary phase temperature, a mechanism which is known as reheating. It is at this moment that the potential energy of the inflating scalar field decays into particles, the Standard Model ones, and standard radiation epoch begins. The main artifact in inflation which allows to solve these two problems has to do with the comoving Hubble radius, $c/(a H)$, which appears in the definition of the *comoving*

horizon (Eq. (1.13)), which we recast here in terms of the scale factor as

$$\eta = \int_0^a \left(\frac{c}{a' H(a')} \right) d \log a'. \quad (1.29)$$

The comoving horizon is the maximum distance a light ray can travel between $t = 0$ and a time t (corresponding to the scale factor a). In the standard Big Bang cosmology, i.e. starting directly with a radiation-dominated era and then moving to matter-domination, the comoving Hubble radius is strictly increasing. Inverting this behaviour is a possible solution to the above mentioned issues and it is what inflation precisely triggers: if the comoving horizon would have been always growing with time, then the comoving scales entering the horizon today should have been completely outside of the horizon at earliest epochs, and thus these scales should be causally disconnected. However, we observe an “almost complete” homogeneity in the CMB; then, to solve this, an accelerated expansion is needed, during which the comoving horizon shrinks. If this happens, then, regions which now would seem to be causally disconnected, were actually inside the horizon during the very early stages of Universe expansion.

We should remark here anyway, that more than the previous questions, one of the most important successes of inflation is to explain how the present large scale structure, the number and variety of gravitational structures we can observe today, are originated. See [52, 53, 54] for a quite complete lecture on this approach and, in general on the early Universe topic.

The second phase of acceleration which our Universe should have undergone (and it is supposedly still undergoing) is the one which we will study in the present work. This period started at relatively later times, approximately at $z \sim 1$, posing end to the matter domination era, and it requires some component of negative pressure, i.e. with EoS $w < 0$, but also being able to give rise to a cosmic acceleration, i.e. $\ddot{a} > 0$. Applying this condition into Friedmann equations we get a more restrictive condition for acceleration, $w < -1/3$ ⁶. This kind of component is what we generally denote as dark energy. The simplest candidate to drive this late-time accelerated phase is the cosmological constant. Although Einstein included it as a purely geometric term, it has acquired nowadays the role of an energy-density component with an EoS parameter $w = -1$. This interpretation has opened new options to find an explanation to the late-time expansion of the Universe, giving rise to a wide class of dark energy models that act as generalizations of the cosmological constant.

⁶Although this is the most usual case, in the literature cases as $w = 1$, known as stiff fluids, are studied in different stages of the Universe [55, 56, 57].

Its reduced density parameter is given by

$$\Omega_\Lambda(a) = \frac{8\pi G\Lambda}{3H^2}. \quad (1.30)$$

Considering this specific kind of dark energy, it is straightforward to compute when this accelerated phase should start by using the condition $\rho_m = \rho_\Lambda$, where ρ_m is the matter energy-density and ρ_Λ is the energy-density component driving the accelerated expansion,

$$\rho_{m,0}(1+z)^3 = \rho_\Lambda, \quad \text{or, using Eq. (1.26): } z_{acc} = \left(\frac{\Omega_\Lambda}{\Omega_{m,0}}\right)^{1/3} - 1. \quad (1.31)$$

Choosing the present values [41] $\Omega_m = 0.31^7$ and $\Omega_r = 8 \cdot 10^{-5}$, assuming spatial flatness and taking into account that Eq. (1.27) evaluated at the present time translates into $\Omega_\Lambda = 1 - \Omega_m - \Omega_r$, we get $z_{acc} \sim 0.3$. At this redshift, matter domination era ends and gives way to the accelerated expansion era. This phase has been confirmed by a big number of observations as SNeIa [58, 59], LSS [60, 61, 62, 63, 64, 65, 66], CMB [41] and more recently, gravitational waves [67, 68].

The model which most successfully fits the majority of the present observational data [41] and therefore has become the consensus scenario is the so called Λ CDM model, supplemented by some inflationary scenario, whose main ingredients are: a flat FLRW Universe governed by the EFE and characterized by a positive cosmological constant; a contribution from photons as detected from CMB radiation; cosmic neutrinos; baryonic (visible) matter; and some non-baryonic matter content, the dark matter. Dark matter has the clustering properties of ordinary matter and does not interact with standard model particles so that its existence can only be probed by gravitational effects on visible matter. More specifically, the type of dark matter which was non-relativistic at the time it decoupled from photons is called Cold Dark Matter (CDM), and it turns out to be the most data compliant choice. Eventually, observations tell us that about the 95% of the overall matter-energy density must be dark. The 68% in the form of dark energy and the rest, in the form of dark matter [41].

The background evolution of the Λ CDM model is given by its Friedmann equation, which can be written as

$$H = H_0 \sqrt{\Omega_r(1+z)^4 + \Omega_m(1+z)^3 + \Omega_k(1+z)^2 + \Omega_\Lambda}, \quad (1.32)$$

⁷We will follow the standard convention for which $\Omega_i(a)$, as a function, is the dimensionless density parameter at any scale factor a , while Ω_i , with no argument specified, will be the dimensionless density parameter at the present time, i.e. $\Omega_i(a=1) = \Omega_i$

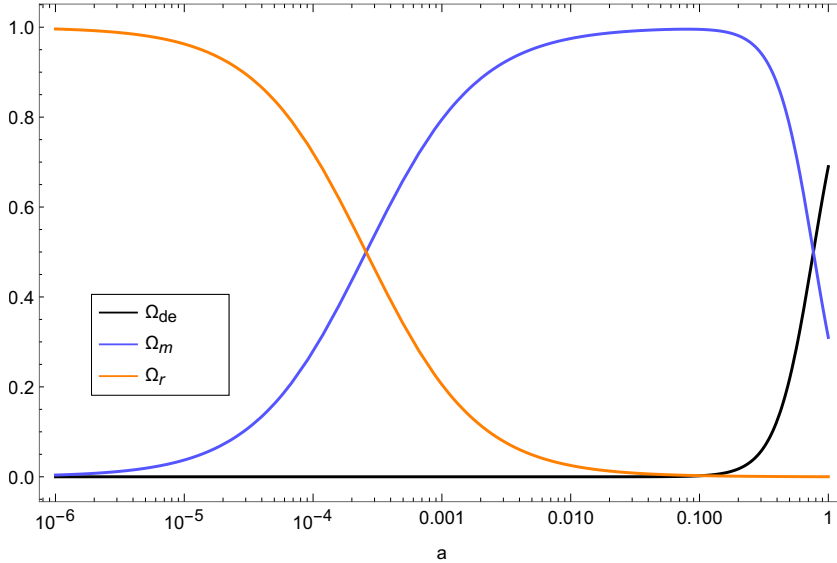


Figure 1.2: Evolution of the principal energy-density contents of the Universe showing the succession of the different epochs. We have chosen the present values given by [41] $\Omega_m = 0.315$, $\Omega_r = 9 \cdot 10^{-5}$ and $\Omega_\Lambda = 1 - \Omega_m - \Omega_r$.

where we are considering radiation, matter, the cosmological constant and the spatial curvature density parameter. The different epochs in the evolution of a Universe filled with the components in Eq. (1.32) are visually shown in Fig. (1.2). Using the same steps followed in Eq. (1.31), we can approximately define the end of radiation domination, $z \simeq 3 \cdot 10^3$ (corresponding to $a \simeq 2 \cdot 10^{-4}$ in the plot); then matter domination, lasting till $z \simeq 0.3$ (corresponding to $a \simeq 0.8$ in the plot), when dark energy in the form of a cosmological constant starts to dominate.

However, it has to be remarked that the Λ CDM model is not fully satisfactory in all its aspects and when compared to all the observational probes we have [69]. Besides not explaining the nature of the dark matter and of the dark energy, this model is burdened with very well-known problems. The cosmological constant can be interpreted as the energy-density of empty space, however, particle physics theories predict a value of Λ which is much larger than the observed one. This fact is called the “cosmological constant problem”. Another issue that is usually discussed is the “coincidence problem”, related to the fact that the fraction of matter and the fraction of dark energy today are of the same order and, besides, are the contents that dominate in the Universe nowadays.

Moreover, despite the favorable experimental results which support the standard paradigm and not forgetting the theoretical issues already mentioned, there are some

important tensions arising when comparing estimations of the cosmological parameters from data obtained within different surveys. One of the tensions that arises is related to matter perturbations. These were originated in the early times of the Universe and then evolved and clustered forming the galaxies and large structures we see today. Before introducing mathematically the corresponding observable, let us recall the basics of linear perturbation theory. As we will not go through the details, we refer the reader to the following reviews [70, 71]. If we first assume matter as a perfect fluid (which is licit as we are working on large scales), then, at the background level, it is completely described by its energy density ρ , the 3-velocity v , the pressure p and a gravitational potential ϕ . Considering now small deviations with respect to these background values and computing the usual linear set of hydrodynamic equations, after some algebra we come up with [72]

$$\ddot{\delta} + 2H\dot{\delta} - 4\pi G\rho\delta = 0, \quad (1.33)$$

where we have assumed pressureless matter and we have defined the fractional amplitude of density perturbations $\delta = \delta\rho/\rho$. This is the equation which describes gravitational instabilities in an expanding Universe. In order to express this physical quantity in a more observational cosmologist friendly way, we define what is called the *growth rate* [73],

$$f = \frac{d \log \delta}{d \log a}. \quad (1.34)$$

This quantity expresses how matter fluctuations, i.e. δ , grow with time. The observable which is commonly used is the normalized growth rate, $f\sigma_8$, where σ_8 is the present linear-theory mass dispersion on a scale of $8h^{-1}$ Mpc [74]. One can see in [41] that the range allowed by *Planck* leaves substantially below some of the data points. Nevertheless, the errors on these measurements are large so they provide no compelling evidence for discrepancy or accordance [75, 76, 77, 78, 79, 80].

Another important tension has to do with the present expansion rate, i. e. the Hubble constant H_0 [81]. The measurement of the Hubble constant is an intriguing task and can be carried out in two main ways. On the one hand we have *indirect model-inferred* values, which can be predicted from a specific cosmological model using multiple cosmological measurements. At the present stage, the most precise and updated constraints of this kind are derived from combining CMB data from *Planck* with other low redshift probes (SNeIa, BAO), using the standard cosmological model, Λ CDM. From this approach, we find $H_0 = (67.4 \pm 0.5) \text{ km s}^{-1} \text{ Mpc}^{-1}$ [41]. On the other hand, we have *direct local measurements*. The best established method of this

sort consists on building a distance ladder to calibrate luminosities of very concrete objects, like Cepheids and SNeIa [82, 83].

In the latest work following this approach [84], the best estimate of the local measured value derived is $H_0 = (74.03 \pm 1.42) \text{ km s}^{-1} \text{ Mpc}^{-1}$. Different methods have been employed for these local measurements, i.e. upgrades in the analysis of water masers in NGC4258 [85], gravitationally-lensed timedelays from quasars [86, 87] analyzed within the H_0 Lenses in COSMOGRAILs Wellspring (H0LiCOW) [88]. However, all the values exceed considerably the early Universe prediction, from 4σ to 6σ .

This list of problems seems to point to Λ CDM more as a phenomenological model to improve the fit to the data than a theoretically well and fully-motivated model. As a consequence, there have been several attempts to propose different alternatives. Many authors do not leave the realm of GR, and explore dynamical alternatives to the cosmological constant, the so-called dark energy models. Many others try to give up with GR itself and propose entirely new alternative theories of gravity, also known as modified gravity theories. In the following sections different models to explain the late-time acceleration (which may ease those inconveniences) are presented.

1.3 Dark energy

We will review here only some of the most-known dark energy models, because a full review of all the possibilities which are now on the market is out of the goal of this thesis. Not all the models which we will describe have been used in our works, but it is interesting to present this selection to show the many and different perspectives which can be adopted when dealing with this topic.

The easiest and more natural generalization of the cosmological constant consists on modeling dark energy (DE) in such a way that its EoS parameter is no more a constant (with the $w = -1$ case corresponding to the cosmological constant). This can be accomplished in the most varied ways, from the theoretical side [89, 90] to the phenomenological one [91, 92, 93, 94, 95, 96, 97, 98, 99, 100, 101, 102, 103, 104, 105, 106]. One can see [107] for a review on this topic.

Among the most common dark energy models studied in the literature where DE is described by a phenomenological equation of state, we can mention the *Chevallier-Polarski-Linder* (CPL) model [95, 96]. In this model the dark energy fluid has a dynamical equation of state which is linear in the scale factor:

$$w(a) = w_0 + w_a(1 - a), \quad (1.35)$$

where w_0 is the value of DE EoS today, while $w_0 + w_a$ is the asymptotic value at early times (i.e. when $a = 0$). The most updated constraints on this model come from latest *Planck* results [41], which provides for example, $w_0 = -0.96_{-0.15}^{+0.16}$ and $w_a = -0.28_{-0.59}^{+0.57}$, obtained by combining *Planck* TT, TE, EE polarization signal with SNeIa and BAO ⁸. We notice that for this combined data both the values of w_0 and w_a are fully consistent with Λ CDM.

More recently the Hubble tension debate has given new attention to the *early dark energy* (EDE) models [108, 109, 110], in which a large (w.r.t to the Λ CDM case) component of DE is present at early times. In one of the many ways in which this can be realized, we have one phenomenological scenario where the EDE term behaves as a constant at early times (adding up to the cosmological constant) and then decays rapidly at late times (where the cosmological constant becomes dominant):

$$E(a) = \sqrt{\Omega_m a^{-3} + \Omega_r a^{-4} + (1 - \Omega_m - \Omega_r - \Omega_{ee}) + \Omega_{ee} \frac{1 + a_c^6}{a^6 + a_c^6}}, \quad (1.36)$$

where Ω_{ee} is the fractional energy density of the early dark energy today, and $a_c = 1/(1 + z_c)$ is the critical value of the scale at which it shifts from the early-time behaviour to the late-time behaviour. In [110], *Planck* measurements of the temperature power spectrum are used to constrain the magnitude of the EDE density and it is shown that its contribution at the time of recombination can never exceed the 2% of the radiation/matter density in the limits $10 \leq z_c \leq 10^5$.

Then, we have the so-called *quintessence* models [111, 112, 113], which are described by a scalar field ϕ with a slowly varying potential $V(\phi)$ responsible for the late-time cosmic acceleration. Assuming that the scalar field interacts with other matter only gravitationally, the energy-density and the pressure are respectively given by

$$\rho_\phi = \frac{1}{2} \dot{\phi}^2 + V(\phi), \quad (1.37)$$

$$p_\phi = \frac{1}{2} \dot{\phi}^2 - V(\phi). \quad (1.38)$$

Thus, its equation of state can be written as

$$w_\phi = \frac{p_\phi}{\rho_\phi} = \frac{\frac{1}{2} \dot{\phi}^2 - V(\phi)}{\frac{1}{2} \dot{\phi}^2 + V(\phi)}. \quad (1.39)$$

which is clearly a time varying EoS, depending on the evolution of the field ϕ . These models are characterized by an EoS satisfying the condition $-1 < w < 1$.

⁸Data from *Planck* Legacy Archive; model `base_w_wa_plikHM_TTTEEE_lowl_lowE_BAO_Pantheon_18_post_lensing_zre6p5` in the PDF tables with 95% limits.

A nice review on quintessence which includes observational constraints on different quintessence models is presented in [114]. In [115] the EoS parameter of the quintessence field in general shows a tendency to the value -1 , not excluding, then, the cosmological constant case. In [116], motivated by the last GW results and by the H_0 tension, the authors observe that larger values of H_0 correspond to more negative EoS parameters of the scalar field. But they conclude that quintessence dark energy models are unlikely to relax the tension between local and CMB measurements.

Going one step forward we have the *k-essence* models [117], where, unlike in quintessence models, scalar fields with non-canonical kinetic terms appear [118],

$$S = \int d^4x \sqrt{-g} \left[\frac{1}{2\kappa^2} R + P(\phi, X) \right], \quad (1.40)$$

where $P(\phi, X)$ is a generic function of the scalar field ϕ and of its kinetic energy $X = -\frac{1}{2}g^{\mu\nu}\partial_\mu\phi\partial_\nu\phi$. In these models the cosmic acceleration should be realized by the kinetic energy of the field. For more details about these models, including some observational constraints, see [119, 120, 121, 122, 123, 124, 125, 126].

Another kind of models that have been widely studied are the *phantom* ones, characterized by having an EoS with $w < -1$. In this models we have

$$\rho_\phi = -\frac{1}{2}\dot{\phi}^2 + V(\phi), \quad (1.41)$$

$$p_\phi = -\frac{1}{2}\dot{\phi}^2 - V(\phi). \quad (1.42)$$

Although they generally present pathologies that made them inviable, as instabilities against small perturbations, in more recent works it has been shown that some particular class of them is consistent with observational data and can yield interesting features [127, 128]. In a more recent study [129], confronting phantom models against data from SNeIa, CMB and BAO, they obtain that the cosmological constant is, statistically, the most preferred dark energy model. However, the results also indicate that $w < -1$ may be preferred over $w > -1$. They finally state that, due to the similar values they obtain, it is not actually possible to distinguish between the cosmological constant and a dynamical dark energy which slightly deviates from it, only at 1σ deviation, so further studies are needed.

Finally, relating the two previous models we have the *quintom models*, which are dynamical scalar fields which are able to move from quintessence to phantom, i.e. they include the crossing point $w = -1$. The easiest Lagrangian which can realize that transition is given by [130]

$$\mathcal{L} = \frac{1}{2}\partial_\mu\phi\partial^\mu\phi - \frac{1}{2}\partial_\mu\sigma\partial^\mu\sigma + V(\phi, \sigma), \quad (1.43)$$

where the quintom fluid consists of a usual scalar field ϕ plus a negative kinetic energy scalar field σ , with $V(\phi, \sigma)$ being the quintom potential. There are some works which show that SNeIa alone seem to favor a quintom-like model [131, 132]. The quintom model is also mildly favored in the combined analysis of CMB, LSS and SNeIa [133, 134]; but in others, the preference is weak [132, 135]. The high interest this kind of scenario attracted has translated into many phenomenological studies that can be found in the literature [136, 137, 138, 139, 140, 141, 142, 143, 144, 145, 146, 147].

All the approaches listed above share the same characteristic: they introduce an extra energy-matter content, either as a parameterized equation of state, or as a scalar field. Nevertheless, there are also approaches which take a perspective which is radically different from this, as we will see below. We can start mentioning the *Ricci dark energy* model [148]. It belongs to the so-called *holographic dark energy* models [149]. The basic idea behind this class of models is that our Universe is in a sense finite and can be described by a two dimensional spherical holographic screen, thus there must be finite size effects. On a theoretical background, there is a big conceptual difference with respect to a simple cosmological constant, however its background evolution can be written as

$$E(a) = \sqrt{\frac{2\Omega_m}{2-\gamma}(1+z)^3 + \Omega_r(1+z)^4 + \left(1 - \Omega_r - \frac{2\Omega_m}{2-\gamma}\right)(1+z)^{4-\frac{2}{\gamma}}}. \quad (1.44)$$

where γ is a constant parameter of the theory. Then, it can be seen that the evolution is completely equivalent to a dark energy model with constant equation of state but with different parameters, if we define $\tilde{\Omega}_m \equiv \frac{2\Omega_m}{2-\gamma}$ and $\tilde{w} \equiv 4 - 2/\gamma$ we clearly see this equivalence. This similarity has been studied in some works as [150]. For a quite complete cosmological study on this kind of models see [151]. Besides, some observational studies have been done within this topic, throwing some hints about their validity. In [152], they analyze the X-ray gas mass fraction observation, SNeIa, BAO and CMB data and also the observational Hubble data, obtaining a slight preference of Λ CDM model with respect to the Ricci dark energy model. In [153], the authors introduce an extension of the holographic Ricci dark energy model by including an interaction between dark energy and matter. Using SNeIa, CMB and BAO observations they find that a nonvanishing interaction rate is favored by the observations. In a more recent work [154], letting the spatial curvature parameter free, it is shown that a flat Universe is observationally disfavoured without the presence of interactions.

Another possible candidate is the *coupled dark energy* [118], which is motivated by the fact that the energy density of dark energy is of the same order as that of dark matter in the present Universe, thus pointing to a possible relation between the two dark components. One interesting example is based on a scalar field (i.e. dark energy) coupled to non-relativistic matter described by the following modified energy conservation equations

$$\dot{\rho}_m + 3H\rho_m = \delta, \quad (1.45)$$

$$\dot{\rho}_\phi + 3H(\rho_m + p_\phi) = -\delta, \quad (1.46)$$

where the subindex m denotes dark matter, ϕ stands for dark energy and δ is an energy exchange term in the dark sector. Some observational studies have shown that coupled dark energy models may relax the Hubble tension [155], on the other side, in a more recent work [156] the obtained results show that there is no evidence of interaction between dark energy and dark matter at 2σ level.

Finally, we want to pay special attention to the *unified models of dark energy and dark matter*, where the two dark components are supposed to be different expressions of the same cosmological fluid. Although these two energy contents are quite different in terms of clustering properties and their EoS, the idea of unifying the whole dark content into a single fluid is very tempting. The kind of models we want to emphasize here are the *Chaplygin-like* models. The Chaplygin gas model was proposed originally by Kamenshchik [157]. These scenarios arose originally as an alternative to quintessence and they are characterized by describing the transition from a Universe filled with dust to an exponentially expanding de Sitter Universe by a single perfect fluid with an exotic equation of state. The background evolution of the original Chaplygin model is given by an EoS where the pressure is related to its energy-density via

$$p = -A/\rho. \quad (1.47)$$

Later, many generalizations of this EoS have been proposed, adding more free parameters to the model, as the *generalized Chaplygin gas*,

$$p = -A\rho^{-\alpha}. \quad (1.48)$$

We recommend [158] for a brief review on these models. Many works based on comparing these models to observational data have been performed, showing their degree of feasibility to explain observations [159, 160, 161, 162, 163, 164]. Concretely, it can be seen that a relaxation in the H_0 tension is obtained [165]. In Chapter V we will study a specific EoS within this kind of approach.

Apart from the Chaplygin-like models, non-linear barotropic equations of state also appear in other works, some of the most recent ones being [166, 167, 168, 169, 170, 171, 172]. They focus on different descriptions as quadratic models to represent dark energy and unified dark matter [171], non-linear EoS for phantom fluids [172] or the Born-Infeld type fluid model [169]. Among the works which have been performed in order to constrain some models of this kind, in [173], for example, the authors analyse a model described by one of the most known functional classes,

$$p = p_0 + w\rho + \beta\rho^2, \quad (1.49)$$

where p_0 , w and β are constants.

We also want to refer to a very recent model with non-linear EoS parameter that has been proposed in [174], the generalized emergent dark energy, for which the DE is negligible at early times but it emerges at late times. Its EoS parameter can be written as [175]

$$w = -\frac{\Delta}{3 \ln 10} \left[1 + \tanh \left(\Delta \log_{10} \frac{(1+z)}{(1+z_t)} \right) \right], \quad (1.50)$$

where Δ is a dimensionless non-negative free parameter and z_t is the transition redshift from the early times behaviour of the fluid, to the late time behaviour. It has been found that, although the dynamics is not very different from that of the standard model, the stability analysis indicates an accelerated phase at early times.

1.4 Modified gravity

Soon after Einstein formulated GR in 1915, the scientific community started to examine it and look for extensions. Hermann Weyl and Arthur S. Eddington, in the 20's, were the first who started considering modifications of GR. While Weyl developed his scale independent theory of gravity [176], Eddington proposed a theory of gravity based solely on a connection (as defined in the previous sections), without introducing a metric [177]. In fact, Eddington performed the earliest parameterization of the post-Newtonian formalism, a calculus tool which expresses Einstein's (non-linear) equations of gravity in terms of the lowest-order deviations from Newton's law of gravitation. This allows approximations to Einstein's equations to be made in the case of weak fields. The parameterized post-Newtonian formalism (PPN) is a version of this formulation where the parameters in which a general theory of gravity can differ from Newtonian gravity are explicitly detailed (for a review on this topic, see [178]).

During the following years, a huge variety of candidate theories of gravity were proposed and the quantity has continued increasing until today. We will review some of the most analyzed ones, emphasizing those ones more relevant for our works.

In the late 50's, a new approach to modify gravity theories was proposed by Pascual Jordan [179, 180], the so-called scalar-tensor theories [181, 182]. The general form of the Lagrangian density is generally written as

$$\mathcal{L} = \frac{1}{16\pi} \sqrt{-g} \left[\phi R - \frac{\omega(\phi)}{\phi} \partial_\mu \phi \partial^\mu \phi - 2\Lambda(\phi) \right] + \mathcal{L}_m(\Psi, g_{\mu\nu}), \quad (1.51)$$

where ϕ is the scalar field which mediates the gravitational interaction, the metric $g_{\mu\nu}$ is the tensorial contribution, $\omega(\phi)$ is an arbitrary function which can be interpreted as the coupling, $\Lambda(\phi)$ is a generalisation of the cosmological constant and \mathcal{L}_m is the lagrangian density of the matter fields Ψ . It can be noticed that this theory reduces to GR in the limit $\Lambda \rightarrow \text{const}$, $\omega \rightarrow \infty$ and $\omega'/\omega^2 \rightarrow 0$.

In the early 60's, Carl H. Brans and Robert H. Dicke would take over Jordan's work to develop their famous scalar-tensor theory of gravity [183], which can be obtained by choosing a constant ω and $\Lambda = 0$ in Eq. (1.51),

$$\mathcal{L} = \frac{1}{16\pi} \left[\phi R - \frac{\omega}{\phi} \partial_\mu \phi \partial^\mu \phi \right] + \mathcal{L}_m(\Psi, g_{\mu\nu}), \quad (1.52)$$

where ω is the dimensionless Dicke coupling constant. Brans-Dicke theory has been constrained at the background and perturbation level using different sources as CMB [184, 185, 186] or primordial nucleosynthesis [187, 188, 189, 190], where the typical limits achieved are about $\omega \gtrsim 300$ or $\omega \lesssim -30$. This model belongs to a most general class of theories which would be developed a decade later, Horndeski's theory [191]. This is the most general theory of gravity in four dimensions whose Lagrangian is constructed out of the metric tensor and a scalar field and leading to second order equations of motion. The reader may refer to [192], where some aspects of this theory in FLRW backgrounds are studied, and also to [193, 194], more centered on the cosmological perturbations.

At this point we find it convenient to mention a mechanism that was introduced by Justin Khoury and Amanda Weltman [195, 196] and which acts as a powerful tool to make a gravitational theory satisfy certain constraints: the chameleon mechanism. If we have a theory which includes a non-minimally coupled scalar field, this scalar can acquire an effective mass parameter, in the presence of other matter fields, that is environmentally dependent. Essentially, one can satisfy the constraints on non-minimally coupled scalar fields that are imposed in dense environments, while having an interesting behaviour in less dense environments, as the existing ones in cosmology.

Following with the alternative theories of gravity including extra fields, a natural extension comes with the vector-tensor theories, first proposed in the 70's [197, 198], which are nowadays studied in the modern form of Einstein-æther theories [199]. The particularity of these models is that they single out a preferred reference frame, where the presence of a Lorentz-violating vector field, i.e. æther, arises. It has been shown that this field can leave imprints on perturbations in the early Universe [200, 201] as well as affect the growth rate of structures [202, 203, 204].

When considering extra fields, another possibility is to consider bimetric theories. The essential idea behind these theories is the introduction of a second metric tensor, more specifically a rank-2 tensor, in the theory. For this reason they are also known as tensor-tensor theories. The idea behind the introduction of a second metric is that one of them describes the geometry of the spacetime and controls the speed of gravity and the other may be the one coupled to some other fields and controls their propagation. This could have implication as having a variable speed of light [205, 206]. The first proposals were done in [207] and conformed the basis of other theories. In order to have some names in mind, but without entering into detail, we can mention the following ones: Drummond's theory, which in fact claimed to mimic dark matter in spiral galaxies [208]; massive gravity, where a single massive spin-2 is included [209, 210, 211, 212] and bigravity, where the two metrics involved are used to build Einstein-Hilbert actions even though just one of them couples to the matter [213, 214, 215, 216]. See [217] for a quite recent review.

We end up with the alternatives with extra fields by noting that there also exists the possibility of adding a scalar field and a vector field, arriving to what is known as the tensor-vector-scalar theories (see [218] for more details on this topic).

Another route one can follow when thinking about modifications of gravity is to consider derivatives higher than second order [219, 220]. In the late 60's and 70's an approach was born to generalize GR consisting on adding higher power curvature corrections to Einstein's theory, which would later lead to the so-called $f(R)$ class of theories [221, 222, 223, 48, 224, 225]. These theories are generalizations of the Einstein-Hilbert action which consider higher order terms in R as, for example, R^2 or scalar curvature invariants as $R_{\mu\nu}R^{\mu\nu}$ in the Lagrangian. In this thesis we will center on the first option, [223]

$$S = \int d^4x \sqrt{-g} [f(R) + \mathcal{L}_m]. \quad (1.53)$$

Although we will dedicate the next subsection to explaining $f(R)$ in detail due to its important role in our work, we want to remark that these models became incredibly

interesting in the 80's due to their ability to give rise to a period of accelerated expansion in the early Universe (i.e. inflation) as well as thanks to their improved renormalization properties [24]. More recently these models have also generated an interest which is mainly related to the gravitational phenomenology at low energies, i.e. the late Universe and, thus, are mostly related to solution of the dark energy problem. It must be said that $f(R)$ theories have a scalar-tensor representation which is analogous but seem to exhibit different behavior in the study of perturbations [226].

From the observational point of view, and taking into account that there will be another entire subsection for this topic, we will just mention some works that have been done about primordial nucleosynthesis in $f(R)$ [227, 228, 229, 230] and also the fact that, despite observations of the CMB and the BAO have allowed to constrain $a(t)$, it has been shown that the arbitrariness when choosing $f(R)$ makes it not possible to falsify a general form of these theories [231, 232, 233, 234, 235, 236, 237]. The consequences on large scale structure due to the modified growth have also been studied [238, 239, 240, 241, 242]. These works encompass a very short overview of some of the topics tackled from the $f(R)$ approach. Let us just add that in analogy with $f(R)$ theories, other approaches will adopt the form of the $f(T)$ and $f(Q)$, where the gravitational force is driven by the torsion, T , or by the non-metricity, Q . We will dedicate more words on the global panorama of these theories in future subsections.

To put an end to this non-exhaustive review of this class of modifications let us say a few words about two sound models which contain non-trivial derivative interaction terms, although they are not higher order derivatives: Galileons [243] and ghost condensates [244]. The first one is inspired in the Dvali-Gabadadze-Poratti (DGP) theory [245], which belongs to the higher dimensional modified gravity theories which will be commented below. Among the variety of galileon extensions we can mention the conformal galileon [243, 246] or the covariant galileon [247, 246]. The late time cosmology of the covariant galileon has been widely studied [248, 249, 250, 251, 252, 253, 254], showing that density perturbations, for example, are a feature that allows to distinguish this model from Λ CDM. The second model is a new kind of fluid whose EoS is the same as the cosmological constant, i.e. $p = -\rho$, but with one difference: it is a physical fluid with a physical scalar excitation around its background. The action for ghost condensate theories can be expressed as [255]

$$S = \int d^4x \sqrt{-g} \left(\frac{R}{16\pi G} + M^4 P(X) \right), \quad (1.54)$$

where M is a mass scale and $P(X)$ is a function of $X = -\frac{1}{2}g^{\mu\nu}\partial_\mu\phi\partial_\nu\phi$ which must have a non-zero minimum at the vacuum expectation value of X . See [244] for more details.

From the observational point of view some works have been done, as [256, 257]. In fact, the growth structure of a theory where these two models merge, i.e. the galileon ghost condensate, has been recently investigated [258].

In the 70's and 80's, the idea of constructing a quantum field theory of gravity [259] stimulated proposals as super-gravity and super-strings, which rely on the introduction of super-symmetry and mean a resurgence in the work by Kaluza and Klein involving higher dimensional spaces. The particularity of Kaluza-Klein theory is that extra dimensions considered are small and compacts [260, 261, 262]. On the other side there is the braneworld paradigm, which is motivated by string theory and the extra dimensions can be much larger [263, 264, 265, 266, 267, 245]. This idea of building a quantum field theory of gravity has attracted a lot of attention, giving rise to different branches of studies which try to develop these ideas, being [268, 269] some of the principal works settling the initial steps.

Although modified gravity and dark energy are intrinsically different, it has to be taken into account that the limits between the dark energy and the modified gravity formulation are not always clearly drawn, i.e. sometimes their phenomenology is similar and make them indistinguishable [270, 271, 272, 273, 274]. In fact, an effective field theory (EFT) of dark energy approach has been recently developed. This framework is a type of approximation which consists on capturing into one single and general formulation a wide class of dark energy and MG models [275, 276]. It is a model independent approach encompassing all single field DE and MG models (once a mapping procedure is provided to write any specific model in the EFT language) and describes both the evolution of the cosmological background and linear perturbations, thus providing an appropriate framework to classify different aspects of MG according to their signatures [277]. A whole and detailed description of this formalism can be found in [278].

As we have said, the number of ways in which GR has been and can be extended is extremely large; for a quite updated non-exhaustive list see, for example, [279, 280, 225].

Formalisms to derive the field equations

There are three main formalisms to derive field equations from the action in gravity theories [280]. The first one is the standard metric formalism (which is the one we adopt in our works, unless something else is clearly specified) in which the field equations are derived by the variation of the action with respect to the metric tensor

$g_{\mu\nu}$. In the case of GR one starts from Eq. (1.1), with the affine connection $\Gamma_{\beta\gamma}^{\alpha}$ depending on $g_{\mu\nu}$ as given in Eq. (1.3).

The second formalism is the Palatini one in which $g_{\mu\nu}$ and $\Gamma_{\beta\gamma}^{\alpha}$ are treated as independent variables when varying the action.

$$S = \frac{1}{2\kappa} \int \sqrt{-g} (g^{\mu\nu} \Gamma R_{\mu\nu}) d^4x + \int \mathcal{L}_m(g_{\mu\nu}, \Psi) d^4x. \quad (1.55)$$

Although for Lagrangians linear in R both variational principles lead to the same field equations, this is not true for a more general action.

Moreover, there is a third version, the metric-affine $f(R)$ formalism, which consists on using the Palatini variation but abandoning the assumption that the matter action is independent of the connection [281]

$$S = \frac{1}{2\kappa} \int \sqrt{-g} (g^{\mu\nu} \Gamma R_{\mu\nu}) d^4x + \int \mathcal{L}_m(g_{\mu\nu}, \Gamma_{\alpha\beta}^{\mu}, \Psi) d^4x. \quad (1.56)$$

1.4.1 $f(R)$ theories

Among the plethora of alternative models proposed, we now focus on the so-called $f(R)$ framework, also referred to as fourth-order theories or extended theories of gravity [221, 282, 223, 225, 283].

The easiest and most basic approach to this kind of theories consists in replacing the Ricci scalar, R , appearing in the Hilbert-Einstein action of GR, with a general function $f(R)$. The reason to choose this type of modification of gravity is, firstly, because $f(R)$ actions are the most logical (even though not the simplest) modification one can consider and secondly, they are also sufficiently general to encapsulate some basic features of higher order gravity. The action is given by [223]

$$S = \int d^4x \sqrt{-g} [f(R) + \mathcal{L}_m], \quad (1.57)$$

where $f(R)$ is an undetermined function of R . Although the $f(R)$ proposals are in principle unspecified, they cannot be arbitrary, but, as any modified gravity theory, they have to be able to satisfy some theoretical and observational requirements:

- To be stable at the classical and semiclassical level; not to contain ghosts; to admit a well-posed Cauchy problem and to have the correct weak-field limit at both the Newtonian and post-Newtonian levels, i.e. they must satisfy Solar System constraints, given that on such scales GR has been experimentally tested and confirmed (see [223] for a detailed analysis on this criteria);

- To fit the cosmological data reproducing the correct cosmological dynamics, the correct behaviour of gravitational perturbations, and to generate cosmological perturbations compatible with the cosmological constraints from Cosmic Microwave Background, Large Scale Structure, Big Bang Nucleosynthesis and gravitational waves.

Some examples of such viable models are in [284, 285, 286, 287, 288, 289]. It is instructive to note that the first model of inflation [284],

$$f(R) = R + \alpha R^2 \quad (\alpha > 0), \quad (1.58)$$

was an $f(R)$ theory. Proposed by Starobinsky, unlike the models such as “old inflation”, this scenario was not plagued by the graceful exit problem, i.e. the period of cosmic acceleration is naturally followed by a radiation-domination epoch with a transient matter-dominated phase. So far, this model seems to be consistent with data for inflation [290].

In [285], another very specific model of $f(R)$ is proposed, this time in order to explain the accelerated expansion without a cosmological constant and it is given by

$$f(R) = R - m^2 \frac{c_1 (R/m^2)^2}{c_2 (R/m^2)^n + 1}, \quad (1.59)$$

where m is a mass scale, $n > 0$ and c_1 and c_2 are dimensionless parameters. This expression comes from setting the following requirements,

$$\lim_{R \rightarrow \infty} f(R) = \text{const.}, \quad (1.60)$$

$$\lim_{R \rightarrow 0} f(R) = 0. \quad (1.61)$$

On the one side, this model mimics Λ CDM in the high redshift regime, well tested with CMB. On the other, it appears to behave as a constant term which might lead the accelerated expansion at low redshifts, as can be seen if we expand $f(R)$

$$\lim_{m^2/R \rightarrow 0} f(R) \simeq -\frac{c_1}{c_2} m^2 + \frac{c_1}{c_2} m^2 \left(\frac{m^2}{R} \right)^n; \quad (1.62)$$

the first term in Eq. (1.62) would play the role of the cosmological constant, being the leading term at low redshifts.

$f(R)$ theories have been intensively analyzed, by comparing them with cosmological probes [291, 292, 293, 294, 295, 296, 297, 298], with the internal dynamics of many different-scale gravitational structures [299, 300, 301, 302, 303, 304, 305], and with cosmological simulations [306, 307, 308, 309, 310, 311, 312], eventually putting either

too weak or too severe (i.e. very consistent with the Λ CDM limits) constraints on their viability. Among the various applications of $f(R)$ theories to cosmology and gravity such as inflation, dark energy, local gravity constraints, cosmological perturbations, and spherically symmetric solutions in weak and strong gravitational backgrounds, we can sum up here the state of the art of $f(R)$ theories giving the principal results and challenges within these models.

We know that the transition from one era to another must be smooth and it has been found in some studies that the exit from radiation era may present problems in many models [313, 314, 315], but more recently it has been proved that the exit of any era can be achieved [316, 313, 317]. It has been also analyzed that instabilities may be a problem for some of these theories due to the order of the field equations [318, 319, 320]. However, the Palatini approach, described by second order field equations, results in avoiding this instability [321]. On the one side, let us notice that $f(R)$ gravity theories are free of ghosts, but generalizations containing higher order terms generally contain ghost. On the other side, exceptions can be found under some conditions [322, 323, 324, 325, 326]. Among the successes of $f(R)$ models we have to underline that some of them exhibit the chameleon mechanism, which allows them to pass observational tests, i.e. model in Eq. (4.2.1) from [327]. Besides, one of the challenges for metric $f(R)$ is related with some instabilities that appear beyond the linear approximation [328, 329]. It pays off to make some numbers in order to understand how $f(R)$ meets the data. In [330], the authors obtain constraints for some cosmological parameters using CMB data and galaxy power spectra. We find it interesting how they use linear theory predictions for the matter spectra finding that the combined data sets give a tight constraint on the $f(R)$ gravity Compton wavelength parameter ⁹, i.e. $\log_{10} B_0 < -4.07$. In a more recent work, they analyze the bounds on maximum structure sizes of the observed Universe, providing a criterion to enable large scale structures to be stable in $f(R)$ theories. They obtain that the existence of stable structures is allowed if the criterion $f'(R_{dS}) \leq 1.37$ is satisfied, being R_{dS} the Ricci scalar [331]. The galactic clustering of an expanding Universe by assuming the gravitational interaction given by $f(R)$ gravity is discussed in [332], where they conclude that the distribution function from the quasi-equilibrium approach could be useful to constrain some classes of $f(R)$ models.

⁹This dimensionless parameter is defined in terms of the first and second derivative of $f(R)$ and can characterize the deviation from GR. A small value of $B(a)$ indicates a small deviation and quasistatic approximation holds, while in the case $B(a) \sim 1$, this approximation breaks down [330].

Apart from all the given references we recommend to see [327, 333, 334, 273] for more details on the theoretical and experimental challenges faced by $f(R)$ in order to satisfy minimal criteria for viability.

One interesting extension of metric $f(R)$ gravity that have been analyzed in this thesis is what are known as $f(R)$ non-minimally coupled theories, first proposed in [335]

$$S = \int \left[\frac{f_1(R)}{2\kappa^2} + (1 + \lambda f_2(R))\mathcal{L}_\dagger \right] \sqrt{-g} d^4x, \quad (1.63)$$

where $f_i(R)$ ($i = 1, 2$) are arbitrary functions of the Ricci scalar R , g is the determinant of the metric $g_{\mu\nu}$, $\kappa^2 = 8\pi G$, λ is a coupling constant with length square units and \mathcal{L}_m is the matter Lagrangian density. Here a small potential coupling appears between the gravitational sector and the matter fields. Those theories have been gathering quite some attention since some years ago to describe different cosmological events. For a non-exhaustive but representative variety of publications on the topic please see [336, 337, 338, 339, 340, 341, 342, 343, 344, 345, 346, 347, 348]. More precisely, in [336], gravitational baryogenesis is analysed finding compatible results with observations, whereas in [337] some inflationary scenarios are studied and examples of observational predictions are given for some of the most common potentials in order to set limits on the scale of the non-minimal coupling. In [338], the degeneracy of Lagrangian densities for a perfect fluid is discussed. On the one hand, one of the motivations of analysing this kind of models is their ability to answer for the dark matter effects which are observed in our Universe. In [339], it is shown that with non-minimally coupled $f(R)$ theories it is possible to mimic known dark matter density profiles through a specific power-law coupling. In [340] it is shown how these theories can give rise to an additional contribution to the field equations, as compared with GR, that can play the role of dark matter. More recently in [341], analytical solutions to the modified field equations are derived and, besides, constraints on the parameters of the model are obtained by comparing their predicted profiles for visible and dark matter with known ones. In [348], the authors discuss an effective model of $f(R)$ gravity containing a non-minimal coupling to the axion scalar field. On the other hand, it is still unanswered the question of which theory could be behind the late-time acceleration of the Universe, then, $f(R)$ non-minimally coupled theories have been also studied as possible candidates for this accelerated behaviour observed nowadays [342, 343, 344]. In [345] the authors studied the evolution of cosmological perturbations within this kind of theories as well as analysing the large-scale structures that are formed. Matter density perturbations are also studied in [346],

where some constraints on a specific model are setted using age of the oldest star clusters and the primordial nucleosynthesis bounds. Finally, in [347] a gravitational waves analysis has been performed within these models. $f(R)$ non-minimally coupled theories will be studied in detail in Chapter 4

1.4.2 $f(Q)$ theories

In GR, the equations of motion impose a torsion and nonmetricity free geometry, where the connection is given by the Christoffel symbols, i.e. Eq. (1.3). Nevertheless, in modified theories of gravity, this will not be the case and two new quantities that we will define now, torsion and non-metricity, can appear.

A basic result in differential geometry states that the general affine connection may be decomposed into the following three independent components [349, 350]:

$$\Gamma^\lambda_{\mu\nu} = \left\{^\lambda_{\mu\nu}\right\} + K^\lambda_{\mu\nu} + L^\lambda_{\mu\nu}, \quad (1.64)$$

where $\left\{^\lambda_{\mu\nu}\right\} \equiv \frac{1}{2}g^{\lambda\beta}(\partial_\mu g_{\beta\nu} + \partial_\nu g_{\beta\mu} - \partial_\beta g_{\mu\nu})$ is the Levi-Civita connection of the metric $g_{\mu\nu}$; the term $K^\lambda_{\mu\nu} \equiv \frac{1}{2}T^\lambda_{\mu\nu} + T_{(\mu}{}^\lambda{}_{\nu)}$ is the contortion, with the torsion tensor defined as $T^\lambda_{\mu\nu} \equiv 2\Gamma^\lambda_{[\mu\nu]}$; and finally the disformation $L^\lambda_{\mu\nu}$ is given by

$$L^\lambda_{\mu\nu} \equiv \frac{1}{2}g^{\lambda\beta}(-Q_{\mu\beta\nu} - Q_{\nu\beta\mu} + Q_{\beta\mu\nu}), \quad (1.65)$$

which is defined in terms of the nonmetricity tensor, $Q_{\alpha\mu\nu} \equiv \nabla_\alpha g_{\mu\nu}$. To complete our inventory of the relevant geometric objects which characterize the spacetime, let us keep in mind that the Riemann tensor is given in terms of the connection by

$$R^\alpha_{\mu\rho\nu} = \partial_\rho \Gamma^\alpha_{\nu\mu} - \partial_\nu \Gamma^\alpha_{\rho\mu} + \Gamma^\alpha_{\rho\lambda} \Gamma^\lambda_{\nu\mu} - \Gamma^\alpha_{\nu\lambda} \Gamma^\lambda_{\rho\mu}. \quad (1.66)$$

Moreover, it will be useful to know that under a shift of the connection, $\hat{\Gamma}^\alpha_{\mu\nu} = \Gamma^\alpha_{\mu\nu} + \Omega^\alpha_{\mu\nu}$ (with $\Omega^\alpha_{\mu\nu}$ an arbitrary tensor), the Riemann tensor transforms as

$$\hat{R}^\alpha_{\beta\mu\nu} = R^\alpha_{\beta\mu\nu} + T^\lambda_{\mu\nu} \Omega^\alpha_{\lambda\beta} + 2\nabla_{[\mu} \Omega^\alpha_{\nu]\beta} + 2\Omega^\alpha_{[\mu|\lambda|} \Omega^\lambda_{\nu]\beta}. \quad (1.67)$$

In order to understand the physical meaning of each quantity, we present an illustration of their effects in Fig. (1.3): the curvature describes the rotation of a vector transported along a closed curve; the torsion gives the non-closure of parallelograms formed when two vectors are transported along each other; the nonmetricity gives the variation of the length of a vector when it is transported [351].

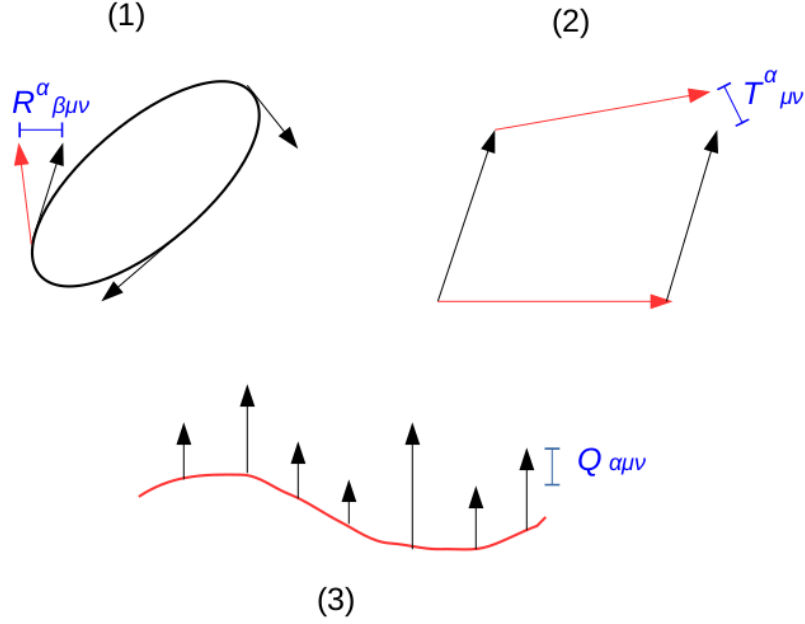


Figure 1.3: (1) Curvature. (2) Torsion. (3) Nonmetricity.

Starting from the usual formulation of GR, where gravity is attributed to the curvature of spacetime, the constraints on the connection being symmetric and torsion-free can be incorporated by adding Lagrange multipliers enforcing those constraints:

$$S = \int d^4x \left(\frac{\sqrt{-g}}{16\pi G} g^{\mu\nu} R_{\mu\nu}(\Gamma) + \lambda_{\alpha}^{\mu\nu} T_{\mu\nu}^{\alpha} + \hat{\lambda}_{\mu\nu}^{\alpha} Q_{\alpha}^{\mu\nu} \right). \quad (1.68)$$

As an alternative, if we identify gravity with the torsion and want to construct an action in this framework, we may consider the most general even-parity second order quadratic form which can be built with the torsion [351],

$$\mathbb{T} = -\frac{c_1}{4} T_{\alpha\mu\nu} T^{\alpha\mu\nu} - \frac{c_2}{2} T_{\alpha\mu\nu} T^{\mu\alpha\nu} + c_3 T_{\alpha} T^{\alpha}, \quad (1.69)$$

where c_1 , c_2 , c_3 are free parameters and $T_{\mu} = T_{\mu\alpha}^{\alpha}$ is the trace of the torsion. Again, introducing appropriate Lagrange multipliers, we have

$$S = - \int d^4x \left(\frac{\sqrt{-g}}{16\pi G} \mathbb{T} + \lambda_{\alpha}^{\beta\mu\nu} R_{\beta\mu\nu}^{\alpha} + \hat{\lambda}_{\mu\nu}^{\alpha} \nabla_{\alpha} g^{\mu\nu} \right). \quad (1.70)$$

Now, we want to know if one can recover GR carefully choosing the parameters. In order to do that one has to take into account that, if nonmetricity vanishes, by using Eq. (1.67) it is possible to arrive to

$$R = \mathcal{R}(g) + \mathring{\mathbb{T}} + 2\mathcal{D}_{\alpha} T^{\alpha}, \quad (1.71)$$

where $\mathcal{R}(g)$ is the Ricci scalar of the Levi-Civita connection, \mathcal{D}_α is the covariant derivative and $\mathring{\mathbb{T}}$ is \mathbb{T} for the choice $c_1 = c_2 = c_3 = 1$. Thus, Eq. (1.71) and the flatness condition ($R = 0$) implies that GR is recovered by

$$S = -\frac{1}{16\pi G} \int d^4x \sqrt{-g} \mathring{\mathbb{T}}. \quad (1.72)$$

This theory is known as Teleparallel Equivalent of GR [352].

Going another step forward one can wonder what happens when considering that gravity is fully represented by the nonmetricity, i.e. a flat and torsion free geometry. Proceeding as before, we can write the most general even-parity second order quadratic form of the non-metricity,

$$\mathbb{Q} = \frac{c_1}{4} Q_{\alpha\mu\nu} Q^{\alpha\mu\nu} - \frac{c_2}{2} Q_{\alpha\mu\nu} Q^{\mu\alpha\nu} - \frac{c_3}{4} Q_\alpha Q^\alpha + (c_4 - 1) \tilde{Q}_\alpha \tilde{Q}^\alpha + \frac{c_5}{2} Q_\alpha \tilde{Q}^\alpha, \quad (1.73)$$

where $Q_\mu = Q_{\mu\alpha}^\alpha$ and $\tilde{Q}_\mu = Q_{\alpha\mu}^\alpha$ are the two independent traces of the nonmetricity. The action considering the corresponding Lagrange multipliers reads

$$S = - \int d^4x \left(\frac{\sqrt{-g}}{16\pi G} \mathbb{Q} + \lambda_\alpha^{\beta\mu\nu} R_{\beta\mu\nu}^\alpha + \lambda_\alpha^{\mu\nu} T_{\mu\nu}^\alpha \right). \quad (1.74)$$

Now, considering a torsion-free connection, Eq. (1.67) throws

$$R = \mathcal{R}(g) + \mathring{\mathbb{Q}} + \mathcal{D}_\alpha(Q^\alpha - \tilde{Q}^\alpha), \quad (1.75)$$

where $\mathring{\mathbb{Q}}$ is \mathbb{Q} for the choice $c_1 = c_2 = c_3 = 1$. In a flat spacetime with $R = 0$, the action becomes

$$S = -\frac{1}{16\pi G} \int d^4x \sqrt{-g} \mathring{\mathbb{Q}}. \quad (1.76)$$

This theory is called Symmetric Teleparallel Equivalent of GR.

In our work we are going to focus on this last description, where gravity is identified with the nonmetricity. Within the scenario of modified gravity alternatives, a natural extension in this formalism is given by $f(\mathring{\mathbb{Q}})$, which from now on we will denote simply as $f(Q)$:

$$S = -\frac{1}{16\pi G} \int d^4x \sqrt{-g} f(Q). \quad (1.77)$$

Here let us remark that, although $\mathcal{L} = \mathring{\mathbb{Q}}$ is equivalent to $\mathcal{L} = \mathcal{R}$ because their only difference is a total derivative, this term is precisely what makes the difference between $f(\mathcal{R})$ and $f(Q)$. Some works have been already performed in this framework [353, 354, 355, 356, 357, 358, 359, 360, 361]. Anyway, as this is a novel approach, it still has to be deeply explored, offering hopefully some insight on different cosmological problems as the late accelerated expansion of the Universe. We will explain more about this field in Chapter 3.

1.5 Observational data

Type Ia Supernovae Type Ia (SNeIa), Baryon Acoustic Oscillations (BAO) and the Cosmic Microwave Background radiation (CMB) are among the most fundamentally important observations which are nowadays used in modern cosmology to infer any insight in the underlying cosmological model background. They constitute the main core around which most of the cosmological analysis is performed, but also additional probes, like early-type galaxies (ETG), quasars (QSO) and gamma ray bursts (GRB) are ongoing further investigations and developments because, although at the present stage they do not achieve the same precision as the mentioned ones at the beginning, they can provide complementary and independent information on the topic. In the next sections, we will provide a general but far-from-exhaustive introduction to the main properties of most of these observational quantities, with a specific highlight on the technological progress which have been at the basis of the achievement of modern cosmology.

1.5.1 Type Ia Supernovae

In cosmology a variety of celestial objects are used, directly or indirectly, in order to extract information about our Universe. The most popular are for sure supernovae (SNe), because they help us to measure distances of very far objects, till $z \sim 2$. However, historically speaking, they are not the first standard candles at all. Actually, they are more properly defined as *secondary* candles because they can be calibrated only after using other objects which are, on purpose, defined as *primary*. The most famous primary standard candles are the Cepheids, which we mentioned in the introduction. They are variable stars whose luminosity follows radial pulsations [362, 363] and, although there are different kinds of variable stars [364], classical Cepheids are more distinguishable due to their characteristic pulsations [365, 366, 367, 368]. As we will see below, these objects are crucial for the calibration of supernovae, and the period-luminosity relation will be a fundamental element. Although this relation was first proposed by Leavitt, it has been continuously improved taking into consideration more features of the cepheids, as the color or the metallicity [369, 370]. For example, the period-luminosity-color relation can be written as [371]

$$M = \alpha \log P + \beta \log(B - V)_0 + \gamma, \quad (1.78)$$

where M is the absolute magnitude, P is the period, $B - V$ refers to the intrinsic color and α, β, γ are constants.

Coming back to SNe, let us say that they are, basically, violently exploding stars whose luminosities after eruption suddenly increase many millions of times over their normal levels, being among the brightest events in the sky, so that they are able to briefly outshine all the stars in the host galaxy. Depending on their origin and their emission and absorption spectral lines they can be classified in different types. Supernovae with no hydrogen features in their spectra had previously all been classified simply as “Type I”, but in the early 1980s, a new classification emerged. This class was subdivided into types Ia and Ib, depending on the presence or absence of a silicon absorption feature at 6150\AA in the supernova’s spectrum (see [372] for more details concerning SNe classification).

In cosmology, we practically deal only with Type Ia Supernovae (SNeIa), because they are “*standardizable*”, as we will explain later, which means that they provide an almost absolute method to measure cosmological distances [373], i.e. they are standard candles. SNeIa are defined by a lack of hydrogen and helium lines and the presence of strong silicon lines in their spectra, and they are thought to occur in a binary system of stars which are orbiting around the same point. There is not much knowledge about the sources of this kind of explosions but the key point is that the supposed mechanism underlying SNeIa always happens in the same way, involves approximately the same masses, and produces the same intrinsic luminosity; this is what makes SNeIa standardizable.

Usually two broad classes of progenitor models are considered. On the one hand, there is the single degenerate model, in which a white dwarf accreting from a binary companion is pushed over the Chandrasekhar mass limit (about one and a half solar masses) [374]. At this point a nuclear chain reaction occurs, causing the white dwarf to explode. On the other hand, there is the double degenerate model, in which gravitational radiation causes an orbiting pair of white dwarfs to merge and exceed the Chandrasekhar mass. As it has been said, one of the stars composing the system must be always a white dwarf star, which is the densest type of self-gravitating stellar-size object, after neutron stars and black holes. White dwarfs are the remnant of a star that was about the size of our Sun. The other star forming the system could be a giant star or even a smaller white dwarf. In the nucleus of white dwarf stars thermonuclear reactions are not happening anymore, so their intense gravity is the feature which unchains the process [375, 376].

The path for SNeIa to become the reference distance measurement for farther celestial objects can be considered to start in 1916, when Vesto Slipher measured velocities of nearby galaxies and found that the vast majority of them was moving

away from us. In Edwin Hubble’s first steps about the cosmic expansion in the 1920s, he used entire galaxies as standard candles. But galaxies, coming in many shapes and sizes, are difficult to match against a standard brightness. They can grow fainter with time, or brighter (by merging with other galaxies). In the 70’s, it was suggested that the brightest member of a galaxy cluster might serve as a reliable standard candle, but in the end, all proposed distant galactic candidates were too susceptible to change. In 1938, Baade and Zwicky proposed SNeIa to measure the cosmic expansion. Many years later, in 1990, The Calan-Tololo SN search in Chile (led by Mario Hamuy) tested the “goodness” of the SNeIa. They found that the fainter a SNeIa is, the sharper is the peak of its brightness [377, 378, 379]. The supernovae that faded faster than the norm were fainter at their peak, and the slower ones were brighter. In fact, one could use the light curve’s time scale to predict peak brightness and thus slightly recalibrate each supernova. But the great majority of SNeIa passed the screening tests and were, in fact, excellent standard candles that needed no such recalibration. In particular, it was found an empiric correlation between the peak luminosity of SNeIa and the shape of their curves [378, 380] described by the linear relation

$$M_{max} = a + b\Delta m_{15}(B). \quad (1.79)$$

where a , b are fit parameters common for every SNeIa and $\Delta m_{15}(B)$ is the measured apparent magnitude decay in the B-band after 15 days from its maximum, identified by the absolute magnitude M_{max} . Of course, the crucial point in the assessment of this relation, was the use of SNeIa whose distance could be estimated by alternative methods [378]. Starting from these initial bunch of SNeIa, extended by later observations, it was possible to calibrate, i.e. to fix the parameters a and b , with higher and higher precision, thus allowing to estimate absolute magnitudes of any newly discovered SNeIa which, combined with the apparent magnitudes measurements, allowed to calculate the luminosity distance of these objects. As for Cepheids, during the years this relation has been constantly updated with new ingredients and insights reaching the present standards. In particular, we remind here two parameters which are crucial in the process of standardization of SNeIa: the stretch, which literally describes the time stretching of the light curve [381, 382, 383], and the SNeIa color at maximum brightness [384, 385]. We will specify more about them in the following sections.

Despite the great theoretical improvements, the main obstacle toward the full exploitation of SNeIa for cosmological uses still was the paucity of data. As reported in [386], in the early 90’s the discovery of a single SNeIa event was thought to be quite hard due to the unpredictability of such events. The turning point was the “SNe on

demand” technique devised by Saul Permuter: by performing repeated imaging of selected areas of the sky at regular intervals (the ideal timing being after any new moon), the teams could identify (many) possible candidates at once and thus plan follow-up observations which would provide both magnitudes, peak brightnesses and spectral features of confirmed SNeIa events. Once the number of observed SNeIa started to grow, the same standardization process based on the relations and parameters described above got improved, leading to the discovery of dark energy, and reaching the high standards we have nowadays.

Even though light curve fitting and calibration have been constantly improving, we do have a limit: SNeIa are very good to estimate distances at relatively large redshifts, but we do not have SNeIa at very low ones. Thus, in order to have it done in the best way possible, one has to rely on some other standard candles, different from SNeIa, and which are abundant at very low redshift; then, in the overlapping regimes, one can use such low redshift probes to calibrate (at higher level) SNeIa [387]. The stellar objects which are used to improve calibration of SNeIa are Cepheids; with the closest Cepheids calibrated using parallax distances measurements [388, 389]. When performing these techniques one must not forget to take into account phenomena that may affect the measurements as the extinction from dust or the shift of the SNeIa spectrum due to the redshift. Thus, to properly determine a precise distance, it requires a well-observed SNeIa light curve in multiple pass bands [390, 391, 392].

After the full standardization procedures are applied, any remaining difference in the peak brightnesses of two SNeIa should be due to a difference in distance to the observer. In 1998, both SCP and High-Z team, had the same key finding: SNeIa looked to be farther (i.e. less luminous) than expected with respect to the common, at that time, cosmological model. If the Universe’s expansion had been expanding at a decelerating rate, the SNeIa should have appeared brighter than what they were found to be. As reported in the historical review of [386], in the context of the then standard cosmological model, with no cosmological constant nor any dark energy component, this could have been achieved only by $\Omega_m < 0$, which was clearly thought unphysical. Relaxing the model, and allowing for a cosmological constant, they found that SNeIa results supported a Universe with $\Omega_m \sim 0.2 - 0.4$, and a negative deceleration parameter, $q = \frac{1}{2}\Omega_m - \Omega_\Lambda$, giving important hints supporting the presence of a dark energy causing the well confirmed accelerated expansion of the Universe that we know today.

As a fact of scientific interest we will say that nowadays the largest combined sample of SNeIa is the Pantheon [393], a compilation of 1048 SNeIa which covers the

redshift range $0.01 < z < 2.26$. This compilation has been used in this thesis as it is a quite powerful probe that allows us to constrain the background evolution of the cosmological parameters.

1.5.2 Cosmic Microwave Background radiation

In order to understand properly the origin and the physics behind CMB, we have to look back into the history of our Universe, and focus on the crucial moment which constitutes the *before and after* crossroad: the recombination epoch, namely, the first moment in the life of our Universe in which baryons and (free) electrons can combine to form neutral hydrogen, due to the lowering density and temperature of the early time cosmic soup after Universe expansion. Recombination is approximately set at $z \approx 1100$, i.e. 380000 years since the beginning. Before recombination, we cannot separate these two components, but we can only recognize a photon-baryon plasma, with photons strongly interacting with the free electrons through Thompson scattering and the free electrons interacting with the baryons through electromagnetic interaction. As for the other components we do have: neutrinos (which have already decoupled from other particles because the weak interaction decouples earlier than the electromagnetic one) and dark matter particles which, whichever they are, only interact with other components by gravitational interactions.

The key point to understand how the CMB was originated, is that this photon-baryon plasma was not homogeneous, but full of over-dense and under-dense regions. The origin of such fluctuations, as they are more commonly defined, is intrinsic to the inflationary era and is, in some sense, the biggest element brought to cosmology by the inflationary scenario. In fact, what inflation basically does is to expand to cosmological scales regions which were many order of magnitudes smaller. Smaller enough in order to have quantum fluctuations [52] which, at the end of inflation, are found to be stretched on scales which have nothing more of quantum origin, but instead constitute the seeds of the large structure of gravitational structures we can see nowadays.

As soon as inflation ends, these quantum fluctuations are translated into perturbations in the density of the plasma. Over-dense regions tend to attract gravitationally plasma and dark matter from the surroundings, thus, the density of these regions therefore tends to grow. This gravitational compression is at some point counteracted by the radiation pressure from the plasma, which grows gradually, eventually stops the compression and starts to dilute matter. The consequent dilution implies cooling down of the matter, a lower radiation pressure until gravity becomes dominant

again, and then a new phase of compression begins. This fight between gravity and pressure induces compressions and rarefactions in the plasma that propagate through the medium as waves with a specific speed (generally called “sound” because these waves of matter propagate in the medium, and not in the vacuum, like sound waves do).

As we have said, perturbations are usually described as temperature fluctuations, by translating compression into higher temperatures and rarefaction into colder ones. We define the temperature fluctuation mathematically as

$$\Theta \equiv \frac{\Delta T}{T}. \quad (1.80)$$

It is interesting to note that even without including gravity, by just considering the case of a perfect fluid consisting on photons and dark matter one can show that Θ behaves as an oscillator in Fourier space [394, 395],

$$\ddot{\Theta}(k) + c_s^2 k^2 \Theta(k) = 0, \quad (1.81)$$

where c_s stands for the speed of these sound waves and k is the wavenumber. The oscillation pattern which is produced sets a characteristic length, the so-called *sound horizon*, r_s , which represents the length traveled by the photon-baryon plasma from the beginning to the recombination epoch. Although all the main ingredients of CMB are already defined, we need to refine the model by including, in first instance, the effects of gravity into Eq. (1.81). The principal consequence of introducing gravity is that maxima and minima will increase in the oscillation. Starting from the perturbed flat FLRW metric

$$ds^2 = - (1 + 2\Psi) dt^2 + a^2 (1 + 2\Phi) (dr^2 + r^2(d\theta^2 + \sin^2 \theta d\phi^2)), \quad (1.82)$$

where we have considered $c = 1$ and we have introduced the spatial curvature perturbation Φ and the metric potential, Ψ , after some algebra, and combining the continuity and Euler equations, one arrives to [395]

$$\ddot{\Theta}(k) + c_s^2 k^2 \Theta(k) = -\frac{k^2}{3} \Psi - \ddot{\Phi}, \quad (1.83)$$

where $c_s^2 \equiv \dot{\rho}_\gamma / \dot{P}_\gamma$ and for a photon (γ) dominated regime it reads $c_s^2 = 1/3$ (at first approximation). Introducing now the contribution of baryons one gets [395]:

$$\left[(1 + R)\dot{\Theta} \right]'(k) + \frac{1}{3} k^2 \Theta(k) = -\frac{k^2}{3} (1 + R)\Psi - \left[(1 + R)\dot{\Phi} \right]', \quad (1.84)$$

where we have defined the quantity $R \equiv (\rho_b + p_b)/(\rho_\gamma + p_\gamma)$, i.e. the baryon-to-photon ratio parameter. In Eq. (1.84) the sound speed reads $c_s^2 = (\dot{\rho}_\gamma + \dot{\rho}_b)/(\dot{p}_\gamma + \dot{p}_b) = 1/(3(1 + R))$. Now, assuming the matter dominated approximation and considering $\dot{R}/R \ll \omega = k c_s$ (change in R slow when compared with the frequency of oscillation) we obtain the solution

$$[\Theta + (1 + R)\Psi] = [\Theta + (1 + R)\Psi](0) \cos(kr_s(z_*)), \quad (1.85)$$

where $r_s(z_*)$ is the sound horizon evaluated at the recombination epoch. We see here that adding baryons changes the overall amplitude of temperature oscillations as well as suppress minima while enhance maxima. Although we will not mention it here, many other effect must be considered when studying this era of the Universe [396, 397, 398, 399, 400, 401].

Let us notice that the signal we are able to notice appears as anisotropies in the temperature fluctuations of the CMB. Besides, the CMB behaves as a black body and for statistically isotropic Gaussian random temperature fluctuations one can adopt a harmonic description, here more specifically, spherical harmonics. The ensemble average of these fluctuations is given by the power spectrum -described by C_l - as [395]

$$\langle \Theta_{lm}^* \Theta_{l'm'} \rangle = \delta_{ll'} \delta_{mm'} C_l. \quad (1.86)$$

This is the variance of Θ integrated over all the Fourier modes. On the other hand, for a statistically homogeneous spatial distribution, the two point function is expressed in terms of the power spectrum

$$\langle \Theta(k)^* \Theta(k') \rangle = (2\pi)^3 \delta(k - k') P(k). \quad (1.87)$$

Combining these two relations we get [395]

$$C_l \simeq \frac{2\pi}{l(l+1)} \Delta_T^2 (l/r_s(z_*)), \quad (1.88)$$

with $\Delta_T^2 = k^3 P(k)/(2\pi)^2$. It is usual to plot instead the quantity

$$\frac{l(l+1)}{2\pi} C_l \simeq \Delta_T^2. \quad (1.89)$$

The physical processes which have been described above take place before recombination, with larger scales perturbations which will need more time to compress and expand again (if they can), while smaller scales fluctuation will be able to do the same process more times. As the Universe expands and cools, reaching a temperature

of around 3000 K, recombination epoch starts: atoms start forming (with electrons bounded to nuclei) and photons cease to be scattered and start propagating freely (but still suffering the cosmological redshift due to the expansion). At this moment all the oscillations get frozen, and the information on the temperature of the inhomogeneities will be imprinted in the energy of the photons now free to move: we will have photons caught at the maximum compression at the moment of recombination; others at the point of maximum expansion; others will have completed two or more oscillations, and so on. All these frozen oscillations are reflected today in the famous power spectrum observed by *Planck* (see Fig. 1.4) in the microwaves band, to which the radiation has been redshifted by the Universe expansion.

We must note here that if one were interested in using CMB data to study cosmological perturbations, the full power spectrum should be used. Instead, as in our case, if one focused only on the cosmological background evolution, some new quantities, the *shift parameters*, can be defined, which have been shown to be sufficient to describe a large variety of dark energy models [402], with few cautionary cases [403].

A useful concept is that of the “last scattered surface” (that, in fact, is receding from us): this is the sphere around the observer such that its radius is the distance each photon has travelled since it was last scattered. The redshift z_* corresponding to the last scattering surface allows us to define the *shift parameters*, which we have used in our analysis when we wanted to include CMB data. A fitting formula can be derived for computing this redshift is derived in [404] ,

$$z_* = 1048 \left[1 + 0.00124(\Omega_b h^2)^{-0.738} \right] \times \left(1 + g_1(\Omega_m h^2)^{g_2} \right) , \quad (1.90)$$

where the factors g_1 and g_2 are given by

$$g_1 = \frac{0.0783(\Omega_b h^2)^{-0.238}}{1 + 39.5(\Omega_b h^2)^{-0.763}} , \quad (1.91)$$

$$g_2 = \frac{0.560}{1 + 21.1(\Omega_b h^2)^{1.81}} . \quad (1.92)$$

Now one can compute the distance the light have traveled until recombination epoch,

$$r_s(z_*) = \frac{c}{H_0} \int_{z_*}^{\infty} \frac{dz'}{E(z')} = \frac{c}{H_0} \int_0^{a_*} \frac{da'}{\sqrt{3(1 + Ra')a'^4 E^2(a')}} , \quad (1.93)$$

with $R = 31500\Omega_b h^2 (T_{CMB}/2.7)^{-4}$, given that $T_{CMB} = 2.725K$ [405]. This is called the sound horizon and characterizes the scale of CMB physics: the modes corresponding to the acoustic peaks before recombination have an harmonic relation with the

length scale $k_n = n\pi/r_s(z_*)$. A mode following this relation has a spatial inhomogeneity of wavelength λ_n which appears in the sky with an angular scale $\theta \simeq \lambda_n/D_M(z_*)$ [395]. Decomposing this in harmonic space, with multipoles defined as $l = 2\pi/\theta$, we get the angular scale of the sound horizon at recombination (and first shift parameter)

$$l_a \equiv \pi \frac{D_M(z_*)}{r_s(z_*)}, \quad (1.94)$$

where $l_n = nl_a$ are the multipoles at which the peaks are. At first approximation this angular scale coincides with the position of the first peak in the temperature power spectrum. We must take into account that the baryons Ω_b shift the positions of the acoustic peak and enhance the compression peaks leaving unmodified the rarefaction ones. Thus, the ratio between the first and second peak amplitudes in CMB power spectrum is a tracer of Ω_b (actually, it is related to $\Omega_b h^2$). Among the other effects in the CMB spectrum which can be used to extract geometric data, there is one related to non-relativistic matter, Ω_m , thus including dark matter. The presence of non-relativistic matter changes the height of the lower multipole peaks compared with the higher ones as well as shifts the position of the peaks. This leads us to the second shift parameter (do not confuse with R in Eq. (1.84)),

$$R \equiv \sqrt{\Omega_m H_0^2} \frac{D_M(z_*)}{c}, \quad (1.95)$$

which describes the scaled distance to the last scattering surface.

Once we have reached this point we may have the question: what else happens between the recombination epoch and today? From that moment on, atoms begin to form and matter start clustering and evolving forming larger structures but not in a random way. We will see in the next section more details about this process.

1.5.3 Baryon Acoustic Oscillations

As we can imagine, the physics behind BAO [406] is intimately related to what we have described for the CMB. Once we understand the CMB as the “photon” part of recombination era physics, BAO can be seen as the “matter” counterpart in that same process. Summing up, as soon as recombination starts, photons are free to move, leaving their imprint in what is now detected as CMB, while the sound waves which were taking place in the plasma stopped at a specific time/radius. After that, the baryons which are left behind are no longer relativistic and start to feel gravitational interaction produced by the dark matter located at the center of the

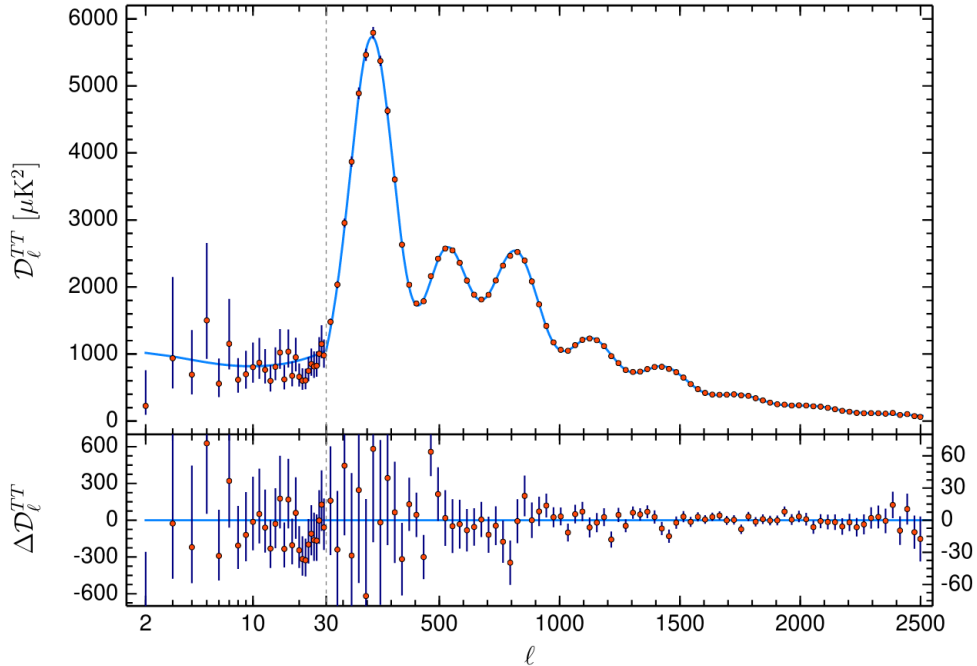


Figure 1.4: Planck 2018 temperature power spectrum. We acknowledge ESA and the Planck Collaboration for this picture. Figure extracted from [41].

over-dense regions, and center of the spherical waves propagation too. In [407] the reader can find a nicely illustrated view of the full process.

Primordial perturbations of the adiabatic form predicted by standard inflation models consist of equal fractional density contrasts in all species. Dark matter perturbations grow in place, slowly at first in the radiation dominated epoch, then faster as the Universe becomes matter dominated. The baryon-photon plasma perturbations, on the other hand, travel away from its origin as a sound wave. At recombination, the baryon part of the wave is left in a spherical shell centered on the original perturbation. Both the dark matter at the center and the baryons on the shell seed gravitational instability, which grows to form the halos in which galaxies form. We therefore expect the distribution of separations of pairs of galaxies (i.e. the two-point correlation function generated by such perturbations) to show a small enhancement at the radius of the shell, with galaxy concentrations in the central dark matter clumps and in the shells induced by the baryons. Thus, the sound horizon mentioned in the past section was also imprinted in the matter perturbations and it is hidden in the correlation function between galaxies as a preferable clustering distance. More specifically, the two-point correlation function describes the probability distribution of two galaxies depending on their separation. We have to take into account that

at the photon decoupling epoch, i.e. last scattering surface, photons stopped feeling the effects of baryons at around $r_s(z_*) = 144.43\text{Mpc}$ [41], but baryons had inertia and stopped feeling the effect of photons a bit later, at the so-called *drag epoch*. The redshift which corresponds to this epoch is well approximated by [408]

$$z_d = \frac{1291(\Omega_m h^2)^{0.251}}{1 + 0.659(\Omega_m h^2)^{0.828}} [1 + b_1(\Omega_b h^2)^{b_2}] , \quad (1.96)$$

$$\begin{aligned} b_1 &= 0.313(\Omega_m h^2)^{-0.419} [1 + 0.607(\Omega_m h^2)^{0.6748}] , \\ b_2 &= 0.238(\Omega_m h^2)^{0.223} . \end{aligned} \quad (1.97)$$

Thus, evaluating the comoving sound horizon at this epoch we find a slightly different value, i.e. $r_s(z_d) = 147.09\text{ Mpc}$ [41]. Thus, over-densities are statistically more likely to be separated by a comoving distance $r_s(z_d)$ than by a bit larger or smaller distances; due to this, a peak should then appear in the correlation function at $r_s(z_d)$, as illustrated in [409]. This converts BAO into a standard ruler, in analogy to SNeIa acting as standard candles: we do have an object (the sound horizon at dragging epoch) of known length (measured by CMB data and fully inferred by theory), imprinted in the BAO, and whose distance can be calculated from the angle it subtends.

However, in this case this ruler is hidden in the sky, because the spherical shells with higher density centered around the original perturbations are randomly superimposed. Moreover, the low proportion of baryons compared to dark matter make this density excess at the BAO scale small compared to the central over density. Nevertheless, through statistical analyses using the two-point correlation function $\xi(r)$ it is possible to detect the BAO signal with big catalogs of galaxies [409].

It has to be said that the computation of the correlation function to get the BAO scale is a challenging work that requires overcoming several difficulties (for further details, see the reviews in [406, 410]). For example, non-linearities due to the evolution of matter which keeps on clustering at smaller scales [411] and peculiar velocities of galaxies which introduce a redshift space distortion [412]. Once all the uncertainties and complications above mentioned have been taken into account, the information of the BAO scale can be extracted from the galaxy surveys, usually with the two-point correlation function, but also computing directly the power spectrum [413].

This increased difficulty for statistical analysis alongside the previous challenges, requires a proper estimator for computing the two-point correlation function [414]. Moreover, the theoretical correlation function must be expanded in spherical harmonics [415] so that the information of the BAO scale longitudinal to the line of sight and

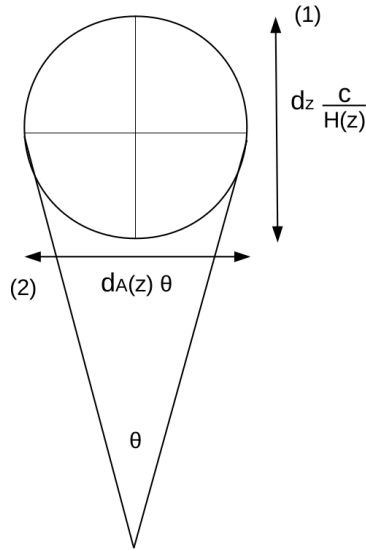


Figure 1.5: Distances measured at the line of sight (1) and at the perpendicular direction (2).

perpendicular to it can be detached (see Fig. 1.5). In this way, the observed redshift depth Δz along the line of sight gives the Hubble function when it is compared to the BAO scale r_s ,

$$H(z) = \frac{c\Delta z}{r_s} \quad (1.98)$$

while the angle $\Delta\theta$ subtended in the sky by the BAO scale perpendicular to the line of sight measures its angular diameter distance, and therefore

$$D_A(z) = \frac{r_s}{\Delta\theta(1+z)}. \quad (1.99)$$

When these two measures cannot be done separately, the spherically averaged correlation function is achieved instead, which blends together the information coming from transverse and longitudinal observations. Nevertheless, in these cases it is still possible to extract BAO information, where the baryon acoustic oscillation scale parameter $A(z)$ is best used, a quantity which does not depend on H_0 [409],

$$A(z) = 100\sqrt{\Omega_m} h^2 \frac{D_V(z)}{c z}, \quad (1.100)$$

and depends on the volume averaged distance,

$$D_V(z) = \left[(1+z)^2 D_A^2(z) \frac{c z}{H(z)} \right]^{1/3}. \quad (1.101)$$

a distance which is approximately the radius of the spherical volume filled by the BAO shell. If one wants to extract the information of the BAO scale along and perpendicular to the line of sight, an anisotropic analysis of the survey must be done so that the two-dimensional two-point correlation function is computed [416]. In this way, the measurement of the Hubble function $H(z)$ and of the angular diameter distance $D_A(z)$, separately, is possible. However, these quantities are quite correlated and are not robust enough with respect to systematics, therefore the following dimensionless quantities are recommended instead [416],

$$\frac{Hr_s(z_D)}{c} = \Delta z, \quad \frac{D_A}{r_s(z_d)} = \frac{1}{\Delta\theta(1+z)} \quad (1.102)$$

These new quantities measure the redshift depth and observed angle of the BAO feature, respectively. We have used the comoving sound horizon r_s as a standard ruler because its size could be given by CMB measurements. If this were unknown, we could still extract information through the fact that we are observing a spherical structure. In this way, the Alcock-Paczynski test can be used [417], which gives the product $D_A(z)H(z)$ from measuring $\Delta z/\Delta\theta$, and its distortion parameter has the following form

$$F = (1+z)D_A H/c \quad (1.103)$$

When there are not enough data to achieve separate analyses along and transverse to the line of sight, one simply relies on to an isotropic analysis, providing a measurement of $D_V(z)/r_s$.

The challenge of the BAO method is primarily statistical: because this is a weak signal at a large scale, one needs to map enormous volumes of the Universe to detect the BAO and obtain a precise distance measurement. Galaxy redshift surveys allow us to make these large three-dimensional maps of the Universe. At low redshift ($z \leq 0.5$), the BAO method strongly complements SNeIa measurements because BAO provides an absolute distance scale and a strong connection to the CMB acoustic peaks from $z = 1000$, while SNeIa allow more precise measurements of relative distances and thus offer a more fine-grained view of the distance-redshift relation. At higher redshift ($z \geq 0.5$), the large cosmic volume and the direct access to $H(z)$ make the BAO method an exceptionally powerful probe of dark energy and cosmic geometry.

The idea of using BAO as standard rulers to learn about cosmological parameters appears to date from 2001. The real foundations, however, of the modern ideas on BAO, their detection and use, were laid by Eisenstein, Blake and Glazebrook [418, 419] and a slew of later papers which developed where they analyze real data.

Among the relevant surveys which have measured the BAO signal, we have to mention the Sloan Digital Sky Survey (SDSS), which is a 2.5-metre wide-angle optical telescope at Apache Point Observatory in New Mexico. The goal of this five-year survey was to take images and spectra of millions of celestial objects. The result of compiling the SDSS data is a three-dimensional map of objects in the nearby Universe: the SDSS catalog. The SDSS catalog provides a picture of the distribution of matter in a large enough portion of the Universe that one can search for a BAO signal by noting whether there is a statistically significant overabundance of galaxies separated by the predicted sound horizon distance.

The SDSS team analyzed the clustering of these galaxies by calculating a two-point correlation function on the data. The BAO signal would show up as a bump in the correlation function at a comoving separation equal to the sound horizon. This signal was detected by the SDSS team in 2005 [420] throwing a value for the sound horizon of approximately 150 Mpc in today's Universe. The Two-degree-Field Galaxy Redshift Survey (2dFGRS) collaboration, previous to the SDSS collaboration, and the SDSS itself reported a detection of the BAO signal in the power spectrum at around the same time in 2005 [421]. Both teams are credited and recognized for the discovery by the community as evidenced by the 2014 Shaw Prize in Astronomy which was awarded to both groups.

The BAO imprint in the Lyman- α forest of quasars was first detected in 2013 [422]. As the light from distant quasars travels through multiple gas clouds with different redshifts, multiple absorption lines are formed (corresponding to Lyman-alpha electron transition of the neutral hydrogen atom). Patches of greater density absorb more light and the absorption lines of neutral hydrogen in the spectrum pinpoint each dense patch by how much they are redshifted. With enough good quasar spectra, close enough together, the position of the gas clouds can be mapped in three dimensions, both along the line of sight for each quasar and transversely among dense patches revealed by other quasar spectra. From these maps the BAO signal is extracted. These measurements allowed the expansion rate to be measured for the first time in the very past of the Universe, showing that at that time the expansion was still decelerating. Since then, the BAO peak in the Lyman- α forest was measured with greater accuracy and separate measurements of $H(z)$ and $D_A(z)$ were obtained.

Another completed and/or ongoing BAO survey which should be mentioned are: the WiggleZ Dark Energy Survey, a large-scale astronomical redshift survey working between 2006 and 2011 [423] and the Extended Baryon Oscillation Spectroscopic Survey (eBOSS) [424], working between 2014 and 2019, which concentrated its efforts

on the observation of galaxies and in particular quasars, in a range of distances (redshifts) currently left completely unexplored by other three-dimensional maps of large-scale structure in the Universe.

1.5.4 Hubble data

An alternative method to constrain the expansion history of the Universe is based on the study of the redshift evolution of “cosmic chronometers”, as suggested by Raul Jimenez and Abraham Loeb [425].

In [426] the authors explain a complementary approach to measure the cosmic expansion which consists on the study of the change in the age of the Universe in terms of the redshift. This method, unlike other techniques, does not depend on integrated quantities, but one needs to find a population of standard clocks in order to obtain the evolution of the relative age of the Universe. In many works [427, 428, 429] it has been shown that the most massive galaxies contain the oldest stellar populations up to $z \sim 1 - 2$. Studying the mass function of these early type galaxies (ETG) it has been found that their massive ends are almost not changing between $0 < z < 0.7$ [430].

It has been shown that the 4000 Å break which appears in the continuum spectrum of different galaxy populations is a feature linearly correlated with the age of these galaxies [426]. Then, it can serve as a good age indicator, i.e. the differential evolution of this break can be considered as a tracer for the differential evolution of the age of these galaxies. The linear relation between this feature (D4000 hereafter) and the age which has been found in the mentioned paper reads

$$D4000 = A \cdot \text{age} + B, \quad (1.104)$$

where A and B are parameters which depend on the metallicity.

On the other hand, the cosmological expansion history is given by

$$H = -\frac{1}{(1+z)} \frac{dz}{dt}. \quad (1.105)$$

Considering this two equations it is straight forward to get

$$H = -\frac{A}{1+z} \frac{dz}{dD4000}, \quad (1.106)$$

where the quantity $dz/dD4000$, or, equivalently, the D4000- z relation for the selected ETGs acts as a standard clock which allows us to measure H_0 .

The differential ages of these objects, then, can be a good indicator for the rate of change of the age of the Universe in terms of z (up to $z \sim 2$), as the majority of their stars formed at $z > 2 - 3$. The problem of this technique is that it relies on the determination of a non-observable parameter using spectra (age of stellar population) and this presents high degeneracies with other parameters as metallicity or dust content [426]. In [431] the authors follow this formalism and present constraints on the cosmological parameters based on the direct determination of $H(z)$ and the combination of CMB, BAO and SNeIa data. Using data from [431, 432, 433] they build a sample of 19 observational $H(z)$ measurements, which they use to study the constraints on the cosmological parameters.

In our work we use a compilation of Hubble parameter measurements estimated by the differential evolution of ETGs used as cosmic chronometers, in the redshift range $0 < z < 1.97$, and recently updated in [434].

1.5.5 Quasars

The word quasar stands for quasi-stellar objects (QSO). They look like stars but they are actually very different, with broad emission lines and they are believed to be galaxies that emit large amounts of X-rays, ultraviolet light and even radio waves. Quasars are believed to be caused by matter falling into a black hole at the centre of the galaxies, causing jets of matter to shoot off at high speed. They are observable up to redshift $z \sim 7$ [435] thus being among the oldest objects that we know about. In the 50's scientists detected them by radio telescopes but were unable to detect a visible object associated with them until the 60's [436, 437].

They are known to be extremely variable and, unlike supernovae, a clear connection between a spectral feature and the luminosity is not available. In short, the use of quasars as standard candles is not straight forward. The fundamental requirement needed to employ these sources for a cosmological purpose is being able to measure a “standard luminosity” from which infer the distance. A possible candidate for that is the existing relation between the luminosities in the X-rays and ultra violet bands [438, 439, 440, 441].

The data [442, 441] we use in this thesis are derived from a method based on the non-linear relation usually employed in many works on quasars [438, 439, 440, 443, 444, 445, 446]. The relation between the UV and X luminosities is given by

$$\log L_X = \beta + \gamma \log L_{UV}. \quad (1.107)$$

From here we can write

$$\log F_X = \beta' + \gamma \log F_{UV} + 2(\gamma - 1) \log D_L, \quad (1.108)$$

where $\beta' = \beta + (\gamma - 1) \log(4\pi)$, F_X and F_{UV} are the fluxes measured at fixed rest frame wavelengths and D_L is the luminosity distance. An additional assumption behind this formula is also that the $L_X - L_{UV}$ relation does not evolve or, at least, its evolution is very weak, as it seems to have been validated in [442]. Then, taking into account that the observed magnitude is given by

$$\mu = 5 \log(D_L/10pc), \quad (1.109)$$

one finds the magnitude in terms of the fluxes arriving to an expression that reads

$$\mu = \frac{5}{2(\gamma - 1)} [\log(F_X) - \gamma \log(F_{UV}) - \beta'], \quad (1.110)$$

where $\gamma = 0.6$ is the average value of the free parameter which relates both fluxes and β' is an arbitrary scaling factor.

1.5.6 Gamma Ray Bursts

When talking about distance indicators we must not forget gamma ray bursts (GRBs). They are used in a similar way to SNeIa but they are valid for measuring distances in a different redshift range, within the gap left between SNeIa and CMB.

GRBs are the most luminous electromagnetic explosions in the Universe. The strong luminosity makes them detectable as far as $z \sim 8$. Their electromagnetic curve is characterized by an initial burst of gamma rays, followed by an afterglow of X-rays, ultraviolet, optical, infrared or radio emissions [447, 448, 449, 450].

The history of the Universe from the CMB at $z \sim 1100$ to the epoch when first stars were formed, $z \sim 10$ is still poorly known and GRBs would be the perfect tool to allow us to unveil the dark Universe. GRBs provide good probes of the formation rate and environmental impact of stars in the high redshift Universe, as the metal enrichment of the intergalactic medium [451].

GRBs are usually classified into two classes: long GRBs and short GRBs. Besides, the nature of their progenitors is uncertain [452]. Some observations show that the progenitors of long GRBs are massive stars, so it is expected that long GRBs are tracers of star formation rate. The progenitors of short GRBs, instead, are mergers of either a double neutron star or a black hole and a neutron star [453]. Among these two kinds of GRBs, the longtype can be turned into “relative standard candles”, using

luminosity correlations that have been found in prompt and afterglow phases [451]. In fact, their infrared and near infrared afterglows are expected to be detectable at very high redshifts [454]. We call them relative standard candles because they are not really standard candles. There are not GRBs at $z < 0.1$ which are cosmology independent, then, GRBs have to be calibrated for each cosmological model and at the same time are used to fit data. See [455, 456] for GRBs calibration issues. However, in [457] an idea about of the distance ladder to calibrate GRBs in a completely cosmology independent way has been proposed. In the same way to the calibration of SNeIa by using Cepheid variables which are primary standard candles, one can calibrate GRBs with a sufficiently large amount of SNeIa.

Many empirical formulas with the peak energy-peak luminosity correlation have been proposed in order to calibrate GRBs. For example, in [457], the correlation between peak energy of the spectrum E and the peak luminosity L satisfy the relation [458]

$$L \propto E^2. \quad (1.111)$$

This way, the GRBs sample at low redshift can be calibrated without assuming any cosmological model, using an empirical formula for the luminosity distance estimated from the one of SNeIa in the same redshift range. Once one has calibrated GRB data, they can be used to constrain parameters of a cosmological model [459].

One important difference between GRBs and SNeIa is that gamma-ray photons suffer from no extinction when they propagate towards us, while the optical photons from supernovae will suffer extinction from the interstellar medium. Thus, GRBs contain a lot of information about high redshift properties of the Universe which cannot be derived from SNeIa. So their combined use with other cosmological probes can bring important and complementary information about the Universe.

1.6 Statistical Analysis

All the mentioned observational probes provide us with the tools to statistically infer the dynamical characteristics of our Universe. There are two main approaches to this problem: frequentist and Bayesian. The former is also known as the classical one, where the notion of probability is tied to the frequency of outcomes over a series of trials. In this approach repeatability of an experiment is the main concept, which clearly fails when dealing with cosmology. The latter, instead, considers that probability expresses a degree of belief in a proposition, based on the available knowledge of the experimenter [460]. Let us keep in mind that, when doing a measurement, we

want to determine the “true” value of a physical quantity, understanding “true” as immune to errors. However this is not possible in practice, and what we measure is the best estimate of the true value and the corresponding uncertainties. The various contributions to the overall uncertainty are classified in terms of statistical uncertainties, which arise from variations in the results of repeated observations under the same conditions, and systematic uncertainties, related to the sources of the experimental errors [461]. On the one hand, statistical uncertainties have the characteristic of vanishing when the number of observations is very large. On the other hand, systematic uncertainties are not possible to treat coherently in a frequentist scenario as there is not a justified consensus on how to consider them [462]. The only way to deal with these and related problems in a consistent way is to abandon the frequentist interpretation of probability introduced at the beginning of this century, and to recover the intuitive concept of probability as degree of belief. Besides, the Bayesian framework can be applied to any thinkable event, independently of the feasibility of making an inventory of all (equally) possible and favorable cases, or of repeating the experiment under conditions of equal probability, what makes it very appropriate for cosmology, where we just have one realisation of our Universe. For more details on this debate please refer to the previous references. Throughout our work we have adhered to the Bayesian approach, and we will just refer to it in the following definitions.

The main goal of any statistical inference approach is to find out the most likely values of the parameters of a theoretical model, given a set of data. In Bayesian Inference this is equivalent to find out the *posterior* probability function which, following Bayes’ theorem, is given by

$$p(\boldsymbol{\theta}, \mathcal{M}|\mathbf{d}) = \frac{\mathcal{L}(\mathbf{d}|\boldsymbol{\theta}, \mathcal{M})\pi(\boldsymbol{\theta}|\mathcal{M})}{\int d\boldsymbol{\theta}\mathcal{L}(\mathbf{d}|\boldsymbol{\theta}, \mathcal{M})\pi(\boldsymbol{\theta}|\mathcal{M})}, \quad (1.112)$$

where \mathbf{d} is the data, \mathcal{M} is the theoretical cosmological model taken into account and characterized by the vector of parameters $\boldsymbol{\theta}$. On the left hand side we have the posterior function which we aim to reconstruct, $p(\boldsymbol{\theta}, \mathcal{M}|\mathbf{d})$. On the right hand side, instead, we have: $\mathcal{L}(\mathbf{d}|\boldsymbol{\theta}, \mathcal{M})$, the likelihood distribution function [463], which is the probability to have the data we have collected, expressed as a function of the model parameters; $\pi(\boldsymbol{\theta}, \mathcal{M})$, the most crucial ingredient in the Bayesian analysis, the prior distribution function of the parameters under investigation, namely, the function which quantifies and qualifies any kind of *a priori* (physically sounding, in our case) probabilistic information we have about the parameters we are concerned with. The denominator, which is basically $p(\mathbf{d}|\mathcal{M})$, is known as evidence and while it appears only as a normalization factor, thus being irrelevant for what concerns fixing the best

fit parameters value, it is crucial in “model selection”, i.e. when we need to state the degree of statistical reliability of one model with respect to another.

While in the frequentist approach the best fit parameters are found by maximizing the likelihood function, in the Bayesian one what we really need to focus on is the posterior, which is an intrinsically different procedure. The two are equivalent only if the priors are flat; in that case the function π is just a normalization factor, and the posterior and the likelihood coincide.

Moreover, if one considers that the measurements are normally distributed around their real value, the likelihood function reads

$$\mathcal{L}(\mathbf{d}|\boldsymbol{\theta}, \mathcal{M}) \propto e^{-\frac{\chi^2(\boldsymbol{\theta})}{2}}, \quad (1.113)$$

where $\chi^2(\boldsymbol{\theta})$ is the so-called *chi-squared function*. In the most general case, thus, maximizing $\mathcal{L}(\mathbf{d}|\boldsymbol{\theta}, \mathcal{M})$ corresponds to minimizing $\chi^2(\boldsymbol{\theta})$, defined as

$$\chi^2(\boldsymbol{\theta}) = \Delta \mathbf{d} \cdot \mathbf{C}^{-1} \cdot \Delta \mathbf{d}^T, \quad (1.114)$$

with $\Delta \mathbf{d} \equiv \mathbf{d}^{obs} - \mathbf{d}(\boldsymbol{\theta})$, where \mathbf{d}^{obs} is the observed data vector and \mathbf{C}^{-1} the inverse of the covariant matrix, which contains the information of the experimental errors. If data points are not correlated, one can write

$$\chi^2(\boldsymbol{\theta}) = \sum_{i=1}^N \left(\frac{\Delta \mathbf{d}}{\sigma_i^{obs}} \right)^2, \quad (1.115)$$

where we have used that $\mathbf{C}_{ij} = \delta_{ij} \sigma_i^2$.

If we are working with multiple data sets, we have to minimize the total χ^2 . If the case where all the observational data mentioned before is used to perform some analysis, the quantity we have to minimize would be

$$\chi^2 = \sum_i \chi_i^2, \quad (1.116)$$

where the subindex i stands for each of the data sets considered. We will describe in the following the expression of the χ_i^2 for the different observational data we have used.

Marginalization

Sometimes one has to minimize over nuisance parameters that are not of interest for our model or that the observations cannot properly measure. For example, for SNeIa

there are parameters that take into account the light-curve shape, the stretch of the luminosity relation, etc.

The general procedure to perform a marginalization is to integrate out of the probability distribution the unwanted parameters [464, 465]. For the specific case of the magnitude of SNeIa,

$$\mu = 5 \log(d_L) + \mu_0, \quad (1.117)$$

we would have to marginalize over μ_0 , which encodes information related to the absolute magnitude and H_0 .

The calculation of the χ^2 for the magnitude -where it is included the dependence on the nuisance parameter μ_0 - is given by Eq. (1.114)

$$\chi^2 = (\mu_{theo} - \mu_{obs})^T \cdot C_{SN}^{-1} \cdot (\mu_{theo} - \mu_{obs}). \quad (1.118)$$

Now, following [465], in order to marginalize over μ_0 we have to compute the integral

$$\tilde{\chi}^2 = -2 \log \left(\int_{-\infty}^{+\infty} e^{-\chi^2/2} \Pi(\mu_0) d\mu_0 \right), \quad (1.119)$$

where $\Pi(\mu_0)$ is the prior distribution. Assuming this prior to be uniform one obtains the marginalized $\tilde{\chi}^2$

$$\tilde{\chi}^2 = a + \log \frac{e}{2\pi} - \frac{b^2}{e}, \quad (1.120)$$

where

$$a = (\mu_{theo} - \mu_{obs}) \cdot C_{SN}^{-1} \cdot (\mu_{theo} - \mu_{obs})^T, \quad (1.121)$$

$$b = (\mu_{theo} - \mu_{obs}) \cdot C_{SN}^{-1} \cdot \mathbf{1}^T, \quad (1.122)$$

$$e = \mathbf{1} \cdot C_{SN}^{-1} \cdot \mathbf{1}^T. \quad (1.123)$$

Type Ia Supernovae

We define

$$\chi_{SN}^2 = \Delta \mathcal{F}^{SN} \cdot C_{SN}^{-1} \cdot \Delta \mathcal{F}^{SN}. \quad (1.124)$$

Here $\Delta \mathcal{F} = \mathcal{F}_{theo} - \mathcal{F}_{obs}$ represents the difference between the theoretical and the observed value of the observable quantity for each SNeIa, which is the distance modulus,

$$\Delta \mathcal{F}^{SN} = \mu(z, \boldsymbol{\theta}) - \mu_{obs}(z). \quad (1.125)$$

The term C_{SN} gives the total covariance matrix and $\boldsymbol{\theta}$, as defined before, stands for the vector of parameters.

In our work we use two SNeIa compilations. The first one is the Joint-Light-curve Analysis compilation [466], made of 740 SNeIa obtained by the SDSS-II (Sloan Digital SkySurvey) and SNLS (Supernovae Legacy Survey) collaborations, covering the redshift range $0.01 < z < 1.39$. In this case we have computed the distance modulus as

$$\mu(z, \boldsymbol{\theta}) = 5 \log_{10}[D_L(z, \boldsymbol{\theta})] - \alpha X_1 + \beta C + \mathcal{M}_B, \quad (1.126)$$

where D_L is given by

$$D_L(z, \boldsymbol{\theta}) = \frac{c}{H_0} (1+z) \int_0^z \frac{dz'}{E(z', \boldsymbol{\theta})}, \quad (1.127)$$

with $E(z, \boldsymbol{\theta}) = H(z, \boldsymbol{\theta})/H_0$ - following [466], only for SNeIa analysis we assume $H_0 = 70 \text{ km/s Mpc}^{-1}$ - and c the speed of light measured here and now. In this case the vector $\boldsymbol{\theta}$ will include cosmologically-related parameters and three other fitting parameters: α and β , which characterize the stretch-luminosity and color-luminosity relationships; and the nuisance parameter \mathcal{M}_B , expressed as a step function of two more parameters, \mathcal{M}_B^1 and Δ_m :

$$\mathcal{M}_B = \begin{cases} \mathcal{M}_B^1 & \text{if } M_{\text{stellar}} < 10^{10} M_{\odot}, \\ \mathcal{M}_B^1 + \Delta_m & \text{otherwise,} \end{cases} \quad (1.128)$$

where M_{stellar} is the mass of the host galaxy. Further details are given in [466].

The second data set we have used is the Pantheon compilation [393]. This set is made of 1048 SNeIa covering the redshift range $0.01 < z < 2.26$. We compute the distance modulus as

$$\mu(z, \boldsymbol{\theta}) = 5 \log_{10}[d_L(z, \boldsymbol{\theta})] + \mu_0, \quad (1.129)$$

where d_L is the dimensionless luminosity distance given by

$$d_L(z, \boldsymbol{\theta}) = (1+z) \int_0^z \frac{dz'}{E(z', \boldsymbol{\theta})} \quad (1.130)$$

Notwithstandingly, our χ_{SN}^2 above would contain the nuisance parameter μ_0 , which in turn is a function of the Hubble constant, the speed of light c and the SNeIa absolute magnitude. This inconvenient degeneracy intrinsic to the definition of the parameters can be dealt with if we marginalize analytically over μ_0 . We refer the reader to [465] for details on this procedure.

The χ^2 estimator for this latter compilation thus reads

$$\chi_{SN}^2 = a + \log \left(\frac{d}{2\pi} \right) - \frac{b^2}{d}, \quad (1.131)$$

where $a \equiv (\Delta \mathcal{F}_{SN})^T \cdot \mathbf{C}_{SN}^{-1} \cdot \Delta \mathcal{F}_{SN}$, $b \equiv (\Delta \mathcal{F}^{SN})^T \cdot \mathbf{C}_{SN}^{-1} \cdot \mathbf{1}$ and $d \equiv \mathbf{1} \cdot \mathbf{C}_{SN}^{-1} \cdot \mathbf{1}$, with $\mathbf{1}$ being the identity matrix.

Baryon Acoustic Oscillations

The χ_{BAO}^2 estimator for Baryon Acoustic Oscillations (BAO) is defined in the following way:

$$\chi_{BAO}^2 = \Delta \mathcal{F}^{BAO} \cdot \mathbf{C}_{BAO}^{-1} \cdot \Delta \mathcal{F}^{BAO}, \quad (1.132)$$

where the quantity involved in \mathcal{F}^{BAO} actually depends on the survey which is considered.

We used data from the WiggleZ Dark Energy Survey, evaluated at redshifts $z = 0.44, 0.6, 0.73$, and given in Table 1 of [60]. In this case we identify

$$\mathcal{F}^{BAO} = \{A(z, \boldsymbol{\theta}), F(z, \boldsymbol{\theta})\}, \quad (1.133)$$

with $A(z)$ and $F(z)$ given by Eqs. (1.100)-(1.103).

We have also considered the data from the SDSS-III Baryon Oscillation Spectroscopic Survey (BOSS) DR12, described in [467]. Here, the quantities to be taken into account are D_M and $H(z)$. More concretely,

$$\mathcal{F}^{BAO} = \left\{ D_M(z, \boldsymbol{\theta}) \frac{r_s^{fid}(z_d, \boldsymbol{\theta})}{r_s(z_d, \boldsymbol{\theta})}, H(z, \boldsymbol{\theta}) \frac{r_s(z_d, \boldsymbol{\theta})}{r_s^{fid}(z_d, \boldsymbol{\theta})} \right\}, \quad (1.134)$$

where all quantities are given by Eqs. (1.15), (1.96) and where $r_s(z_d)$ is the sound horizon evaluated at the dragging redshift and $r_s^{fid}(z_d)$ is the same sound horizon but calculated for a given fiducial cosmological model used. The sound horizon is defined as:

$$r_s(z, \boldsymbol{\theta}) = \int_z^\infty \frac{c_s(z')}{H(z', \boldsymbol{\theta})} dz' \quad (1.135)$$

with the sound speed

$$c_s(z) = \frac{c}{\sqrt{3(1 + \bar{R}_b(1+z)^{-1})}}, \quad (1.136)$$

and

$$\bar{R}_b = 31500 \Omega_b h^2 (T_{CMB}/2.7)^{-4} \quad (1.137)$$

with $T_{CMB} = 2.726$ K.

We have taken into account the point $D_V(z = 1.52) = 3843 \pm 147 \frac{r_s(z_d)}{r_s^{fid}(z_d)}$ Mpc obtained by using the clustering of quasars [468]¹⁰ from the extended Baryon Oscillation Spectroscopic Survey (eBOSS), with D_V given by Eq. (1.101).

¹⁰The data is D_V in units of $\frac{r_s(z_d)}{r_s^{fid}(z_d)}$. Then, the quantity we have considered is $D_V \frac{r_s^{fid}(z_d)}{r_s(z_d)}$.

Finally, we have also added data points from Quasar-Lyman α Forest from SDSS-III BOSS DR11 [469]. Here we have

$$\mathcal{F}^{BAO} = \{d_A(z, \boldsymbol{\theta})/r_s(z_d, \boldsymbol{\theta}), H(z, \boldsymbol{\theta})/r_s(z_d, \boldsymbol{\theta})\}, \quad (1.138)$$

with d_A and $r_s(z_D)$ defined in Eqs. (1.18),(1.96) and (1.135).

Cosmic Microwave Background

The χ_{CMB}^2 estimator for the Cosmic Microwave Background (CMB) is defined as

$$\chi_{CMB}^2 = \Delta \mathcal{F}^{CMB} \cdot \mathbf{C}_{CMB}^{-1} \cdot \Delta \mathcal{F}^{CMB}, \quad (1.139)$$

where , following [470], we define

$$\mathcal{F}^{CMB} = \{l(\boldsymbol{\theta}), R(\boldsymbol{\theta}), \Omega_b h^2\}. \quad (1.140)$$

Hubble data

For these measurements one can construct a χ_H^2 estimator as follows:

$$\chi_H^2 = \sum_{i=1}^{24} \frac{(H(z_i, \boldsymbol{\theta}) - H_{obs}(z_i))^2}{\sigma_H^2(z_i)}, \quad (1.141)$$

where $\sigma_H(z_i)$ stand for the observational errors on the measured values $H_{obs}(z_i)$, and $\boldsymbol{\theta}$ is the vector of the cosmological background parameters.

Quasars

In our work we use the quasar data from [442] consisting on 808 objects covering the redshift range $0.06 < z < 6.28$. As before we compute the theoretical distance modulus using Eq. (1.129) and marginalize over the additive constant terms so that the the final χ^2 is given by Eq. (1.131) where now we have: $a \equiv (\Delta \mathcal{F}^Q)^T \cdot \mathbf{C}_Q^{-1} \cdot \Delta \mathcal{F}^Q$, $b \equiv (\Delta \mathcal{F}^Q)^T \cdot \mathbf{C}_Q^{-1} \cdot \mathbf{1}$ and $d \equiv \mathbf{1} \cdot \mathbf{C}_Q^{-1} \cdot \mathbf{1}$.

Gamma Ray Bursts

In our work we have considered the so-called Mayflower sample, consisting on 79 Gamma Ray Bursts (GRBs) covering the redshift range $1.44 < z < 8.1$ [471]. As before, we compute the theoretical distance modulus using Eq. (1.129) and marginalize over the constant additive term so that the the final χ^2 is given by Eq. (1.131) with $a \equiv (\Delta \mathcal{F}^G)^T \cdot \mathbf{C}_G^{-1} \cdot \Delta \mathcal{F}^G$, $b \equiv (\Delta \mathcal{F}^G)^T \cdot \mathbf{C}_G^{-1} \cdot \mathbf{1}$ and $d \equiv \mathbf{1} \cdot \mathbf{C}_G^{-1} \cdot \mathbf{1}$.

1.6.1 Monte Carlo Markov Chain (MCMC)

In order to find the value of the parameters which minimize the χ^2 of a specific model, the simplest and usual approach is the grid method. This process consists on constructing a grid by dividing the physical range of each parameter in fine intervals, so that the value of χ^2 will be defined by a point in the parameter space. But if one has to deal with models with a large number of parameters and data (as it happens in cosmology), the grid approach is not the most convenient both in terms of time and hardware budget. To address these multi-dimensional problems, the Monte Carlo Markov Chain (MCMC) method is more useful [472].

More concretely, the purpose of a Markov Chain Monte Carlo algorithm is to construct a sequence (or chain) of points (“samples”) in parameter space. The crucial property of the chain is that the density of samples is proportional to the posterior *pdf* thus allowing to reconstruct a map of the posterior distribution [460, 472, 473]. The Markov nature of such chains is reached when the sequence of random variables is such that the probability of the $(t + 1)$ -th element in the chain only depends on the value of the t -th element. The crucial property of Markov chains is that they can be shown to converge to a stationary state (i.e., which does not change with t) where successive elements of the chain are samples from the target distribution, in our case the posterior $p(\boldsymbol{\theta}|\mathbf{d})$.

One of the most used algorithm for the acceptance-rejection sampling is the Metropolis-Hastings [474], where we want to remark the important role of the proposal density function, $q(\boldsymbol{\theta}'|\boldsymbol{\theta})$, which is defined in order to pick the subsequent trial points and represents the conditional probability to have $\boldsymbol{\theta}'$ given $\boldsymbol{\theta}$. The steps are the following:

- We start from an initial point for the vector parameters $\boldsymbol{\theta}$;
- A new point $\boldsymbol{\theta}'$ is taken employing a proposal density function $q(\boldsymbol{\theta}'|\boldsymbol{\theta})$;
- The transition kernel $T(\boldsymbol{\theta}, \boldsymbol{\theta}')$, i.e. the conditional probability to move from one state to another, must satisfy the condition

$$p(\boldsymbol{\theta}'|\mathbf{d})T(\boldsymbol{\theta}', \boldsymbol{\theta}) = p(\boldsymbol{\theta}|\mathbf{d})T(\boldsymbol{\theta}, \boldsymbol{\theta}'). \quad (1.142)$$

In this way we guarantee that the Markov chain recovers the posterior distribution $p(\boldsymbol{\theta}|\mathbf{d})$;

- The previous condition corresponds to setting the probability to accept a point at

$$g(\boldsymbol{\theta}, \boldsymbol{\theta}') = \min \left\{ 1, \frac{p(\boldsymbol{\theta}'|\mathbf{d})q(\boldsymbol{\theta}', \boldsymbol{\theta})}{p(\boldsymbol{\theta}|\mathbf{d})q(\boldsymbol{\theta}, \boldsymbol{\theta}')} \right\}, \quad (1.143)$$

where $T(\boldsymbol{\theta}, \boldsymbol{\theta}') = g(\boldsymbol{\theta}, \boldsymbol{\theta}')q(\boldsymbol{\theta}, \boldsymbol{\theta}')$;

- To decide whether to accept the new state or not, a random number u from the range $[0, 1]$ is generated and compared with $g(\boldsymbol{\theta}, \boldsymbol{\theta}')$. Then, only if $g \geq u$ the new state will be accepted. Otherwise, it is rejected and the next step will start with the same previous step $\boldsymbol{\theta}$. In fact, if the numerator in Eq. (1.143) is bigger than the denominator, one already ensures that new state will be automatically accepted.

Burn-in period and chain convergence

When doing an MCMC chain one usually observes that there is an initial burn-in region where the chain has not arrived to the equilibrium distribution. This occurs due to the lack of information at choosing the initial $\boldsymbol{\theta}$, which make it to be far from the true value. This is why initial samples in the chain must be discarded. The length of the burn-in period can be assessed by looking at the evolution of the posterior density as a function of the number of steps in the chain. When the chain is started at a random point in parameter space, the posterior probability will typically be small and becomes larger at every step as the chain approaches the region where the fit to the data is better [460]. Thus, as we go through each step of the chain, we observe how the χ^2 stabilizes. This can be seen in Fig. (1.6).

Another issue is presented by the assessment of chain convergence, which aims at establishing when the MCMC process has gathered enough samples so that the Monte Carlo estimate is sufficiently accurate. We recommend to see [475, 476] for diagnostic tools and criteria. To avoid running multiple chains, we have followed the method developed in [477], where the spectral analysis of a single chain is performed, and some test diagnostics can be evaluated to establish convergence.

1.6.2 Model selection

Finally, in order to set up the reliability of one model with respect to others, the Bayesian Evidence is generally recognized as the most reliable statistical comparison tool even if it is not completely immune to problems, like its dependence on the choice of priors [478]. The Evidence, \mathcal{E} , is defined as the probability of the data D given

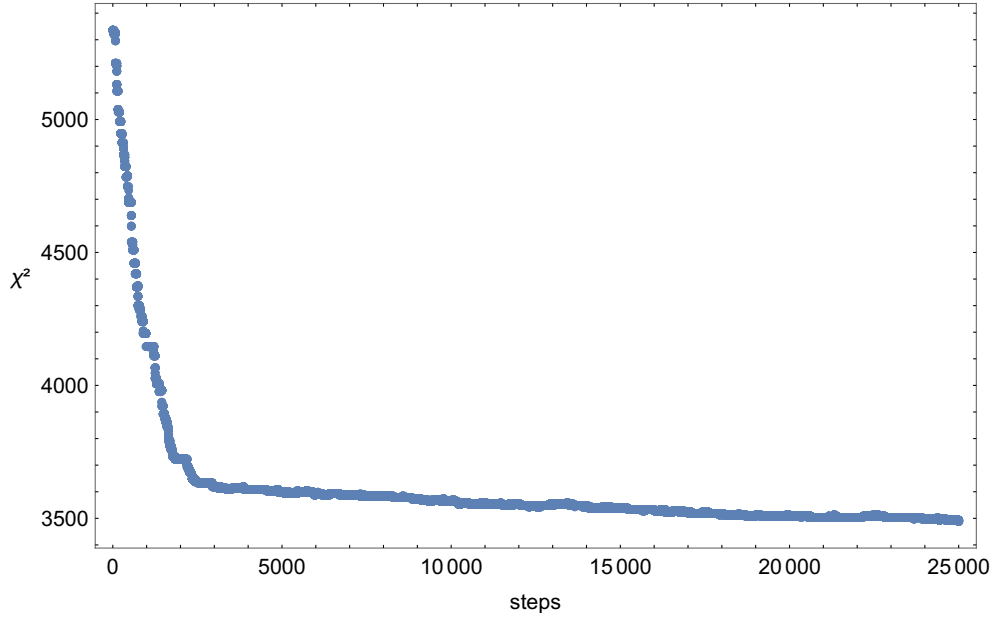


Figure 1.6: Burn-in and stabilization of the MCMC chain.

the model M with a set of parameters θ , $\mathcal{E}(M) = \int d\theta \mathcal{L}(D|\theta, M) \pi(\theta|M)$. We calculate it using the algorithm described in [479], whose main steps we will detail below. The main idea within this method is that it breaks up the prior volume into a large number of equal smaller volumes and orders them by the maximum value of the likelihood inside them. Denoting X as the fraction of total prior mass such that $dX = P(\theta|M)$ and the likelihood $P(D|\theta, M) = L(X)$, the equation for the evidence reads,

$$\mathcal{E} = \int_0^1 L dX. \quad (1.144)$$

Then, we have now a one-dimensional integral in which the integrand is positive and decreasing. If we assume that it is possible to evaluate the likelihood as $L_j = L(X_j)$, where the X_j are a sequence of decreasing values between 0 and 1, then the evidence can be computed as

$$\mathcal{E} = \sum_j \mathcal{E}_j, \text{ with } \mathcal{E} = \frac{L_j}{2}(X_{j-1} - X_{j+1}). \quad (1.145)$$

The above summation is achieved following these steps:

- We sample N points randomly from within the prior and compute their likelihoods. At the beginning we have the full prior range available, $0 \leq X_0 \leq 1$.

- We select the point with the lowest likelihood and the prior volume corresponding to this point, X_j , can be estimated probabilistically. We can compute the average volume decrease as $X_j/X_{j-1} = t$, where t is the expectation value of the largest of N random numbers from $(0, 1)$, which is $N/(N + 1)$.
- Now we increment the evidence by $\mathcal{E}_j = L_j(X_{j-1} - X_{j+1})/2$.
- We will discard the lowest likelihood point and replace it with a new point, uniformly distributed within the remaining prior volume $(0, X_j)$. The new point must satisfy the constraint on likelihood of $L > L_j$.
- Finally, we will repeat second to fourth steps until the evidence has been estimated to some desired accuracy.

This algorithm is stochastic thus, in order to take into account possible statistical variance, we have run it ~ 100 times obtaining a distribution of values from which we extract the best value of the evidence as the median of the distribution with the corresponding error.

Once the Bayesian Evidence is calculated, one can obtain the Bayes Factor, defined as the ratio of evidences of two models, M_i and M_j , $\mathcal{B}_j^i = \mathcal{E}_i/\mathcal{E}_j$. If $\mathcal{B}_j^i > 1$, model M_i is preferred over M_j , given the data. Although, even if the Bayes Factor $\mathcal{B}_j^i > 1$, one is not able yet to state how much better is model M_i with respect to model M_j . For this, we followed the widely-used Jeffreys' Scale [480]. In general, Jeffreys' Scale states that: if $\ln \mathcal{B}_j^i < 1$, the evidence in favor of model M_i is not significant; if $1 < \ln \mathcal{B}_j^i < 2.5$, the evidence is substantial; if $2.5 < \ln \mathcal{B}_j^i < 5$, is strong; if $\ln \mathcal{B}_j^i > 5$, is decisive. Negative values of $\ln \mathcal{B}_j^i$ can be easily interpreted as evidence against model M_i (or in favor of model M_j). In [478], it is shown that the Jeffreys' scale is not a fully-reliable tool for model comparison, but at the same time the statistical validity of the Bayes factor as an efficient model-comparison tool is not questioned: a Bayes factor $\mathcal{B}_j^i > 1$ unequivocally states that the model i is more likely than model j .

Chapter 2

$f(R)$ gravity

It is a very well established matter nowadays that many modified gravity models can offer a sound alternative to GR for the description of the accelerated expansion of the universe. But it is also equally well known that no clear and sharp discrimination between any alternative theory and the classical one has been found so far. In this chapter, we attempt at formulating a different approach starting from the general class of $f(R)$ theories – introduced in Sec. 1 – as test probes: we try to reformulate $f(R)$ Lagrangian terms as explicit functions of the redshift, i.e., as $f(z)$.

The most common approach when one tries to accomplish this task is to first propose an $f(R)$ expression at the level of the Lagrangian, with the requirement that it satisfies some priors (e.g. Solar System constraints), then to solve the corresponding dynamical equations, and finally to test them against the data. The main obstacle in this procedure is that the fourth order differential equations which come out from a very general $f(R)$ Lagrangian are not analytically solvable. For cosmological applications, consider that the Friedmann equations can result to be quite complicated third order differential equation in H [481], the expansion rate function which is generally needed in order to calculate cosmological distances, and we might miss an easy analytical expression for it (see [482] for an application to the famous model from [285]). In order to overcome such difficulties, thus, either one needs to fix a functional form for the $f(R)$ function so as to obtain analytically manageable equations [291], or some phenomenological ansätze for an H compatible with the given $f(R)$ have to be proposed [483]. Alternatively, one can go the other way around, that is, to recover analytically a specific $f(R)$ model from any requested standard cosmology [484] or given any $H(t)$ proposal [485, 481], or to reconstruct numerically the $f(R)$ from the data [231]. It has not to be forgotten, on the other hand, that for $f(R)$ theories a scalar-tensor equivalence holds [486], meaning that a scalar field can be introduced,

coupled to gravity (geometrically described by a standard $f(R) = R$) and following a given potential, which is completely equivalent to the given $f(R)$ model.

In all the previous cases, anyway, there are some flaws, or limitations: in one way or another, we need to make assumptions at some step, so that the results will be always somewhat biased by these choices and will not be as general as they should or as we would like; in some cases, the relation between $f(R)$ and H is generally approximate and some information might be lost (especially if advocating the scalar-tensor equivalence). One usual approach is to take into account that the $f(R)$ cosmology should mimic the Λ CDM model as much as possible given that, at the end of the day, this model gives the best description to most of the cosmological data available nowadays. Thus, the $f(R)$ cosmology should recover a matter dominated stage at high redshift, and should show accelerated expansion at low redshift, ideally, without a true cosmological constant, but through purely geometrical terms. Apart from setting some general limits based on these considerations, there really is not much more information one can provide a priori in order to yield sensible $f(R)$ theories.

Our present study is precisely related to this topic. We want to explore this problem but using a different approach, a sort of *practical poor cosmologist* approach. The vast amount of probes in cosmology provides us with a big variety of measurements usually corresponding to specific values of the redshift; thus, we think it would be interesting to have gravity models which are described in terms of this observable, so that we are provided with a more straightforward way to test the models against the observations. Studies exist in the literature where the redshift formulation appears [483], however they are not focused on constructing a sensible $f(z)$ model but rather on proposing ansätze both for the Hubble function H and for the $f(R)$ function, and then fitting the parameters in order to do a cosmographic reconstruction. Our present analysis will seek a way to provide reasonable $f(z)$ models since the beginning, i.e., from the action, so that at a later stage one can numerically solve the dynamics of the Universe, to test their validity and study their deviation with respect to the Λ CDM scenario.

We begin by introducing briefly how we build $f(R)$ as a function of the redshift z . The expression of the derivatives of $f(R)$ with respect to R , and of R with respect to time are provided in terms of derivatives with respect to the redshift z . We then consider various different dark energy and modified gravity scenarios and calculate the corresponding high and low redshift limits to validate the choice of our proposals. We will also describe the observational data used in our analysis and we will end up with a discussion of the obtained results and some conclusions.

2.1 From $f(R)$ to $f(z)$

We consider the most general $f(R)$ -type modification to the Einstein-Hilbert action described by the action [223]

$$S = \int d^4x \sqrt{-g} [f(R) + \mathcal{L}_m], \quad (2.1)$$

where g is the determinant of the metric $g_{\mu\nu}$ and \mathcal{L}_m is the Lagrangian of any considered energy-matter component. In order to obtain the field equations one has to vary the action with respect to the metric field, $g_{\mu\nu}$, ending up with

$$R_{\mu\nu} f_R - \frac{1}{2} g_{\mu\nu} f + (g_{\mu\nu} \square - \nabla_\mu \nabla_\nu) f_R = T_{\mu\nu}^m, \quad (2.2)$$

where $R_{\mu\nu}$ is the Ricci tensor, \square and ∇ are respectively the d'Alembertian and Laplacian operators, $T_{\mu\nu}^m$ is the stress energy tensor, and we define $f_R \equiv df/dR$. We assume a background Friedmann-Lemaître-Robertson-Walker (FLRW) metric in spherical coordinates

$$ds^2 = -c^2 dt^2 + a(t)^2 \left[\frac{dr^2}{1 - kr^2} + r^2 (d\theta^2 + \sin^2 \theta d\phi^2) \right], \quad (2.3)$$

with c , the speed of light in vacuum and $a(t)$, the scale factor, and we restrict our considerations to spatially flat spaces ($k = 0$), with matter and radiation as the only contribution to the stress-energy tensor. Thus we will consider $f(R)$ as a purely geometrical contribution even if, as stated before, we can always find a scalar field, entering the stress-energy tensor, and completely equivalent to the original proposed $f(R)$. Finally, we obtain the generalized Friedmann equations which govern the dynamics of the universe at large scales, namely [481]

$$\begin{aligned} H^2 &= \frac{1}{3f_R} \left(\rho_m + \rho_r + \frac{Rf_R - f}{2} - 3H\dot{R}f_{2R} \right), \\ -3H^2 - 2\dot{H} &= \frac{1}{f_R} \left[\dot{R}^2 f_{3R} + (2H\dot{R} + \ddot{R}) f_{2R} + \frac{1}{2}(f - Rf_R) \right], \end{aligned} \quad (2.4)$$

where $\cdot \equiv d/dt$ and we have defined $f_{2R} \equiv d^2 f/dR^2$, $f_{3R} \equiv d^3 f/dR^3$, together with the energy conservation equation for standard energy-matter perfect fluids:

$$\dot{\rho}_X(t) + 3H(t) \left[\rho_X(t) + 3 \frac{p_X(t)}{c^2} \right] = 0, \quad (2.5)$$

where the suffix X stands for matter, radiation or any fluid in the stress-energy tensor.

For our goals, the next step is to perform a change of variables in order to have all the derivatives appearing in Eq. (2.4) in terms of the redshift. First, we note that by combining the generalized Friedmann equations we obtain

$$R = -3(H^2)_z(1+z) + 12H^2, \quad (2.6)$$

which is the usual definition for the Ricci scalar for homogeneous and isotropic flat FLRW spacetimes. From this, we calculate

$$\begin{aligned} R_z &= 9(H^2)_z - 3(1+z)(H^2)_{2z}, \\ R_{2z} &= 6(H^2)_{2z} - 3(1+z)(H^2)_{3z}. \end{aligned} \quad (2.7)$$

where the subindex z means derivative w.r.t. the redshift. Finally, one gets:

$$\begin{aligned} f_R &= R_z^{-1} f_z, \\ f_{2R} &= (f_{2z} R_z - f_z R_{2z}) R_z^{-3}, \\ f_{3R} &= \frac{f_{3z}}{R_z^3} - \frac{f_z R_{3z} + 3f_{2z} R_{2z}}{R_z^4} + \frac{3f_z R_{2z}^2}{R_z^5}, \\ \dot{R} &= -(1+z) H R_z, \\ \ddot{R} &= (1+z) H [H R_z + (1+z)(H_z R_z + H R_{2z})]. \end{aligned} \quad (2.8)$$

Here we will provide $f(R)$ as $f(z)$, we will solve Eq. (2.4) numerically for H , and we will compare it to observational data. In terms of the redshift, the first Friedmann equation Eq. (2.4) now reads:

$$H^2 = \frac{\rho_f}{3} + \frac{R_z [(1+z)^4 \Omega_r + \Omega_m (1+z)^3]}{f_z}, \quad (2.9)$$

with

$$\rho_f = \frac{R_z}{f_z} \left[\frac{1}{2} \left(\frac{R f_z}{R_z} - f \right) + \frac{3(1+z) H^2 (R_z f_{2z} - R_{2z} f_z)}{R_z^2} \right]. \quad (2.10)$$

Clearly, here we have a third order differential equation, for which we need to set initial conditions for H , H_z and H_{2z} ; we will discuss in the next section how we choose such initial conditions.

2.1.1 Requirements for $f(z)$ proposals

Once we have the equation for H , the next step is to provide a “good” $f(z)$ model to test against data. We know that a spatially flat Λ CDM universe can be expressed as the $f(R)$ theory:

$$f_\Lambda(R) = R - 2\Lambda. \quad (2.11)$$

If we assume the universe filled with matter and radiation, then the first Friedmann equation can be cast into the following form:

$$H^2(z) = \Omega_m (1+z)^3 + \Omega_r (1+z)^4 + (1 - \Omega_m - \Omega_r), \quad (2.12)$$

where we have defined the dimensionless density parameters as

$$\Omega_i = \frac{8\pi G\rho_i}{3H_0^2}, \quad (2.13)$$

with $i = m, r$ indicating, respectively, matter and radiation, and $1 - \Omega_m - \Omega_r$ corresponding to the cosmological constant. To get f_Λ in terms of the redshift we can use Eqs. (2.6), thus obtaining

$$R(z) = 12(1 - \Omega_m - \Omega_r) + 3\Omega_m(1 + z)^3, \quad (2.14)$$

$$f_\Lambda(z) = 6(1 - \Omega_m - \Omega_r) + 3\Omega_m(1 + z)^3. \quad (2.15)$$

Here we have normalized by H_0^2 , the Hubble constant $H_0 \equiv H(z = 0)$, just to simplify notation, and we will keep this notation for the whole analysis.

Taking this into account we would like to choose an $f(z)$ which is somehow the simplest generalization of the latter expression, that is, a polynomial with more terms and not only a constant and a third-degree one. In order to set some restrictions when choosing a specific model, a useful analysis is to study the high and low redshift limit of R and $f(R)$ for the case of Λ CDM and other different models of dark energy or modified gravity theories. At the end of the day, even if Λ CDM may not be the model which really underlies our universe, it is the one which, so far, best describes it. Thus, any generalization, should have a behaviour which should follow its same trends. If we were able to detect some special feature, we could propose a reasonable $f(z)$ according to this.

Actually, Eqs. (2.14) - (2.15) exactly provide us with such information; it is straightforward and somehow trivial to verify that the high and low redshift limits of Λ CDM for both the Ricci scalar and the $f_\Lambda(R)$ function (which in this case are identical, because of GR) read

$$\lim_{z \rightarrow \infty} R(z) = \lim_{z \rightarrow \infty} f_\Lambda(z) = 3\Omega_m(1 + z)^3, \quad (2.16)$$

$$\lim_{z \rightarrow 0} R(z) = \lim_{z \rightarrow 0} f_\Lambda(z) = \text{const}. \quad (2.17)$$

Let us generalize a little bit such scenario, considering the most popular and common dark energy model used in the usual references, the CPL model,

$$w(a) = w_0 + w_a(1 - a). \quad (2.18)$$

The well-known expression for the first Friedmann equation in this case is:

$$H^2 = \Omega_m a^{-3} + \Omega_r a^{-4} + (1 - \Omega_m - \Omega_r) e^{3w_a(a-1)} a^{-3(1+w_0+w_a)}, \quad (2.19)$$

from this, we can compute the Ricci scalar:

$$R(a) = 3\Omega_m a^{-3} + 3(1 - \Omega_m - \Omega_r) [1 - 3w(a)] \exp(3w_a(a - 1)) a^{-3(1+w_0+w_a)}. \quad (2.20)$$

As we are still working in the context of General Relativity, $f_{CPL} = R$ and the CPL dark energy fluid is included in the stress-energy tensor. Let us notice that $w(a = 1) = w_0$ has to be negative today, in order to lead to the observed accelerated expansion of the universe; and we can further assume the strong prior $w_0 + w_a < 0$, as confirmed by observations [487], which implies that the universe was matter dominated at early times. Accordingly,

$$\lim_{z \rightarrow \infty} R(z) = 3\Omega_m(1 + z)^3, \quad (2.21)$$

while for the low redshift limit one finds:

$$\lim_{z \rightarrow 0} R(z) = 3(1 - \Omega_m - \Omega_r)(1 - 3w_0) + 3\Omega_m = \text{const.} \quad (2.22)$$

Setting $w_0 = -1$ we would get the limit for the Λ CDM model.

Another possibility is given by the “early dark energy” models [108, 109]. We will focus on the model discussed in [110],

$$H(a)^2 = \Omega_m a^{-3} + \Omega_r a^{-4} + (1 - \Omega_m - \Omega_r - \Omega_{ee}) + \Omega_{ee} \frac{(1 + a_c)^2}{a^6 + a_c^6}, \quad (2.23)$$

where Ω_{ee} is the fractional energy density of the early dark energy today, and $a_c = 1/(1 + z_c)$ is the critical value of the scale at which it shifts from the early-time behaviour to the late-time behaviour. Computing the Ricci scalar in terms of the redshift, one gets

$$R(z) = 12(1 - \Omega_{ee} - \Omega_m - \Omega_r) + 3\Omega_m(1 + z)^3 + \frac{6\Omega_{ee}(1 + a_c)^2}{a_c^6 + \frac{1}{(1+z)^6}} \left(2 - \frac{3}{1 + (1 + z)^6 a_c^6} \right). \quad (2.24)$$

Taking the limits one finds:

$$\begin{aligned} \lim_{z \rightarrow \infty} R(z) &= 3\Omega_m(1 + z)^3, \\ \lim_{z \rightarrow 0} R(z) &= 12(1 - \Omega_{ee} - \Omega_r) - 9\Omega_m + 6\Omega_{ee} \frac{(1 + a_c)^2}{1 + a_c^6} \left(2 - \frac{3}{1 + a_c^6} \right) \\ &= \text{const.} \end{aligned} \quad (2.25)$$

Thus, in these two cases, we qualitatively recover the same limits as Λ CDM. While this is somehow expected, because both the CPL parametrization and the early dark energy models are generalizations of the cosmological constant and contain it as a

special case, we are also interested in exploring the limits of more radically different approaches. For example, we will consider the Ricci dark energy model [148]. An interesting feature here is that Λ CDM is not explicitly included in this model. This difference, anyway, as it happens in many cases, does not necessarily translate into a difference in the quantitative description of the observational data. In this model the cosmological evolution is governed by

$$H^2 = \frac{2\Omega_m}{2-\gamma}(1+z)^3 + \Omega_r(1+z)^4 + \left(1 - \Omega_r - \frac{2\Omega_m}{2-\gamma}\right)(1+z)^{4-\frac{2}{\gamma}}, \quad (2.26)$$

from which the Ricci scalar reads

$$R(z) = \frac{6\Omega_m(1+z)^3}{2-\gamma} + 6(1+z)^4 A_\gamma(z) \left(1 - \Omega_r - \frac{2\Omega_m}{2-\gamma}\right), \quad (2.27)$$

with

$$A_\gamma(z) \equiv \frac{(1+z)^{-2/\gamma}}{\gamma}. \quad (2.28)$$

One can notice that the first term in R will dominate as far as $\gamma < 2$. And, actually, this parameter has been constrained with observational data [488] to be $\gamma = 0.325_{-0.010}^{+0.009}$, so that one can write

$$\lim_{z \rightarrow \infty} R(z) = \frac{6\Omega_m(1+z)^3}{2-\gamma}. \quad (2.29)$$

The low redshift limit exhibits, like in the previous cases, a constant behaviour:

$$\lim_{z \rightarrow 0} R(z) = \frac{6}{\gamma} \left(1 - \frac{2\Omega_m}{2-\gamma} - \Omega_r\right) + \frac{6\Omega_m}{2-\gamma} = \text{const.} \quad (2.30)$$

We also consider another well-known example of modified gravity, the Dvali-Gabadadze-Porrati (DGP) model [489], in which gravity leaks off the four dimensional Minkowski brane into the five dimensional bulk Minkowski space-time and such setting should yield a self-acceleration of the universe without introducing dark energy. The dynamics for this model is given by the modified Friedmann equation [490]

$$H(z) = \sqrt{\Omega_m(1+z)^3 + \Omega_r(1+z)^4 + \Omega_{r_c}} + \sqrt{\Omega_{r_c}}. \quad (2.31)$$

As in the previous case, the Λ CDM model is not a sub-case within this theory. Plugging Eq. (2.31) into Eq. (2.6) we get:

$$R(z) = 3\Omega_m(1+z)^3 + 12\sqrt{\Omega_{r_c}}h(z) + 24\Omega_{r_c} + \frac{3\sqrt{\Omega_{r_c}}}{h(z)}(4\Omega_{r_c} + \Omega_m(1+z)^3), \quad (2.32)$$

with

$$H(z) \equiv \Omega_{r_c} + \Omega_m(1+z)^3 + \Omega_r(1+z)^4, \quad (2.33)$$

and

$$\Omega_{r_c} = \frac{1}{4r_c^2 H_0^2}, \quad (2.34)$$

where r_c is the cross-over scale that governs the transition between four-dimensional behavior and five-dimensional behavior. One can easily see that as $z \rightarrow \infty$, the biggest contribution corresponds to

$$\lim_{z \rightarrow \infty} R(z) = 3\Omega_m(1+z)^3, \quad (2.35)$$

while for the low redshift limit we have:

$$\lim_{z \rightarrow 0} R(z) = 3\Omega_m + 12\sqrt{\Omega_{r_c}} h_\Omega + 24\Omega_{r_c} + \frac{3\sqrt{\Omega_{r_c}}}{h_\Omega} (4\Omega_{r_c} + \Omega_m) = \text{const.}, \quad (2.36)$$

with

$$h_\Omega \equiv \sqrt{\Omega_{r_c} + \Omega_m + \Omega_r}. \quad (2.37)$$

It is important to note that the four-dimensional part of the total DGP action has $f_{DGP}(R) = R$. A generalization of this model can be found in [491].

2.1.2 Final proposals

Given the previous examples and reminding that for all of them we have $f(R) = R$, we can see that in many relevant cases in the literature these hold:

$$\lim_{z \rightarrow \infty} R(z) \propto (1+z)^3, \quad (2.38)$$

$$\lim_{z \rightarrow \infty} f(z) \propto (1+z)^3, \quad (2.39)$$

$$\lim_{z \rightarrow 0} R(z) \propto \text{const.}, \quad (2.40)$$

$$\lim_{z \rightarrow 0} f(z) \propto \text{const}; \quad (2.41)$$

then, we can conclude that it is a reasonable choice to propose polynomial expressions with a maximum third-degree term as extensions of the $f_\Lambda(R)$. Anyway, one could ask what would happen with more general $f(R)$ models alternative to those described above. For example, in [292], the authors consider the model

$$f(R) = \beta R^n. \quad (2.42)$$

Following [292] it is easy to deduce that

$$R \propto (1+z)^{3/n}, \quad (2.43)$$

from which we have

$$f(R) \propto (1+z)^3. \quad (2.44)$$

This result is not in contrast with previous high redshift limits. Again, in [292], another $f(R)$ model is considered which is given by

$$f(R) = \alpha \ln R. \quad (2.45)$$

Again, we obtain

$$R \propto -\frac{1}{2(9A(1+z)^3+4)^2} \left\{ 3(9A+4) \exp^{\frac{3}{2}A[(1+z)^3-1]} \right. \\ \left. \times [9A(1+z)^3(9A(1+z)^3-10)-32] \right\}, \quad (2.46)$$

with $A = \Omega_m H_0^2 \alpha^{-1}$. In this case,

$$\lim_{z \rightarrow \infty} R(z) \propto \exp^{(1+z)^3-1}, \quad (2.47)$$

which implies that

$$\lim_{z \rightarrow \infty} f(R) \propto (1+z)^3. \quad (2.48)$$

Thus, again, we have the same high redshift limit. Note also that in both the $f(R)$ models we have just considered, the low redshift limit is not a constant, which means, they do not include a cosmological constant. Of course, we cannot check here all possible models, as this would be out of the purpose of the present analysis, and would be a gigantic, yet useless, exercise, also because even the more commonly used, as the one in [285], can not have an analytical solution for H [482].

But it is clear, that the limits we have described so far, clearly depict a possible trend which we use as guideline for our proposals. Thus, we are going to choose different models to see how much each model deviates with respect to Λ CDM. Let us notice that some of the models will contain a constant term (so they might resemble a Λ CDM model) and others will not. The latter may have more interest if we want to provide fully alternative theories to the standard model of cosmology. Finally and all in all, the models we have decided to focus on are:

1. $f_0 + f_3(1+z)^3$
2. $f_0 + f_1(1+z) + f_2(1+z)^2 + f_3(1+z)^3$
3. $f_0 + f_2(1+z)^2 + f_3(1+z)^3$
4. $f_0 + f_1(1+z) + f_3(1+z)^3$

5. $f_{12}(1+z)^{1/2} + f_3(1+z)^3$
6. $f_{12}(1+z)^{1/2} + f_1(1+z) + f_2(1+z)^2 + f_3(1+z)^3$
7. $f_{14}(1+z)^{1/4} + f_3(1+z)^3$
8. $f_{14}(1+z)^{1/4} + f_1(1+z) + f_2(1+z)^2 + f_3(1+z)^3$

2.2 Observational test

We have used the combination of various current observational data to constrain the $f(R) = f(z)$ models described previously. We have only considered the observational data related to the expansion history of the universe, i.e., those describing the distance-redshift relations. Specifically, we use the Type Ia Supernovae data from the JLA (Joint-Light-curve Analysis) compilation [492]; the cosmic microwave background distance priors from [470]; the Baryon Acoustic Oscillations data from WiggleZ Dark Energy Survey [60], the data from the SDSS-III Baryon Oscillation Spectroscopic Survey (BOSS) DR12, described in [467], data points from Quasar-Lyman α Forest from SDSS-III BOSS DR11 [469]; the expansion rate data from early-type galaxies (ETG) [434] and a gaussian prior on H_0 derived from the Hubble constant value given in [39], $H_0 = 69.6 \pm 0.7$.

The complete set of free parameters in our analysis is $\Omega_m, \Omega_b, h, f_i, \alpha, \beta, \mathcal{M}_B, \Delta_m$, where f_i are the parameters corresponding to the various polynomial degrees we have considered for each of the proposed parametrizations of $f(z)$. We will focus in our comments only on the matter density parameter Ω_m and on the f_i parameters, given that the other parameters are fully limited by imposed priors (e.g., Ω_b and h), or are independent of the cosmological background (e.g., SNeIa parameters, $\alpha, \beta, \mathcal{M}_B, \Delta_m$). In Tables 2.1 and 2.2 we report the results obtained for such parameters in terms of the corresponding confidence levels, for the two different choices of the pivot redshift we have described in the previous section, i.e., $z_{piv} = 10$ and $z_{piv} = 100$. We also show the values of the Bayesian Evidence ratios, as defined in the previous section.

2.2.1 Model 1: Λ CDM

First, let us concentrate on the results for Λ CDM. As we have shown in previous sections, for Λ CDM, not only $f(z)$ depends only on f_0 and f_3 , but we also have the further conditions $f_0 = 6(1 - \Omega_m - \Omega_r)$ and $f_3 = 3\Omega_m$. Note that we have always left

Table 2.1: Results for $z_{piv} = 10$.

model	Ω_m	f_0	$f_{1/4}$	$f_{1/2}$	$f_1 (10^{-2})$	$f_2 (10^{-2})$	f_3	\mathcal{B}_Λ^i	$\ln \mathcal{B}_\Lambda^i$
1	$0.310^{+0.015}_{-0.011}$	$4.60^{+0.63}_{-0.85}$	-	-	-	-	$0.93^{+0.05}_{-0.03}$	1	0
2	$0.314^{+0.012}_{-0.012}$	$5.06^{+1.75}_{-1.74}$	-	-	$0.5^{+1.6}_{-1.0}$	$-1.1^{+2.3}_{-1.8}$	$0.94^{+0.03}_{-0.04}$	0.95	-0.05
3	$0.314^{+0.015}_{-0.011}$	$4.04^{+0.87}_{-0.99}$	-	-	-	$0.6^{+0.4}_{-1.1}$	$0.94^{+0.04}_{-0.03}$	1.05	0.05
4	$0.313^{+0.015}_{-0.012}$	$4.43^{+0.62}_{-0.95}$	-	-	$0.02^{+0.14}_{-0.05}$	-	$0.94^{+0.04}_{-0.04}$	1.23	0.21
5	$0.312^{+0.013}_{-0.009}$	-	-	$1.00^{+0.15}_{-0.19}$	-	-	$0.94^{+0.04}_{-0.03}$	1.11	0.10
6	$0.313^{+0.012}_{-0.013}$	-	-	$0.99^{+0.17}_{-0.17}$	$0.05^{+0.04}_{-0.05}$	$0.001^{+0.002}_{-0.001}$	$0.94^{+0.04}_{-0.04}$	0.91	-0.10
7	$0.314^{+0.015}_{-0.013}$	-	$1.91^{+0.34}_{-0.39}$	-	-	-	$0.94^{+0.05}_{-0.04}$	1.07	0.06
8	$0.313^{+0.015}_{-0.012}$	-	$1.91^{+0.31}_{-0.38}$	-	$0.09^{+0.09}_{-0.07}$	$(-0.09^{+0.19}_{-0.19}) \cdot 10^{-3}$	$0.94^{+0.04}_{-0.04}$	1.06	0.06

f_0 and f_3 free in our MCMC analysis, so that it is interesting to check if the previous conditions are “automatically” verified by the Λ CDM case.

A straightforward check shows that the model (1), corresponding to Λ CDM, really satisfies Eq. (2.15): from Ω_m , we can calculate $3\Omega_m = 0.93^{+0.05}_{-0.03}$ for $z_{piv} = 10$ and $3\Omega_m = 0.89^{+0.02}_{-0.02}$ for $z_{piv} = 100$, which perfectly agrees with the corresponding free estimations of f_3 . We can also calculate $6(1 - \Omega_m - \Omega_r) = 4.14^{+0.06}_{-0.09}$ for $z_{piv} = 10$ and $6(1 - \Omega_m - \Omega_r) = 4.21^{+0.04}_{-0.04}$ for $z_{piv} = 100$, which also agree with our free estimations of f_0 , mainly because of the larger errors on this parameter than on Ω_m .

Before discussing generalizations and/or deviations from Λ CDM, let us note that the value of Ω_m does not really change from one case to another; there is a small trend toward smaller values for $z_{piv} = 100$ than for $z_{piv} = 10$, but all the values are perfectly consistent at 1σ level.

Table 2.2: Results for $z_{piv} = 100$.

model	Ω_m	f_0	$f_{1/4}$	$f_{1/2}$	$f_1 (10^{-2})$	$f_2 (10^{-2})$	f_3	\mathcal{B}_Λ^i	$\ln \mathcal{B}_\Lambda^i$
1	$0.298^{+0.006}_{-0.006}$	$4.44^{+2.37}_{-2.40}$	-	-	-	-	$0.89^{+0.02}_{-0.02}$	1	0
2	$0.313^{+0.012}_{-0.015}$	$6.00^{+2.72}_{-3.14}$	-	-	$-4.5^{+16.8}_{-30.5}$	$-2.6^{+2.0}_{-2.9}$	$0.94^{+0.04}_{-0.04}$	0.86	-0.15
3	$0.303^{+0.010}_{-0.008}$	$4.46^{+2.00}_{-2.95}$	-	-	-	$0.07^{+0.76}_{-0.84}$	$0.91^{+0.03}_{-0.02}$	1.09	0.09
4	$0.298^{+0.007}_{-0.007}$	$4.06^{+2.64}_{-3.01}$	-	-	$-0.002^{+0.002}_{-0.001}$	-	$0.89^{+0.02}_{-0.02}$	0.90	-0.10
5	$0.301^{+0.006}_{-0.006}$	-	-	$1.51^{+0.75}_{-0.69}$	-	-	$0.90^{+0.02}_{-0.02}$	1.24	0.22
6	$0.300^{+0.007}_{-0.007}$	-	-	$1.45^{+0.81}_{-0.94}$	$-3.5^{+2.9}_{-1.4}$	$-0.03^{+0.03}_{-0.01}$	$0.90^{+0.02}_{-0.02}$	1.01	0.008
7	$0.299^{+0.006}_{-0.006}$	-	$2.70^{+0.97}_{-1.07}$	-	-	-	$0.90^{+0.02}_{-0.02}$	1.12	0.11
8	$0.298^{+0.006}_{-0.006}$	-	$2.07^{+0.66}_{-0.65}$	-	$-0.007^{+0.004}_{-0.008}$	$(-0.013^{+0.008}_{-0.011}) \cdot 10^{-3}$	$0.90^{+0.02}_{-0.02}$	1.08	0.07

2.2.2 Models 2-4

Now, considering case by case, let us consider model (2), which generalizes Λ CDM by adding intermediate powers corresponding to the f_1 and f_2 parameters. Given the very good agreement of Λ CDM with cosmological background data, we expect small deviations from it, if any. Actually, we can see how f_1 and f_2 are $\mathcal{O}(10^{-2}) - (10^{-3})$ at 1σ confidence level. What is even more important, is that they are also consistent with zero, at 1σ for $z_{piv} = 10$ and maximum at 2σ for $z_{piv} = 100$. Thus, we can conclude that any $f(z)$ with this form is basically indistinguishable from Λ CDM at the present stage of observational data.

We also note that the simultaneous presence of both f_1 and f_2 seems to be tied to some degeneracy between the two parameters. In fact, for the models (3) and (4), where only one of the two parameters is present, the corresponding likelihoods are much more regular and far less noisy than in the case of model (2).

Anyway, we also stress that models (2), (3) and (4) have in common the presence of a constant term f_0 which, in some way, can bias the possible detection of any departure from Λ CDM because it can always be considered as representing a cosmological constant (on the limit $z \rightarrow 0$). Actually, note that also for models (2) (3) and (4) the same relations we have described for the Λ CDM case still hold. Eventually, a departure or agreement for them could tell us about the effective reliability and weight of the terms f_1 and f_2 . In particular, we find that the relation $3\Omega_m = f_3$ is always perfectly satisfied by all models for both the pivot redshift values we have considered. The same holds true for the condition $6(1 - \Omega_m - \Omega_r) = f_0$, except for model (2), which exhibits a value of f_0 clearly different from all the other cases, even if with larger errors.

Thus, we are not in the position to establish if the role of f_1 and f_2 is really effective and/or needed, or not: such relations should not hold in models (2) (3) and (4), because for them $f(z) \neq f_\Lambda(z)$, but we find a good agreement, so that one might be led to think we are not actually detecting any deviation from the Λ CDM model. Moreover, the new parameters f_1 and f_2 are very small so that their role is really less significant than those of f_0 and f_3 . But we cannot avoid to comment that these results strongly depend on the present observational status; in the future, more precise data could help to discriminate between one model or another.

2.2.3 Models 5-8

More interesting are, from some point of view, models from (5) to (8), which explicitly avoid the introduction of the constant term f_0 so that they are not reducible to Λ CDM in any way. On the one hand, the first point to note is that, even in these cases, the parameters f_1 and f_2 , when included, must be very small in the light of observations, ranging from $\mathcal{O}(10^{-2})$ to $\mathcal{O}(10^{-7})$. On the other, we see that the parameters corresponding to the lowest degree powers 1/2 and 1/4 are very well constrained and the likelihood profiles have a very regular Gaussian shape. Furthermore, they seem to provide an equally good fit for the data with respect to Λ CDM with the same number of theoretical parameters.

Thus, the point to be understood here is: are these low degree terms a real possible alternative to the cosmological constant, or should we consider them as a “smeared” version of the standard case only due to the low (for such type of discrimination) accuracy of the data? In fact, we have to consider that the power of the redshift we are considering might be low enough so that, due to the observational constraints we are using, they are actually mimicking the effective behaviour of a constant.

A possibly obvious trend is that the higher the degree, the smaller the value of the corresponding parameter f_i is (seen by comparing f_0 to $f_{1/4}$ and $f_{1/2}$); but this trend might be expected, given that $f_{1/2}$ and $f_{1/4}$ are by construction coupled to redshift dependent terms which could compensate the magnitude value with time dependence.

2.2.4 Bayesian Evidence

As we have mentioned before, apart from the information one can extract from the values of the parameters which best agree with the data, we have also computed the Bayes factor for each one of our proposed models against Λ CDM, the reference model. This statistical tool should provide us information about the reliability of each model. In general, we can see how $|\ln \mathcal{B}_\Lambda^i| < 1$ so that there is no statistical significant preference for one model with respect to another.

2.3 Lessons from $f(R)$ vs. $f(z)$

In this chapter we have introduced a different approach to convert general $f(R)$ theories in $f(z)$ models, which should be more easily connected to observational data and thus could shed some light on the explanation of the accelerated expansion of

the universe and provide a more straightforward formulation to perform tests against observations.

The most attractive scenario would be to be able to solve the Friedmann equations analytically to find $H(z)$ solutions by proposing some $f(z)$ or viceversa. However, as we have mentioned in the introduction, this formulation is not possible in general, neither when studying the problem in terms of the Ricci scalar nor in terms of the redshift.

Then, what we have done has been to start from some $f(z)$ ansätze and perform the analysis numerically. By studying some of the most known dark energy models we have been able to find some general potentially interesting features in order to shed some light on the expression of our proposals and restrict their arbitrariness by imposing some physically well-sounded and expected trends. In particular, we have found that a simple algebraic expression of a polynomial including just a constant and a third-degree term can describe the general behaviour whatever $f(R) = f(z)$ model is expected to have in order to mimic Λ CDM at both high and low redshift. We need to stress that this polynomial does not need to include powers higher than degree three, as we have seen by analysing different dark energy models. Even if such analysis cannot be exhaustive, we know that Λ CDM works fine with most of the data we have and we expect that, if any, deviations from it might be small.

Thus, we have selected eight proposals varying the number of free parameters in order to analyze their viability according to the data. In particular, we have included middle-degree terms in between the constant and the third-degree one, checking for their compatibility with observations and their statistical soundness. And we have also proposed models with no constant term at all, so that they cannot be reduced at a Λ CDM scenario in any way.

A general conclusion we can extract is that there are some $f(z)$ polynomial models which are competitive with Λ CDM at the background level. We were especially interested in models (5) and (7) because they explicitly do not include a Λ -like term and, in fact, we have evidence indicating that these models are as reliable as Λ CDM when it comes to analyse observational data. Even though the Bayesian Evidence does not claim any significant difference with respect to Λ CDM, we still think this is an interesting result, which could be a useful guide when formulating and studying manageable alternative models of gravity. Moreover, we want to stress and keep in mind that $f(z)$ theories will probably not be the definitive answer to explain why the universe is expanding at an accelerated rate; but that was not really our objective here. Our goal was rather to provide a different perspective on how to relate the

theoretical proposal of a modified gravity with observationally related quantities, and how to extract any kind of useful information which might contribute to the development of observationally reliable theories of gravity.

Chapter 3

$f(Q)$ gravity

As anticipated in the Sec. 1, GR is traditionally described in terms of the Levi-Civita connection, which conforms the basis of Riemannian geometry. This choice relies on the assumption of a torsion and nonmetricity free geometry. Within this framework, the Ricci curvature scalar R acts as the building block of the spacetime. Although this is usually done for historical reasons, it is important to keep in mind that the connection has a more general expression [349, 350] and GR can be described in terms of different geometries from the Riemannian one. One of the alternatives is what is called teleparallel gravity [352], where the gravitational force is driven by the torsion, T . Although this formalism was formally proposed in [352], Einstein himself already used such a framework in one of his unified field theory attempts [493]. Another possible alternative is symmetric teleparallel gravity [353], where one considers a vanishing curvature and torsion, and it is the nonmetricity, Q , that mediates the gravitational interaction. Some other interesting cases can be thought as, for example, a geometry where torsion carries part of the gravitational force and nonmetricity carries the rest. Along with the increasing interest on extended theories of gravity, all these alternative geometries have been explored due to the fact that the intrinsic implications and features of the gravitational theories could be different to the ones corresponding to Riemannian geometry [354, 355, 356, 357, 358, 359, 360].

Indeed, by making assumptions on the affine connection, one is essentially specifying a metric-affine geometry [361]. Recall that the metric tensor $g_{\mu\nu}$ can be considered as a generalization of the gravitational potential, and it is essentially used to define notions such as angles, distances and volumes, while the affine connection $\Gamma^\mu_{\alpha\beta}$ defines parallel transport and covariant derivatives. In this context, as mentioned in a previous section, general affine connection may be written as the following decomposition [349, 350]:

$$\Gamma^\lambda_{\mu\nu} = \left\{ \begin{smallmatrix} \lambda \\ \mu\nu \end{smallmatrix} \right\} + K^\lambda_{\mu\nu} + L^\lambda_{\mu\nu}, \quad (3.1)$$

where $\{\overset{\lambda}{\underset{\mu\nu}{\}}\} \equiv \frac{1}{2}g^{\lambda\beta}(\partial_\mu g_{\beta\nu} + \partial_\nu g_{\beta\mu} - \partial_\beta g_{\mu\nu})$ is the Levi-Civita connection of the metric $g_{\mu\nu}$; the term $K^\lambda_{\mu\nu} \equiv \frac{1}{2}T^\lambda_{\mu\nu} + T_{(\mu}{}^\lambda{}_{\nu)}$ is the contortion, with the torsion tensor defined as $T^\lambda_{\mu\nu} \equiv 2\Gamma^\lambda_{[\mu\nu]}$; and the disformation $L^\lambda_{\mu\nu}$ is given by

$$L^\lambda_{\mu\nu} \equiv \frac{1}{2}g^{\lambda\beta}(-Q_{\mu\beta\nu} - Q_{\nu\beta\mu} + Q_{\beta\mu\nu}), \quad (3.2)$$

which is defined in terms of the nonmetricity tensor, $Q_{\alpha\mu\nu} \equiv \nabla_\alpha g_{\mu\nu}$.

In this work we will focus on a torsion and curvature free geometry, which is exclusively defined by the nonmetricity $Q_{\alpha\mu\nu}$. As this is a novel approach, no cosmological tests have been carried out so far, and its exploration will hopefully offer some insight on the late accelerated expansion of the universe. Within the scenario of modified gravity alternatives, we will take as an initial point the idea of generalizing Q -gravity in an analogous manner to what has been done with $f(R)$ theories. We will start from the $f(Q)$ -type of theories presented in [359] and rewrite some proposals in the redshift approach [494] analyzed in the previous Sec. 2 in order to explore the cosmological background evolution within this kind of geometry.

The analysis is organized as follows. We set the stage in Sec. 3.1, by briefly outlining the general formalism of $f(Q)$ gravity. In Sec. 3.2, we reformulate the $f(R)$ Lagrangian as an explicit function of the redshift, and provide reasonable $f(z)$ models from the outset, which are to be tested at a later stage, by numerically solving the gravitational field equations, in order to test their validity and study their deviation with respect to the Λ CDM scenario. In Sec. 2.2, we discuss our results and finally conclude in Sec. 2.3.

3.1 Setting the stage: $f(Q)$ gravity

Consider the proposal of $f(Q)$ gravity given by the following action [359]:

$$S = \int \left[\frac{1}{2}f(Q) + \mathcal{L}_m \right] \sqrt{-g} d^4x, \quad (3.3)$$

where $f(Q)$ is an arbitrary function of the nonmetricity Q , g is the determinant of the metric $g_{\mu\nu}$ and \mathcal{L}_m is the matter Lagrangian density.

The nonmetricity tensor is defined as

$$Q_{\alpha\mu\nu} = \nabla_\alpha g_{\mu\nu}, \quad (3.4)$$

and its two traces as follows:

$$Q_\alpha = Q_\alpha{}^\mu{}_\mu, \quad \tilde{Q}_\alpha = Q^\mu{}_{\alpha\mu}. \quad (3.5)$$

It is also useful to introduce the superpotential

$$4P^\alpha{}_{\mu\nu} = -Q^\alpha{}_{\mu\nu} + 2Q_{(\mu}{}^\alpha{}_{\nu)} - Q^\alpha g_{\mu\nu} \quad (3.6)$$

$$-\tilde{Q}^\alpha g_{\mu\nu} - \delta_{(\mu}^\alpha Q_{\nu)}. \quad (3.7)$$

One can readily check that $Q = -Q_{\alpha\mu\nu}P^{\alpha\mu\nu}$ (with our sign conventions that are the same as in Ref. [359]).

The energy-momentum tensor is given by

$$T_{\mu\nu} = -\frac{2}{\sqrt{-g}} \frac{\delta\sqrt{-g}\mathcal{L}_m}{\delta g^{\mu\nu}}, \quad (3.8)$$

and for notational simplicity, we introduce the following definition

$$f_Q = f'(Q). \quad (3.9)$$

Varying the action (3.3) with respect to the metric, one obtains the gravitational field equation given by

$$\frac{2}{\sqrt{-g}} \nabla_\alpha (\sqrt{-g} f_Q P^\alpha{}_{\mu\nu}) + \frac{1}{2} g_{\mu\nu} f \quad (3.10)$$

$$+ f_Q (P_{\mu\alpha\beta} Q_\nu{}^{\alpha\beta} - 2Q_{\alpha\beta\mu} P^{\alpha\beta}{}_\nu) = -T_{\mu\nu}, \quad (3.11)$$

and varying (3.3) with respect to the connection, one obtains

$$\nabla_\mu \nabla_\nu (\sqrt{-g} f_Q P^{\mu\nu}{}_\alpha) = 0. \quad (3.12)$$

With the formalism of $f(Q)$ gravity specified, we will next consider cosmological applications, by reformulating the $f(Q)$ Lagrangian as an explicit function of the redshift, namely, as $f(z)$. We will provide reasonable $f(z)$ models from the outset, i.e. at the level of the action, so that at a later stage one can numerically solve the dynamics of the universe, to test their validity and study their deviation with respect to the Λ CDM scenario.

3.2 The $f(z)$ approach

3.2.1 Cosmology

Considering a FLRW universe represented by the following isotropic, homogeneous and spatially flat line element

$$ds^2 = -dt^2 + a^2(t)\delta_{ij}dx^i dx^j, \quad (3.13)$$

and taking into account the energy-momentum tensor of a perfect fluid, given by $T_{\mu\nu} = (\rho + p) u_\mu u_\nu + p g_{\mu\nu}$, where ρ and p are the thermodynamic energy density and isotropic pressure, we obtain the Friedmann and Raychadhuri equations, given by [495]

$$3H^2 = \frac{1}{2f_Q} \left(-\rho + \frac{f}{2} \right), \quad (3.14)$$

$$\dot{H} + 3H^2 + \frac{\dot{f}_Q}{f_Q} H = \frac{1}{2f_Q} \left(p + \frac{f}{2} \right), \quad (3.15)$$

respectively, where the overdot is defined as $\cdot \equiv d/dt$. In addition to this, consider the energy conservation equation for standard energy-matter perfect fluids:

$$\dot{\rho}_i + 3H(\rho_i + 3p_i) = 0, \quad (3.16)$$

where the suffix i stands for matter, radiation or any other fluid in the stress-energy tensor.

As our goal is to propose $f(z)$ models and find the evolution of the background we will manipulate Eq. (3.14) and write it in terms of the redshift. We perform thus a change of variable taking into account that in a FLRW geometry, $Q = 6H^2$ holds and then $f_Q = f_z/6H_z^2$ getting

$$H^2 = \frac{(H^2)_z}{f_z} \left(-\rho + \frac{f}{2} \right). \quad (3.17)$$

where the subindex z denotes the derivative with respect to the redshift.

Here we will follow an analogous approach to the one outlined in the previous section and published in [494]: we will reformulate an $f(Q)$ model as an explicit function of redshift, $f(z)$, solve Eq. (3.17) numerically, and then we will apply the obtained $H(z)$ to observational data.

3.2.2 Specific $f(z)$ proposals

In order to select some $f(z)$ models that could be interesting to study we first take a look at an $f(Q)$ model that mimics a Λ CDM background expansion, which is $f_\Lambda(Q) = -Q$. This can be clearly seen by replacing this expression in Eq. (3.17). Assuming a universe filled with matter, radiation and a cosmological constant, the Friedmann equation reads

$$H^2(z) = \Omega_m(1+z)^3 + \Omega_r(1+z)^4 + (1 - \Omega_m - \Omega_r), \quad (3.18)$$

where $\Omega_i = 8\pi\rho_i/(3H_0^2)$ is the dimensionless density parameter, and $i = m, r$ refers to matter and radiation, respectively.

Then, $f_\Lambda(Q)$ in terms of z gives

$$f_\Lambda(z) = -6(1 - \Omega_m - \Omega_r) - 6\Omega_m(1+z)^3 - 6\Omega_r(1+z)^4. \quad (3.19)$$

Here we can notice that a Λ CDM background in the redshift formalism would be described by a constant term, a third degree term and a fourth degree one. Now, we would like to choose $f(z)$ models which are somehow generalizations of Eq. (3.19). To do that we have found useful to make use of the tendencies we observe in f_Λ . Even if Λ CDM is not the definitive model to explain the late-time expansion of the universe, it does describe this late phase quite satisfactorily. Then, it is reasonable to propose models which satisfy the trends it shows at low and high redshift, that is,

$$\lim_{z \rightarrow 0} f(Q(z)) \propto \text{const}, \quad (3.20)$$

$$\lim_{z \rightarrow \infty} f(Q(z)) \propto (1+z)^4. \quad (3.21)$$

In fact, due to the relation between Q and H this will be satisfied at least for all the dark energy models studied in [494].

3.2.3 Models considered

As in [494], we will propose simple but well-motivated polynomial generalizations of the most fundamental model $f_\Lambda(z)$. As the high and low redshift limits lie within a constant term and a fourth degree polynomial, we have constructed our proposals by adding some terms consisting on powers of $(1+z)$ which are within these two limits. Moreover, we have selected small powers as this allows us to introduce small modifications that may induce changes in the background evolution but preserving the desired behaviour.

In the following analysis, we consider the following models:

1. $f_0 + f_3(1+z)^3 + f_4(1+z)^4$,
2. $f_{12}(1+z)^{1/2} + f_3(1+z)^3 + f_4(1+z)^4$,
3. $f_{12}(1+z)^{1/2} + f_1(1+z) + f_2(1+z)^2 + f_3(1+z)^3 + f_4(1+z)^4$,
4. $f_{14}(1+z)^{1/4} + f_3(1+z)^3 + f_4(1+z)^4$,
5. $f_{14} + f_1(1+z) + f_2(1+z)^2 + f_3(1+z)^3 + f_4(1+z)^4$,

$$6. f_{16}(1+z)^{1/6} + f_3(1+z)^3 + f_4(1+z)^4,$$

$$7. f_{16}(1+z)^{1/6} + f_1(1+z) + f_2(1+z)^2 + f_3(1+z)^3 + f_4(1+z)^4,$$

where the factors f_i are free parameters corresponding to each model.

3.3 Results of the observational tests

In order to test our models, we use the expansion rate data from early-type galaxies, Type Ia Supernovae, Quasars, Gamma Ray Bursts, Baryon Acoustic Oscillations data and Cosmic Microwave Background distance priors. After implementing the MCMC code, we have obtained the values for the background parameters that appear in Table 3.1. There are some general results that can be summarized before analyzing in detail model by model. It can be noticed that the parameters Ω_m and Ω_b do not present a relevant variation from one model to another, being in perfect agreement with *Planck*'s predictions [41] in every case. Some more interesting feature can be observed in the value of the Hubble constant, defined as $H_0 = 100 h$. With respect to the existing tension between the value obtained by local measurements [84] and the one predicted by *Planck*, our result for H_0 are perfectly consistent with the *Planck* value.

3.3.1 Model 1: Λ CDM

The first model we have considered consists on a constant term plus a third and a fourth degree term. These are exactly the terms which correspond to a $f(z)$ theory mimicking a Λ CDM background in the Q -formalism, i.e., Eq. (3.19). According to this equation, one may expect that the values of f_0 , f_3 and f_4 are somehow related with Ω_m and Ω_r (an analog computation was done in [494]). In fact, we could identity the quantities

$$f_0 = -6(1 - \Omega_m - \Omega_r), \quad (3.22)$$

$$f_3 = -6\Omega_m, \quad (3.23)$$

$$f_4 = -6\Omega_r. \quad (3.24)$$

If we substitute here the values of Ω_m , Ω_r for Λ CDM according to Table 3.1 we obtain the following numerical values for Eqs. (3.22)-(3.24):

$$f_0 = -4.1, \quad f_3 = -1.88, \quad f_4 = -0.00053. \quad (3.25)$$

Comparing with the values of f_0 , f_3 , f_4 in the table for this model, we see that for the parameters f_3 and f_4 there is an agreement at 1σ level. Nevertheless, we can also see that the parameter f_0 agrees in the order of magnitude but presents a discrepancy with respect to the one in the table.

Table 3.1: Results

model	Ω_m	Ω_b	h	f_0	f_{16}	f_{14}	f_{12}	f_1	f_2	f_3	f_4	\mathcal{B}_Λ^i	$\ln \mathcal{B}_\Lambda^i$
1	$0.313^{+0.007}_{-0.007}$	$0.046^{+0.002}_{-0.002}$	$0.69^{+0.02}_{-0.02}$	$-9.6^{+0.7}_{-0.8}$	-	-	-	-	-	$-1.95^{+0.04}_{-0.04}$	$-0.00046^{+0.00004}_{-0.00004}$	1	0
3	$0.317^{+0.006}_{-0.007}$	$0.047^{+0.003}_{-0.002}$	$0.69^{+0.02}_{-0.02}$	-	-	-	$-22.1^{+1.7}_{-2.2}$	$8.2^{+2.2}_{-3.3}$	$-0.5^{+0.3}_{-0.5}$	$-2.06^{+0.09}_{-0.10}$	$-0.00039^{+0.00004}_{-0.00005}$	0.394	-0.931
4	$0.317^{+0.007}_{-0.007}$	$0.047^{+0.002}_{-0.002}$	$0.69^{+0.02}_{-0.02}$	-	-	$-14.3^{+1.3}_{-1.4}$	-	-	-	$-2.06^{+0.05}_{-0.04}$	$-0.00040^{+0.00004}_{-0.00004}$	0.712	-0.339
5	$0.315^{+0.007}_{-0.006}$	$0.047^{+0.003}_{-0.003}$	$0.69^{+0.02}_{-0.02}$	-	-	$-13.0^{+1.6}_{-2.1}$	-	$2.2^{+0.9}_{-1.0}$	$-0.28^{0.46}_{-0.27}$	$-1.99^{+0.06}_{-0.05}$	$-0.00045^{+0.00005}_{-0.00004}$	0.791	-0.234
6	$0.314^{+0.009}_{-0.008}$	$0.046^{+0.003}_{-0.002}$	$0.69^{+0.02}_{-0.02}$	-	$-12.5^{+1.2}_{-1.4}$	-	-	-	-	$-2.06^{+0.05}_{-0.04}$	$-0.00042^{+0.00004}_{-0.00004}$	0.917	-0.087
7	$0.315^{+0.008}_{-0.007}$	$0.047^{+0.003}_{-0.002}$	$0.69^{+0.02}_{-0.02}$	-	$-12.2^{+1.2}_{-1.0}$	-	-	$0.05^{+0.14}_{-0.07}$	$0.004^{+0.037}_{-0.053}$	$-2.01^{+0.04}_{-0.04}$	$-0.00042^{+0.00003}_{-0.00004}$	1.011	0.011

3.3.2 Models 2-3

These two models do not include a constant term which could play the role of an effective cosmological constant. Instead, they are characterized by including a $1/2$ power in the polynomial; and model 3 also presents a term of degree one and a second degree term, corresponding to the parameters f_1 and f_2 . It must be noticed that model 2 does not appear in the table as it does not reach a χ^2 which stabilizes and, moreover, it is higher than all other cases, which means it is clearly discarded by data. For model 3 it is not possible to make a concrete interpretation of the values of f_1 and f_2 , because the corresponding histograms are highly irregular and far from being Gaussian, so that the error bars are just an approximate and indicative estimation of their parameter space width. However, there is one interesting manner we can extract information from these two quantities: when looking at the parameters f_3 and f_4 , we see their values are not very far (and statistically consistent) with those from model 1. Thus, we can infer that the role played by f_1 and f_2 is marginal. Moreover, the Bayes Factor of model 3 is the highest in the sample; which means that it is the most disfavoured by data.

3.3.3 Models 4-7

As well as models 2 and 3, models 4-7 do not include a constant term, but they perform much better. Model 4 consists on a $1/4$ polynomial term plus a third and a fourth degree term. Model 5 includes the same free parameters plus the f_1 and f_2 terms. The value of f_{14} does not vary significantly between these two models, presenting an agreement at 1σ level. On the one hand, it is interesting to notice

that the parameter f_1 is consistent with zero at approximately 2σ , while f_2 contains zero at 1σ . Thinking about results for model 3, these results could confirm that the presence of any effect of such order on cosmological scales can be quite confidently discarded. Finally, for f_3 and f_4 , the obtained values are quite in concordance with those of model 1.

Model 6 and 7 have been constructed in a similar way. Model 6 is described by a $1/6$ polynomial term plus the usual third and fourth degree ones, while model 7 contains, in addition, f_1 and f_2 parameters. Again, the quantity corresponding to the smallest power, f_{16} in this case, does not vary a lot between model 6 and 7. Moreover, in this case we have found more significant results for f_1 and f_2 , as they are both consistent with zero at 1σ level. Again, f_3 and f_4 seem not to depend much on the model, having similar values in every model. Thus, we can infer from these results that cosmological data shows a statistical preference for small-degree terms, i.e. for a lower-degree dependence of the additional terms with redshift. In other words, even in the $f(Q)$ approach, data seem to confirm that any alternative solution must behave closely as a cosmological constant, at least for what concerns the cosmological background.

With respect to the reliability of the models in comparison with the Λ CDM model, the differences in the Bayes factor and Jeffrey's scale are so small that we cannot extract much information from them. Although one cannot set decisive conclusions about the preference of one model with respect to the standard Λ CDM, this new formalism seems to be a viable alternative within the study of the late-time expansion of the universe.

3.4 Lessons from $f(Q)$ vs. $f(z)$

Within the context of modified gravity we have chosen a novel geometrical scenario based on the nonmetricity, Q , to obtain observational constraints for the background quantities of the late-time universe. We have selected the $f(Q)$ type of theories and followed the $f(z)$ approach to give some phenomenologically motivated models to test against observational data. We have used a wide variety of observational data sets to check the validity of our proposals. As an interesting result we have seen that degree one and second degree terms, i.e., f_1 and f_2 , are, in general, compatible with zero. Moreover, the values we obtain for the rest of parameters are very similar for a model with and without these two parameters, not showing a significant dependence

on their presence. This result coincides with the one obtained in the Sec. 2, whose approach we are following.

We have also found that some of the modified parameters that we introduce, f_3 and f_4 more specifically, could be related in some way with the background parameters Ω_m and Ω_r . Finally, an interesting result we want to remark is that the value obtained for the Hubble parameter, H_0 , lies close to the *Planck* estimation.

From the statistical point of view we cannot have a clear interpretation from the Bayes factor and Jeffrey's scale. In general, we obtain values that are not conclusive so we cannot extract information about the preferability of our polynomial models with respect to the Λ CDM. Nevertheless, the consistency of the value of the background parameters can be considered as a hint pointing to continue the study of alternative theories of gravity within this kind of approach. This analysis can be understood as a first step in the observational study of a new class of modified gravity theories which lay in a geometry described by the nonmetricity. By going deeper in the cosmological and observational studies of these yet unexplored theories we may find interesting information which may contribute to our understanding of the evolution of the late-time universe.

Chapter 4

Non-minimal $f(R)$ gravity

One of the most straightforward approaches to modify GR is within the framework of $f(R)$ metric gravity, explained in detail in Sec. 1. If we also consider a coupling between the gravitational and the matter sector, we arrive to what are known as $f(R)$ non-minimally coupled theories, introduced in Sec. 1.

In our work, we further analyse $f(R)$ non-minimally coupled theories as a mean to successfully describe the late-time acceleration of the universe. We firstly construct two setups within the framework of [335] which mimic a Λ CDM universe. The action describing this theory is described by two functions, $f_1(R)$ and $f_2(R)$, the first one would take the role of a typical $f(R)$ metric theory and the second one is non-minimally coupled to matter through a small coupling constant, λ .

In the first setup that we consider, we fix $f_2(R) = R$ and compute $f_1(R)$ analytically, in the second one, we fix $f_1(R) = R - 2\kappa^2\Lambda$ and find an analytical solution for $f_2(R)$. Besides, we analyse each setup for two different energy-density contents in the universe, ρ , so that we obtain different physical solutions analytically for each one. Secondly, in order to get an order of magnitude of the parameters of the model for the two setups considered, we perform a cosmographic study and we map it to the current observational values fitting Λ CDM. Moreover, we analyse in detail the physical meaning of the coupling parameter, λ , which, as we will see later, can be interpreted as a parameter intimately related to the late speed up of the universe.

We begin reviewing $f(R)$ non-minimally coupled theories, providing some more details about them; then we calculate the analytical solutions for our theory in the two selected setups; in a subsequent section we perform a cosmographic analysis including a study of the effects of the coupling constant on the value of the cosmographic quantities and as a final point, we sum up the obtained results.

4.1 Non-minimally coupled $f(R)$

We consider a model which includes a non-minimal coupling between geometry and matter. The action is the one described in the introduction, i.e.

$$S = \int \left[\frac{f_1(R)}{2\kappa^2} + (1 + \lambda f_2(R))\mathcal{L} \right] \sqrt{-g} d^4x. \quad (4.1)$$

4.1.1 Field equations

From the variation of the action 4.1 with respect to the metric one gets the modified Einstein's equations [335]:

$$F_1 R_{\mu\nu} - \frac{1}{2} f_1 g_{\mu\nu} - (\nabla_\mu \nabla_\nu - g_{\mu\nu} \square) F_1 = 2\lambda\kappa^2 (\nabla_\mu \nabla_\nu - g_{\mu\nu} \square) \mathcal{L} F_2 + (1 + \lambda f_2) \kappa^2 T_{\mu\nu} - 2\lambda\kappa^2 F_2 \mathcal{L} R_{\mu\nu}, \quad (4.2)$$

where $F_i(R) \equiv \frac{df_i(R)}{dR}$ ($i = 1, 2$), $\square = g^{\mu\nu} \nabla_\mu \nabla_\nu$, $T^{\mu\nu}$ is the energy momentum tensor and $R_{\mu\nu}$ is the Ricci tensor. Taking the covariant derivative of Eq. (4.2) one can deduce the following modified conservation equation for the energy momentum tensor [335]:

$$\nabla^\mu T_{\mu\nu} = \frac{\lambda F_2}{1 + \lambda f_2} [g_{\mu\nu} \mathcal{L} - T_{\mu\nu}] \nabla^\mu R. \quad (4.3)$$

4.1.2 Dynamics of a homogeneous and isotropic Universe

Now, considering a perfect fluid in a flat FLRW scenario

$$ds^2 = -dt^2 + a(t)^2 [dr^2 + r^2(d\theta^2 + \sin^2 \theta d\phi^2)], \quad (4.4)$$

one can compute the ‘‘conservation’’ or ‘‘no conservation’’ equation of the energy momentum tensor [342] by taking the $\mu = 0$ component of Eq. (4.3)

$$\dot{\rho} + 3H(p + \rho) = \frac{\lambda F_2}{1 + \lambda f_2} [-\mathcal{L} - \rho] \dot{R}, \quad (4.5)$$

where $\cdot \equiv d/dt$, ρ is the matter density, p is the pressure and $H = \dot{a}/a$. From here, we note that if $\mathcal{L} = -\rho$, $\dot{\rho}$ is conserved. We will assume this is the case from now on.

As we are interested in computing the dynamics of our model, we take the 00 component of Eq. (4.2) in order to obtain the Friedmann equation [342]

$$3H^2 = \tilde{\kappa}^2 (\rho + \rho_{f_1} + \rho_{f_2}), \quad (4.6)$$

where

$$\tilde{\kappa}^2 \equiv \frac{\kappa^2(1 + \lambda f_2)}{F_1 + 2\lambda\kappa^2\mathcal{L}F_2}, \quad (4.7)$$

$$\rho_{f_1} \equiv \frac{-6H\partial_t F_1 + F_1 R - f_1}{2\kappa^2(1 + \lambda f_2)}, \quad (4.8)$$

$$\rho_{f_2} \equiv \frac{-6H\lambda\partial_t(\mathcal{L}F_2) + \lambda\mathcal{L}F_2 R}{1 + \lambda f_2}. \quad (4.9)$$

The theory reduces to GR for $f_1 = R - 2\Lambda\kappa^2$ and a vanishing f_2 , while for a vanishing f_2 we recover the standard metric $f(R)$ theory. Here we have a second order differential equation on f_1 and f_2 . We want to solve this equation analytically, if possible. Our procedure will consist on fixing a simple f_1 (f_2) and solving for f_2 (f_1).

4.2 Λ CDM geometry within non-minimally coupled $f(R)$ gravity

We are interested in solving Eq. (4.6) analytically. In order to do this we consider reasonable to assume a Λ CDM expansion, as in [496], i.e.

$$H^2 = \frac{\kappa^2}{3} \left(\frac{\rho_0}{a^3} + \Lambda \right). \quad (4.10)$$

Therefore, the scalar curvature reads

$$R = \kappa^2 \left(\frac{\rho_0}{a^3} + 4\Lambda \right). \quad (4.11)$$

Consequently,

$$a = \left(\frac{\rho_0}{R/\kappa^2 - 4\Lambda} \right)^{1/3}, \quad (4.12)$$

and

$$3H^2 = R - 3\kappa^2\Lambda. \quad (4.13)$$

As we have two undetermined functions the way we are going to proceed is to specify one of them and solve for the other one. We are going to study the two simplest cases which seem interesting to us:

- Set $f_2 = R$ and find f_1 .
- Set $f_1 = R - 2\Lambda\kappa^2$ and find f_2 .

We also take $\mathcal{L} = -\rho$, so the energy-momentum tensor is conserved in Eq. (4.3), as already stated above. In the present study, we will study two different cases of fluids: dust and a perfect fluid.

4.2.1 An arbitrary f_1 with $f_2 = R$

Inserting Eqs. (4.11) - (4.13) in Eq. (4.6) and letting f_1 as an undetermined function of R and $f_2 = R$ one obtains

$$a_2(R)f_1'' + a_1(R)f_1' + a_0f_1 = \frac{\kappa^2}{3}(\rho + \rho_\lambda), \quad (4.14)$$

where the prime stands for the derivative with respect to R and

$$a_2(R) \equiv -(R - 3\kappa^2\Lambda)(R - 4\kappa^2\Lambda), \quad (4.15)$$

$$a_1(R) \equiv \left(\frac{R}{6} - \kappa^2\Lambda\right), \quad (4.16)$$

$$a_0 \equiv \frac{1}{6}, \quad (4.17)$$

$$\rho_\lambda \equiv 2\lambda(R - 3\kappa^2\Lambda) \left(3\frac{d\rho}{dR}(R - 4\kappa^2\Lambda) + \rho\right). \quad (4.18)$$

The first step is to find the homogeneous solution. We can see that the homogeneous part fo Eq.(4.14) is an hypergeometric differential equation and, in fact, it coincides with the differential equation obtained in minimal $f(R)$ gravity, which has been already computed in the literature. In [496] it was wrongly stated that there cannot be any real valued function of Ricci scalar that can mimic a Λ CDM expansion for a vacuum universe but one can take a look at [497], where an exhaustive analysis of the solutions is performed. Just notice that these solutions are given in terms of hypergeometric functions, so the convergence and integral representation of these functions in the physically possible regions must be adecuately studied. In our case we are interested in the late-universe Cosmology, and the solution can be written as [498]

$$f_1 = c_0 \left(\frac{\Lambda}{R - 4\Lambda}\right)^{p_+ - 1} {}_2F_1\left(q_+, p_+ - 1; r_+; -\frac{-\Lambda}{R - 4\Lambda}\right), \quad (4.19)$$

where c_0 , p_+ , q_+ and r_+ are real constants and $c_0 \equiv -\bar{\omega}_1$, according to the notation in [497]. The fact of having just one independent solution with the integration constant c_0 is due to the divergence that appears in the other linearly independent solution when $R \rightarrow \infty$. To avoid this we set to zero the other integration constant. See [497] for more details. As we can notice, the terms including ρ are found exclusively on the right hand side of the differential equation 4.14, so the homogeneous solution is the same regardless of the content but the particular solution will change. We have calculated the particular solution for the two different cases stated above: dust and perfect fluid.

4.2.1.1 Dust: $\rho = \rho_m$

The first scenario we consider is a universe which contains just dust. In this case the matter density can be written as

$$\rho = \frac{R}{k^2} - 4\Lambda. \quad (4.20)$$

Inserting this into Eq. (4.14) one gets

$$a_2(R)f_1'' + a_1(R)f_1' + a_0f_1 = \frac{4}{3}\lambda a_2(R) + \frac{1}{3}(R - 4\kappa^2\Lambda). \quad (4.21)$$

One can compute a particular solution proposing a second order polynomial on R . Then one finds

$$f_1 = 2\Lambda\kappa^2(4\kappa^2\Lambda\lambda - 1) + (1 - 4\kappa^2\Lambda)R + \frac{8}{9}\lambda R^2. \quad (4.22)$$

If $\lambda = 0$, we recover GR: $f_1 = R - 2\Lambda\kappa^2$. We see that by considering a vanishing cosmological constant Λ and a constant coupling the matter and the curvature term induces in this case a particular solution f_1 which is similar to Starobinsky inflationary model [499], even though this latter scenario refers to the early universe. In this particular case λ is proportional to the square of the scalaron mass.

4.2.1.2 Perfect fluid with constant EoS parameter: $\rho = \rho_w$

Now we consider that the geometry still corresponds to a Λ CDM universe but filled with a perfect fluid with constant equation of state (EoS) parameter w ; i.e. its energy density reads:

$$\rho = \frac{\rho_0}{a^{3(1+w)}}. \quad (4.23)$$

Therefore, by recalling Eq. (4.12), we obtain

$$\rho = \rho_0 \left(\frac{\frac{\rho_0}{R}}{\frac{R}{\kappa^2} - 4\Lambda} \right)^{-(1+w)}. \quad (4.24)$$

Then, the Friedmann equation reads

$$a_2(R)f_1'' + a_1(R)f_1' + a_0f_1 = -\frac{1}{3}\rho_0^{-w}a_2(R)(R/\kappa^2 - 4\Lambda)^w \times \left(\frac{1}{R - 3\kappa^2\Lambda} + 2\lambda - 6(1+w)\lambda \right). \quad (4.25)$$

If $w = 0$, we recover Eq. (4.21). We have not been able to find a particular solution for a general w so we will consider $w = -1/3$. This case is interesting as it lies at the

boundary of the set of matter fields that obey the strong energy condition. In GR such fluids give rise to a Milne Universe [500] which is a coasting universe, and the Ricci scalar is proportional to the square of the Hubble parameter. For this specific EoS one gets

$$f_1 = a (R/\kappa^2 - 4\Lambda)^{2/3} + b (R - 3\kappa^2\Lambda) (R/\kappa^2 - 4\Lambda)^{2/3}, \quad (4.26)$$

where

$$a \equiv \frac{\kappa^2 \sqrt[3]{\rho_0}}{3} (3\kappa^2 \lambda \Lambda + 2),$$

$$b \equiv \kappa^2 \lambda \sqrt[3]{\rho_0}.$$

Here we can check that by making $\lambda = 0$ one recovers the perfect fluid solution in minimally coupled $f(R)$ theories given in [496].

Finally, due to the linearity of the differential equation 4.25, as the coefficients a_i do not depend on the fluid, it is easy to see that the particular solution for a universe containing both dust and a perfect fluid with EoS parameter $w = -1/3$ is the sum of the previous particular solutions, i.e. Eq. (4.22) and Eq. (4.26).

4.2.2 An arbitrary f_2 with $f_1 = R - 2\kappa^2\Lambda$

In this case we fix f_1 and let f_2 as an undetermined function. We have to solve the following differential equation

$$6\lambda \left[\rho a_2(R) f_2'' - \left(\rho a_1(R) - a_2(R) \frac{d\rho}{dR} \right) f_2' - a_0 \rho f_2 \right] = \rho + \Lambda - \frac{R - 3\kappa^2\Lambda}{\kappa^2}. \quad (4.27)$$

Let us notice that if $\lambda = 0$, one obtains that the content of the universe can just be dust

$$\rho = \frac{R}{\kappa^2} - 4\Lambda. \quad (4.28)$$

This is consistent with Eq. (4.10), as we are assuming a Λ CDM background. Let us note that in this case ρ cannot be collected as a simple inhomogeneous term in the differential equation Eq. (4.27). Then, in this case, both the homogeneous and particular solution will be affected by the choice of ρ . We will solve this equation for dust and for a perfect fluid.

4.2.2.1 Dust: $\rho = \rho_m$

The equation in a universe filled with dust reads

$$6\lambda (R - 4\kappa^2\Lambda) \left(a_2(R)f_2'' + \left(\frac{5}{6}R - 2\kappa^2\Lambda \right) f_2' - a_0f_2 \right) = 0. \quad (4.29)$$

As we can notice, the right hand side will be always zero no matter the coupling constant one chooses. Assuming $\lambda \neq 0$ we note that we have an homogeneous differential equation with the following analytical solutions:

$$f_2 = \frac{c_1}{\sqrt[3]{R - 4\kappa^2\Lambda}} + \frac{6}{5}c_2\sqrt{R - 3\kappa^2\Lambda} + \frac{9}{5}c_2\sqrt{R - 3\kappa^2\Lambda} {}_2F_1\left(\frac{5}{6}, 1; \frac{4}{3}; 4 - \frac{R}{\kappa^2\Lambda}\right), \quad (4.30)$$

where c_1 and c_2 are integration constants and can be fixed by setting initial conditions on f_2 and f_2' . The integral representation of the hypergeometric function is well defined in the range $4\kappa^2\Lambda \leq R < \infty$ [498], and as we are interested in the physical range, that is, $R \geq 4\kappa^2\Lambda$, this term is perfectly defined. One should have special care with the c_1 term, as in the limit $R \rightarrow 4\kappa^2\Lambda$ one would have zero at the denominator. However, taking a look at how this term appears in the action -that is, multiplied by the Lagrangian- one can see that there are no problems at this point. Our solution is perfectly defined.

4.2.2.2 Perfect fluid with constant EoS parameter: $\rho = \rho_w$

Now the equation which has to be solved is

$$6\lambda \left[(R - 4\kappa^2\Lambda)^w a_2(R)f_2'' - [a_1(R) - (w + 1)(R - 3\kappa^2\Lambda)] f_2' - a_0f_2 \right] = 1 - \left(\frac{\rho_0}{\frac{R}{\kappa^2} - 4\Lambda} \right)^w. \quad (4.31)$$

If $w = 0$, one recovers the differential equation for a dust dominated universe, Eq. (4.29). If $\lambda = 0$, one gets $\rho_0 = R/\kappa^2 - 4\Lambda$, so this would be the only solution fixing $f_1 = R - 2\Lambda\kappa^2$. Firstly, let us take a look at the homogeneous equation

$$\lambda \left[a_2(R)f_2'' - \left(a_1(R) - (w + 1)(R - 3\kappa^2\Lambda) \right) f_2' - a_0f_2 \right] = 0. \quad (4.32)$$

As the RHS does not depend on the coupling constant, the specific election of λ will not affect the homogeneous solution. Assuming $\lambda \neq 0$ and performing the change of variable

$$x = \frac{R}{\kappa^2\Lambda} - 3,$$

we can rewrite the previous equation as follows:

$$(1-x)xf_2'' + \left[\frac{1}{6}(x-3) - (w+1)x \right] f_2' + \frac{f_2}{6} = 0. \quad (4.33)$$

We have found a solution which is valid for any value of w which is given by:

$$f_{2,h} = C_1 {}_2F_1 \left(a_1, b_1, c_1; \frac{R}{\kappa^2 \Lambda} - 3 \right) + \quad (4.34)$$

$$C_2 \left(\frac{R}{\kappa^2 \Lambda} - 3 \right)^{7/6} {}_2F_1 \left(a_2, b_2, c_2; \frac{R}{\kappa^2 \Lambda} - 3 \right)$$

with

$$a_1 = w_1 - \tilde{w}, \quad (4.35)$$

$$b_1 = w_1 + \tilde{w}, \quad (4.36)$$

$$c_1 = -\frac{1}{6}, \quad (4.37)$$

$$a_2 = w_2 - \tilde{w}, \quad (4.38)$$

$$b_2 = w_2 + \tilde{w}, \quad (4.39)$$

$$c_2 = \frac{13}{6}. \quad (4.40)$$

where we have defined $w_1 \equiv -\frac{1}{12} + \frac{w}{2}$, $w_2 \equiv \frac{13}{12} + \frac{w}{2}$ and $\tilde{w} \equiv \frac{1}{12} \sqrt{25 - 12w + 36w^2}$. Here we are giving the solution around the point $R = 3\kappa^2 \Lambda$. As we said, we are interested in the physical region, that is, $R \geq 4\kappa^2 \Lambda$, and in this region the variable of our function, x , goes from 1 to ∞ . The condition for a well-defined integral representation in our case would apply to the region $(-\infty, 1)$ [498]. In order to have our solution defined within those limits, we change the variable to $1-x$. This transformation also appears in the previous reference. Rewriting the solution Eq. (4.34), we have:

$$f_{2,h} = C_1 {}_2F_1 \left(a_1, b_1, 1 + a_1 + b_1 - c_1; 4 - \frac{R}{\kappa^2 \Lambda} \right) + \quad (4.41)$$

$$C_2 \left(4 - \frac{R}{\kappa^2 \Lambda} \right)^{-w} {}_2F_1 \left(c_2 - a_2, c_2 - b_2, 1 + c_2 - a_2 - b_2; 4 - \frac{R}{\kappa^2 \Lambda} \right)$$

The following step would be to find an analytical particular solution. In order to find a particular solution one would have to solve Eq. (4.31). The problem is that it is not straight forward to find an analytical solution for this equation, not even for a specific w , however one can find it by solving it numerically. Finally, the total solution will be the sum of the homogeneous solution and the particular one.

4.3 Cosmography within non-minimally coupled $f(R)$ gravity

In this section, we apply the cosmographic approach described in [501, 293, 502, 503, 294, 504, 505, 506] and adapt it to non-minimally coupled $f(R)$ gravity. In order to reduce the arbitrariness and complete our study we have considered the same two scenarios discussed before. In the first one, we set $f_2(R) = R$ so we can rename $f \equiv f_1$ for simplicity. In the second one, we will consider $f_1(R) = R - 2\kappa^2\Lambda$ renaming $f \equiv f_2$ when doing the computations. We will consider that the universe is filled by dust. The procedure we will follow is the one described, for example, in [506], where firstly one has to write the scalar curvature and derivatives in terms of the cosmographic parameters.

$$R = 6H^2(1 - q), \quad (4.42)$$

$$\dot{R} = 6H^3(j - q - 2), \quad (4.43)$$

$$\ddot{R} = 6H^4(s + q^2 + 8q + 6), \quad (4.44)$$

$$\ddot{\ddot{R}} = 6H^5(l - s - 2(q + 4)j - 6(3q + 8)q - 24). \quad (4.45)$$

4.3.1 An arbitrary f_1 with $f_2 = R$

The first step is to use the modified Friedman Eq. (4.6) and Raychaudhuri equations to obtain expressions for f and f_{RRR} . We obtain the Raychaudhuri equation taking the derivative of the Friedmann equation, Eq. (4.6). We then get:

$$f = \kappa^2 2\rho + (R - 6H^2)f_R - 6H\dot{R}f_{RR} - 24H^2\lambda\kappa^2\rho, \quad (4.46)$$

$$f_{RRR} = -\frac{\kappa^2\rho + 2\dot{H}f_R + (\ddot{R} - H\dot{R})f_{RR} + \lambda\kappa^2\rho(8\dot{H} - 12H^2)}{(\dot{R})^2}. \quad (4.47)$$

Differentiating the Raychaudhuri equation with respect to the cosmic time, we obtain the third equation that we need:

$$\begin{aligned} \ddot{H} &= \frac{\kappa^2}{2} \left[3H + \dot{R} \frac{f_{RR}}{f_R} \right] \frac{\rho}{f_R} - \frac{1}{2} \left(\ddot{R} - \dot{H}\dot{R} - H\ddot{R} \right) \frac{f_{RR}}{f_R} + \frac{(\ddot{R}\dot{R} - H\dot{R}^2)}{2} \left(\frac{f_{RR}}{f_R} \right)^2 \\ &- \frac{1}{2} \left(3\ddot{R}\dot{R} - H\dot{R}^2 \right) \frac{f_{RRR}}{f_R} + \frac{\dot{R}^3}{2} \frac{f_{RRR}f_{RR}}{f_R^2} - \frac{\dot{R}^3}{2} \frac{f_{RRRR}}{f_R} \\ &- \frac{\lambda\kappa^2\rho}{2f_R} \left(g_1(t) + \frac{f_{RR}}{f_R} g_2(t) \right), \end{aligned} \quad (4.48)$$

where

$$g_1(t) = 36H^3 - 48H\dot{H} + 8\ddot{H}, \quad (4.49)$$

$$g_2(t) = 12H^2\dot{R} - 8\dot{H}\dot{R}. \quad (4.50)$$

Since at the present time $f(R)$ should not deviate too much from GR, we can approximate our theory by its Taylor expansion around R_0 up to second order¹, being R_0 the present value of the scalar curvature:

$$f(R) \simeq f(R_0) + f_R(R_0)(R - R_0) + \frac{f_{RR}(R_0)}{2}(R - R_0)^2 + O(R - R_0)^3. \quad (4.51)$$

Then, we can ignore the terms containing f_{RRR} and f_{RRRR} in Eq. (4.48).

Now we have three equations and we can express f , f_R and f_{RR} in terms of the cosmographic parameters using Eqs. (4.42)-(4.45) and

$$\dot{H} = -H^2(1 + q), \quad (4.52)$$

$$\ddot{H} = H^3(j + 3q + 2), \quad (4.53)$$

which come from the basic formulas of cosmography. Please note that from now on, Ω_m and all the cosmographic parameters refers to quantities evaluated today. The cosmographic dimensionless quantities we compute are given by

$$\frac{f(R_0)}{6H_0^2} = \frac{A_0\Omega_m + \lambda H_0^2\Omega_m C_0}{D}, \quad (4.54)$$

$$f_R(R_0) = \frac{A_1\Omega_m + \lambda H_0^2\Omega_m C_1}{D}, \quad (4.55)$$

$$\frac{f_{RR}(R_0)}{(6H_0^2)^{-1}} = \frac{A_2\Omega_m + \lambda H_0^2\Omega_m C_2}{D}, \quad (4.56)$$

where the explicit expression of the coefficients A_i , C_i with $i = 1, 2, 3$ and D are shown in the Appendix.

We can get an order of magnitude of the cosmographic parameters by computing them for a given dark energy phenomenological parameterisation. The best and simplest one is the Λ CDM model.

$$j = 1, \quad (4.57)$$

$$q = \frac{3\Omega_m}{2} - 1, \quad (4.58)$$

$$s = 1 - \frac{9\Omega_m}{2}. \quad (4.59)$$

¹Although in reference [506], the authors expand up to third order we will carry the expansion only up to $o(R - R_0)^3$. This way we do not need to fix $f_R = 1$.

Afterwards, we take the latest Planck results [40] to compute the cosmographic parameters choosing a specific value for² λ :

$$\Omega_m = 0.315, \quad q = -0.54025, \quad j = 1, \quad s = -0.37925, \quad \lambda H_0^2 = \frac{1}{10^{15}}. \quad (4.60)$$

One obtains:

$$\frac{f(R_0)}{6H_0^2} = 0.84675, \quad f_R(R_0) = 1, \quad \frac{f_{RR}(R_0)}{(6H_0^2)^{-1}} = 3.98651 \cdot 10^{-15}. \quad (4.61)$$

It can be shown that if the model is close enough to Λ CDM, then f and f_R are decreasing functions of λ . We have assumed the latest Planck data. Likewise, it can be shown that f_{RR} is an increasing function of λ . Consequently, and under the assumption $f_2(R) = R$, this result can be interpreted as follows: the larger the non-minimal coupling in the action Eq. (4.1), the smaller the pure gravitational part; i.e. $f_1(R)$.

4.3.2 An arbitrary f_2 with $f_1 = R - 2\kappa^2\Lambda$

Following a procedure similar to the one used previously:

$$\begin{aligned} \kappa^2\lambda\rho f &= \kappa^2\lambda\rho(12H^2 + R)f_R - 6\kappa\lambda\rho H\dot{R}f_{RR} + 3H^2 - \kappa^2\Lambda - \kappa^2\rho \\ 2\kappa^2\lambda\rho\dot{R}^2 f_{RRR} &= \kappa^2\rho(1 + f\lambda) + \kappa^2\lambda\rho(2\dot{H} - 24H^2) f_R \\ &\quad + \kappa^2\lambda\rho(14H\ddot{R} - 2\ddot{R})f_{RR} + 2\dot{H}. \end{aligned} \quad (4.62)$$

One can note that if one sets $\lambda = 0$, one gets $3H^2 = \kappa^2(\rho + \Lambda)$ in the Friedmann equation and $2\dot{H} = -\kappa^2\rho$ in the Raychaudhuri equation. This is completely consistent with the background we are fixing in Eq. (4.10).

We obtain a third equation deriving the Raychaudhuri equation with respect to the cosmic time,

$$\begin{aligned} -6(H\ddot{H} + \dot{H}^2) &= 3\kappa^2\rho(\dot{H} - 3H^2) + \kappa^2\lambda\rho\left[(-9H^2 + 3\dot{H})f\right. \\ &\quad + (216H^4 - 162H^2\dot{H} + 24H\ddot{H} + 6\dot{H}^2)f_R \\ &\quad + (-198H^3\dot{R} + 60H^2\ddot{R} + 66H\dot{H}\dot{R} - 6H\ddot{R} - 6\dot{H}\ddot{R} \\ &\quad + \dot{R}(\dot{R} - 6\ddot{H}))f_{RR} \\ &\quad \left. + (60H^2\dot{R}^2 - 18H\dot{R}\ddot{R} - 6\dot{H}\dot{R}^2)f_{RRR} - 6\dot{R}^3Hf_{RRRR}\right] \end{aligned} \quad (4.64)$$

²Despite not having quantitative information about the order of magnitude of the coupling parameter, we estimate it to be sufficiently small so that it does not produce a drastical deviation from Einstein-Hilbert action.

As before, we can ignore the terms containing f_{RRRR} and f_{RRR} . Using an approach analogous to the one in Subsec. 4.3.1, we can express f , f_R and f_{RR} in terms of the cosmographic parameters considering dust as the only matter content. Again, note that from now on, Ω_m and all the cosmographic parameters refers to quantities evaluated at present. Similarly to the previous case, we compute the following dimensionless quantities:

$$\lambda\Omega_m f(R_0) = \frac{A_0\Omega_m + B_0 + C_0 \frac{\kappa^2\Lambda}{H_0^2}}{3D}, \quad (4.65)$$

$$\lambda\Omega_m \frac{f_R(R_0)}{(6H_0^2)^{-1}} = \frac{A_1\Omega_m + B_1 + C_1 \frac{\kappa^2\Lambda}{H_0^2}}{D}, \quad (4.66)$$

$$\lambda\Omega_m \frac{f_{RR}(R_0)}{(6H_0^2)^{-2}} = \frac{A_2\Omega_m + B_2 + C_2 \frac{\kappa^2\Lambda}{H_0^2}}{D}, \quad (4.67)$$

where the values of the coefficients appear explicitly in the Appendix.

Computing the parameters for a Λ CDM model, one gets

$$\lambda\Omega_m f(R_0) = 0, \quad \lambda\Omega_m \frac{f_R(R_0)}{(6H_0^2)^{-1}} = 0, \quad \lambda\Omega_m \frac{f_{RR}(R_0)}{(6H_0^2)^{-2}} = 0. \quad (4.68)$$

This is a result that is completely consistent with our model. Taking a look at Eq. (4.62) one can see that the only way to have a Λ CDM background is when λ is exactly zero. Nevertheless, we are interested in having a non-null coupling constant. This means that we have to relax the condition $\Omega_\Lambda = 1 - \Omega_m$ and leave Ω_Λ unfixed. The value of the coupling constant would affect the value of the density of the cosmological constant. In order to see it qualitatively one can see Fig. (4.1). It is straight forward to notice that in the limit $\lambda \rightarrow 0$, the value of Ω_Λ tends to exactly $1 - \Omega_m$. Something interesting that one can observe is that the higher the coupling constant λ is, the lower is the dark energy density Ω_Λ . This is a very desirable feature, as one of the motivations of introducing a coupling to matter is that it could play, in some way, the role of dark energy.

4.4 Lessons from non-minimally coupled $f(R)$ gravity

In the present chapter, we have considered an $f(R)$ modified gravity model characterized by having a non-minimal coupling to matter. A good representative of this kind of models was first proposed in [335] and it corresponds to a metric gravity extension of the well known $f(R)$ gravity. Within this framework, we have two functions: $f_1(R)$,

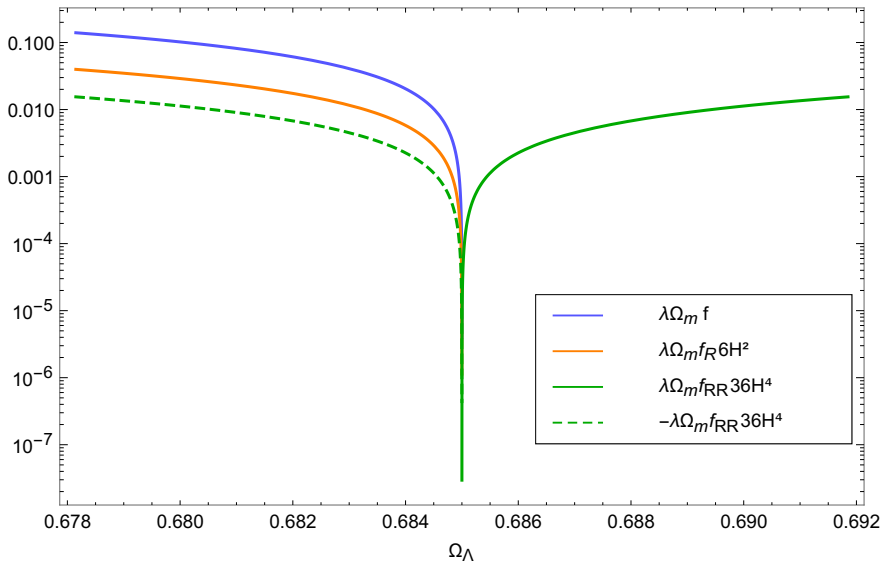


Figure 4.1: Here the dimensionless quantities given in Eqs. (4.65)-(4.67) are represented as a function of Ω_Λ .

uncoupled to matter, and $f_2(R)$, which takes into account the coupling of gravity to matter (see Eq. (4.1)). Our main interest resides on getting exact analytical solutions for this theory in the context of the late-time cosmology. For this purpose, we have selected two simple and physically meaningful scenarios; i. e. we have obtained two $f(R)$ non-minimally coupled models that mimic a Λ CDM setup.

For the first case, we have chosen $f_2(R) = R$, i.e. a small coupling of gravity to matter. Then $f_1(R)$ has to satisfy Eq. (4.14). Solving this equation, we have obtained a physically meaningful solution which exactly mimics a Λ CDM expansion for a vacuum universe, which is in contrast with what it is affirmed in [496]. Then, we have considered that the universe is filled up with some energy-density content and we have analysed two different scenarios. For a dust-dominated universe, the solution is described by the usual $R - 2\kappa^2\Lambda$ plus a polynomial correction on R driven by the coupling constant, λ . It is interesting to notice how in this solution a term naturally appears which acts as an effective cosmological constant. For a perfect fluid-dominated universe, we have been able to find an analytical solution once we have chosen the specific equation of state parameter $w = -1/3$, which can be interpreted as an energy-density mimicking an open universe. The obtained solution is also characterised by a polynomial behaviour on R .

For the second case, we have chosen $f_1(R) = R - 2\kappa^2\Lambda$. Then $f_2(R)$ has to satisfy Eq. (4.27). We have considered the two scenarios previously considered. In the dust-

dominated universe, the solution we have found is also given by polynomial terms but also including R in a denominator, then we have studied it carefully in order to ensure that there was no divergence in the range which is physically interesting for us. For the perfect fluid-dominated universe, taking into account that the differential equation we are solving is inhomogeneous, we want to emphasise that we have been able to find the homogeneous solution which is valid for every constant equation of state parameter, w . However, we have not been able to find an analytical particular solution for this case in order to have a complete analytical solution. Though, it is possible to get it numerically.

Finally, to complete our study and get a qualitative idea of the information these two models can bring to us, we have performed a cosmographic analysis. In the first case we want to mention that the quantities f and f_R are decreasing functions of λ and this can be interpreted as “the stronger the coupling to matter, the weaker the weight of the pure gravitational part of the action”, that is, f . On the other side, for the second case, we have obtained that the only case which allows for an exact Λ CDM background corresponds to $\lambda = 0$. Then, to allow non-zero values of λ , we let the parameter Ω_Λ free. The way λ affects the value of Ω_Λ shows us a desirable result because the higher is λ , the lower is Ω_Λ . This satisfies the main motivation of our research, as the non-minimally coupled term may be understood as playing the role of the cosmological constant, that is, of being the responsible of the late-time acceleration of the universe.

Chapter 5

Umami Chaplygin model

Chaplygin-like models arose originally as an alternative to quintessence, the latter describing a new type of matter which is represented by a scalar field, and whose behaviour describes the transition from a universe filled with dust to an exponentially expanding universe. Chaplygin-like models are characterized by describing this transition in terms of a single perfect fluid with an exotic equation of state. This means that we have dark matter and dark energy unified in a single fluid [157]. Many generalizations of this scenario have been proposed since then, the most studied in the literature are modified Chaplygin, extended Chaplygin and generalized Chaplygin proposals; see [158] for a brief review. The interesting feature of the specific model we present here is that our non-linear equation of state at late times does not have a de Sitter universe as a limit case but a fluid with a constant equation of state parameter w . Apart from the Chaplygin-like models, non-linear barotropic equations of state also appear in other works, one of the most recent ones being [167]. They focus on different descriptions, such as quadratic models to represent dark energy and unified dark matter [171], non-linear EoS for phantom fluids [172] or the Born-Infeld type fluid model [169].

In the present study we analyze a phenomenological generalization of the Chaplygin cosmological model, which we call *umami* Chaplygin model. We will treat our fluid in a polyvalent way in order to extract as much information as we can. We consider three different cosmological background scenarios in which our fluid can play three different roles: only as a dark energy component, as a dark matter and dark energy component and as a dark plus baryonic matter and dark energy component. The two last cases are the most intriguing ones because in that case we realize the idea of having all the “dark” behaviour unified into a single fluid. With such analysis we explore the possibility of unifying the dark fluids into one single component within the context of GR.

We will test this hypothesis against the main available data related to the cosmological background described in Sec. 1. Final results point to a positive (albeit not strong) evidence in favor of a possible unification of dark energy and dark matter with the *umami* fluid.

5.1 Model

We study what we have named the *umami* Chaplygin model described by the following equation of state:

$$p = -\frac{\rho}{\frac{1}{|w|} + \frac{\rho^2}{|A|}} \quad (5.1)$$

where p and ρ are the pressure and the energy density of our fluid and w and A are real constants. Let us note that, on one hand, at high energy density the pressure of the fluid behaves as

$$p \rightarrow -\frac{|A|}{\rho}, \quad (5.2)$$

which is the equation of state of the original form of the Chaplygin fluid. On the other hand, the low energy density limit gives

$$p \rightarrow -|w|\rho, \quad (5.3)$$

which is the equation of state of a perfect fluid with negative effective EoS parameter; thus, the fluid will be playing the role of some dark energy component.

We assume the fluid independently fulfills the usual conservation equation,

$$\dot{\rho} + 3H(\rho + p) = 0, \quad (5.4)$$

where $\cdot \equiv d/dt$ and, once again, $H = \dot{a}/a$ is the Hubble parameter. This can be solved analytically thus obtaining the following implicit expression for ρ :

$$\rho^{\frac{1}{1-|w|}} \left| |A| - |A||w| + |w|\rho^2 \right|^{\frac{|w|}{2(|w|-1)}} = \rho_0^{\frac{1}{1-|w|}} \left| |A| - |A||w| + |w|\rho_0^2 \right|^{\frac{|w|}{2(|w|-1)}} a^{-3}, \quad (5.5)$$

where the subindex 0 means that the quantity is evaluated at the present time.

To set up the background cosmological evolution we have solved Eq. (5.5) numerically in order to find ρ . Given the non-linearity of the solution and for practical reasons, instead of working with the variable ρ , we switch to the dimensionless matter parameter,

$$\bar{\Omega}_f \equiv \frac{\rho}{\rho_{c,0}}, \quad (5.6)$$

where $\rho_{c,0} = 3H_0^2/8\pi G$ is the critical density of the Universe at the present time. Note that the defined $\bar{\Omega}_f$ parameter is not fully equivalent to the standard dimensionless density parameter Ω_f , which should have been defined as ρ/ρ_c . The two versions are equivalent only in the present-time limit, i.e. $\bar{\Omega}_{f,0} = \Omega_{f,0}$, which is the case we are mostly interested in, if we want to compare our results with the literature. Thus, Eq. (5.5) will become:

$$\begin{aligned} \bar{\Omega}_f^{\frac{1}{1-|w|}} \left| |\bar{A}| - |\bar{A}| |w| + |w| \bar{\Omega}_f^2 \right|^{\frac{|w|}{2(|w|-1)}} &= \\ \bar{\Omega}_{f,0}^{\frac{1}{1-|w|}} \left| |\bar{A}| - |\bar{A}| |w| + |w| \bar{\Omega}_{f,0}^2 \right|^{\frac{|w|}{2(|w|-1)}} a^{-3}, \end{aligned} \quad (5.7)$$

where also the parameter A has been redefined as

$$\bar{A} \equiv A/\rho_{c,0}^2. \quad (5.8)$$

The solution to Eq. (5.7) allows us to add the *umami* fluid in a more direct observationally related form into the expression of the Friedmann equation obtained after the standard assumption of a FLRW metric background.

In particular, we have studied three different scenarios, where the *umami* fluid plays different roles:

$$E_1(z) = \sqrt{\Omega_m(1+z)^3 + \Omega_r(1+z)^4 + \bar{\Omega}_f(z) + \Omega_k(1+z)^2} \quad (5.9)$$

$$E_2(z) = \sqrt{\Omega_b(1+z)^3 + \Omega_r(1+z)^4 + \bar{\Omega}_f(z) + \Omega_k(1+z)^2} \quad (5.10)$$

$$E_3(z) = \sqrt{\Omega_r(1+z)^4 + \bar{\Omega}_f(z) + \Omega_k(1+z)^2} \quad (5.11)$$

where $E(z) \equiv H(z)/H_0$ is the dimensionless Hubble parameter, and $\Omega_m, \Omega_b, \Omega_r$ are the normalized densities of total matter (baryons and dark matter), baryons-only and radiation today, while $\Omega_k \equiv k/H_0^2$ corresponds to the spatial curvature. In the first scenario our fluid $\bar{\Omega}_f$ represents only a dark energy component; in the second one, we unify the dark matter and dark energy content into $\bar{\Omega}_f$; finally, in the third scenario, $\bar{\Omega}_f$ would include the total matter content and the dark energy.

We have to pay special attention to the two latter models: in principle, we have no clue about which fraction of our *umami* fluid should behave as dark energy and/or dark matter. We are giving here a phenomenological proposal, with no physical insight about its possible physical origin. For that, in case 2, we define the parameter $f_{\Omega_{DM}}$ which is the fraction of $\bar{\Omega}_f$ that corresponds to dark matter. In this way we have that the total matter content is $\Omega_m = \Omega_b + f_{\Omega_{DM}} \cdot \bar{\Omega}_f$. In model 3, something similar happens. We need to know which part of our fluid accounts for dark matter

Table 5.1: Background primary parameters for the the three *umami* Chaplygin models considered and for the standard Λ CDM dark energy model, plus Bayesian Evidence ratios.

model	$f_{\Omega_{DM}}$	f_{Ω_b}	Ω_k	h	w	\tilde{A}	Ω_m	Ω_b	\mathcal{B}_Λ^i	$\ln \mathcal{B}_\Lambda^i$
Λ CDM	-	-	$-0.002_{-0.002}^{+0.002}$	$0.669_{-0.006}^{+0.006}$	-1	-	$0.320_{-0.006}^{+0.007}$	$0.050_{-0.001}^{+0.001}$	1	0
1	-	-	$-0.001_{-0.002}^{+0.002}$	$0.665_{-0.007}^{+0.007}$	$-0.98_{-0.01}^{+0.02}$	$3.4_{-1.3}^{+1.4}$	$0.323_{-0.007}^{+0.007}$	$0.050_{-0.001}^{+0.001}$	0.40	-0.91
2	$0.285_{-0.007}^{+0.008}$	-	$-0.004_{-0.007}^{+0.006}$	$0.69_{-0.01}^{+0.01}$	$-0.85_{-0.06}^{+0.07}$	$0.50_{-0.07}^{+0.08}$	$0.320_{-0.007}^{+0.008}$	$0.047_{-0.002}^{+0.001}$	1.31	0.27
3	$0.271_{-0.007}^{+0.008}$	$0.046_{-0.001}^{+0.001}$	$-0.003_{+0.006}^{-0.007}$	$0.69_{-0.01}^{+0.01}$	$-0.81_{-0.07}^{+0.08}$	$0.52_{-0.08}^{+0.08}$	$0.319_{-0.007}^{+0.008}$	$0.046_{-0.002}^{+0.002}$	1.14	0.13

and baryonic matter, respectively. In this case we have $\Omega_m = (f_{\Omega_b} + f_{\Omega_{DM}}) \cdot \bar{\Omega}_f$, where f_{Ω_b} is the fraction of baryons in $\bar{\Omega}_f$.

In order to describe numerically the general function $\bar{\Omega}_f(a)$ (where a is the scale factor) and save time when performing the statistical data analysis, we have built a grid on the parameters $\{a, \bar{\Omega}_{f,0}, w, \bar{A}\}$ and defined the final *umami* density function as an interpolating function on this grid. The chosen grid is:

$$1 \cdot 10^{-11} < a < 1 \quad (5.12)$$

$$0.3 < \bar{\Omega}_{f,0} < 1.5 \quad (5.13)$$

$$-1 < w < -0.015 \quad (5.14)$$

$$-500000 < \bar{A} < -0.025 \quad (5.15)$$

We want to stress that we keep $w > -1$ in order to avoid phantom fields and the ‘‘singular’’ value $w = -1$. The range of A is large enough to cover all the possible physically meaningful values for our model; but we need to specify also that the grid is not globally uniform. That is because as well as for $w \leq -1$ and for some combination of $w > -1$ values with some ranges of the A parameter, the numerical solution of Eq. (5.5) may not be physical or not univocal. In fact, for some combinations we might have negative densities or two positive solutions with one branch leading to increasing density in time. While this could be considered meaningful in some singularity scenarios [507], we have avoided them and stuck to a more standard evolution of the cosmological background.

5.1.1 Results

In Table 5.1 we summarize the mean values of the background parameters

$$\{f_{\Omega_{DM}}, f_{\Omega_b}, \Omega_k, h, w, \tilde{A}, \Omega_m, \Omega_b\},$$

obtained for each of the scenarios considered. It can be seen that the results for all our models are in agreement with the values obtained in *Planck* 2018 [41].

We are mostly interested in the parameters directly related with baryonic and dark matter, as they change from one model to other when considered as part of the *umami* fluid. In order to make the comparison more direct, we show in Table 5.2 the value of $\Omega_b h^2$ and $\Omega_{DM} h^2$ obtained by *Planck* 2018 for the full data combination with varying Ω_k^1 , and by us from the MCMCs run for each one of the three scenarios we have considered. We also show the value of H_0 , which has also a special importance due to the existing tension between the values given by local measurements [508] and indirect measurements by Planck [509]. To compute the statistics for $\Omega_{DM} h^2$ we take into account that $\Omega_{DM} = f_{\Omega_{DM}} \bar{\Omega}_{f,0}$, with $\bar{\Omega}_{f,0} = 1 - \Omega_b - \Omega_r - \Omega_k$ for model 2 and $\bar{\Omega}_{f,0} = 1 - \Omega_r - \Omega_k$ for model 3. Also, for the statistics of $\Omega_b h^2$, we take into account that in model 3 $\Omega_b = f_{\Omega_b} \bar{\Omega}_{f,0}$.

As a general tendency we can see how the *umami* fluid is generally disfavored with respect to a cosmological constant when considered as dark energy fluid only. Instead, when we consider the possibility to describe both dark matter and dark energy by one single fluid, the Bayesian Evidence becomes positive, indicating a general trend in favor of the alternative model. But it is also true that the value of the evidence is too low to set any strong preference toward it against Λ CDM. At least, it works equally good.

Another interesting point is that the value of H_0 increases slightly in models 2 and 3, tending to *solve* the H_0 tension. It is also true, however, that the corresponding error also increases. If we focus now on Ω_b and Ω_m we notice that they decrease in models 2 and 3. With respect to Ω_k , in models 2 and 3 this parameter gets bigger but so the error does, and it is always consistent with zero.

We also want to pay attention to another interesting result of our analysis: the columns of Table 5.1 corresponding to the *umami* parameters, \tilde{A} and w . In order to analyze in detail these results and to be able to compare the models, we focus on the pressure and the effective equation of state parameter, respectively defined as

$$\bar{p} \equiv c^2 w_{\text{eff}} \bar{\Omega}_f, \quad (5.16)$$

where

$$w_{\text{eff}} \equiv \frac{-1}{\frac{1}{|w|} + \frac{\bar{\Omega}_f^2}{|\tilde{A}|}}. \quad (5.17)$$

¹https://wiki.cosmos.esa.int/planck-legacy-archive/index.php/Cosmological_Parameters

Table 5.2: Comparison of the secondary baryonic and dark matter background parameters and of the Hubble parameter H_0 from our analysis with those derived from *Planck* 2018 data.

	$\Omega_b h^2$	$\Omega_{DM} h^2$	H_0
Planck18 (68%)	$0.02240^{+0.00015}_{-0.00015}$	$0.1196^{+0.0014}_{-0.0014}$	$67.95^{+0.64}_{-0.64}$
Planck18 (95%)	$0.02240^{+0.00030}_{-0.00030}$	$0.1196^{+0.0027}_{-0.0027}$	$67.9^{+1.3}_{-1.2}$
model 1	$0.02231^{+0.00016}_{-0.00016}$	$0.12042^{+0.0014}_{-0.0014}$	$66.50^{+0.68}_{-0.67}$
model 2	$0.02227^{+0.00016}_{-0.00017}$	$0.1286^{+0.0046}_{-0.0049}$	$68.73^{+1.13}_{-1.27}$
model 3	$0.02227^{+0.00015}_{-0.00016}$	$0.1308^{+0.0045}_{-0.0046}$	$69.27^{+1.21}_{-1.23}$

So, as we did with the energy density, we redefine the pressure normalizing over $\rho_{c,0}$ so that we have $\bar{p} \equiv \frac{p}{\rho_{c,0}}$.

Looking at the plot of \bar{p} in Fig. 5.1 one can notice how the pressure of the *umami* is negative during the whole expansion history of the universe, but exhibiting different limiting behaviours at early times depending on the scenario we consider. For model 1 we see an almost constant evolution with a quite abrupt and faster decrease at early times, but still leading to a finite negative pressure. This is not really surprising, as in model 1 the *umami* fluid has been considered as a dark energy-only fluid.

For models 2 and 3, the results are very similar between them, as expected, because at the level of the background the role of the baryonic matter is somehow minor with respect to that one played by dark matter. But differently from model 1 we now see a smooth transition from a region with negative pressure at late times, where dark energy dominates, to a region with pressure close (tending) to zero at early times, when we know that matter should be dominating the expansion of the Universe. Note that our data probe the cosmological expansions for $a > 0.138$.

These different trends are related to the quantity \tilde{A} , which drives this transition between a matter domination epoch and a dark energy domination epoch. We notice that the obtained value is much bigger for model 1 than for models 2 and 3. To understand its role it must always be taken into account the comparison of its value with respect to $\bar{\Omega}_f$. The bump that appears in Fig. 5.1 for model 1 occurs where the density starts to be comparable with \tilde{A} . For models 2 and 3 its mean value is much lower, so that its effects appear at smaller scale factor.

All these considerations are confirmed by the effective equation of state parameter, w_{eff} . In Fig. 5.1 we see that in the case where the *umami* fluid behaves only like dark energy we do not have a clear statistical difference between the *umami* and a

standard Λ CDM scenario. We have some more evident changes in the cases 2 and 3, where the equation of state parameter shows a clear transition on its tendency.

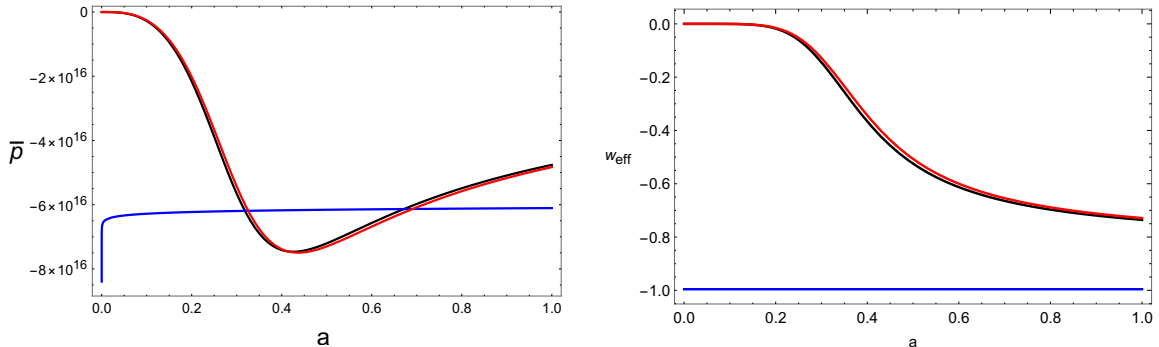


Figure 5.1: (*Left panel.*) Evolution of the pressure with the scale factor for each of the models considered. The blue line corresponds to model 1, where the *umami* is just dark energy (DE), the black one corresponds to model 2, where the *umami* is dark energy plus dark matter (DE+DM) and the red one corresponds to model 3, where the *umami* is dark energy plus the total matter (DE+TM). (*Right panel.*) Same as before, but for the effective equation of state parameter.

The leading fact we want to remark here is that the mean values we obtain for w_{eff} and \tilde{A} are significantly different from what it is obtained in a model where dark energy is considered independently from the matter content, as for example Λ CDM. This means that we have a model which is drastically different from Λ CDM and that is well-fitting the data in a statistical satisfactory way.

Finally, an interesting point to explore is to study which energy conditions are satisfied (and when) for each of the proposed *umami* fluids. Energy conditions can be understood as requirements that can be applied to the energy-density content of a theory when one does not specify this content explicitly. These are imposed boundary conditions that attempt to encapsulate the statement that pressure must be positive. In cases as ours, where dark energy is considered, one can expect some of these conditions not to be accomplished. We have considered the energy conditions as summarized in [510], and described in terms of our quantities:

- Null energy condition (NEC): $c^2\bar{\Omega}_f + \bar{p} \geq 0$
- Weak energy condition (WEC): $c^2\bar{\Omega}_f + \bar{p} \geq 0$ and $\bar{\Omega}_f \geq 0$
- Strong energy condition (SEC): $c^2\bar{\Omega}_f + \bar{p} \geq 0$ and $c^2\bar{\Omega}_f + 3\bar{p} \geq 0$

We have studied these conditions for every scenario, including the cosmological constant scenario, and we have found some interesting results. First of all, NEC and WEC conditions are perfectly satisfied by every model. As expected, Λ CDM violates the SEC condition and a similar behaviour is found in model 1, in which our *umami* plays the role of a fully dark energy component. On the other hand, models 2 and 3 exhibit a much more interesting evolution of the quantity corresponding to the strong energy condition. In Fig. 5.2 we have plotted the energy density, the pressure and the WEC and SEC conditions for these two models. In both plots we see that there is cusp in the SEC condition, related to a change from negative (at large scale factor) to positive (at small scale factors) values, which means that SEC is violated when the *umami* behaves as a dark energy fluid (at large scale factor), but is satisfied when its behaviours resemble that of a pressureless matter component (at low scale factor).

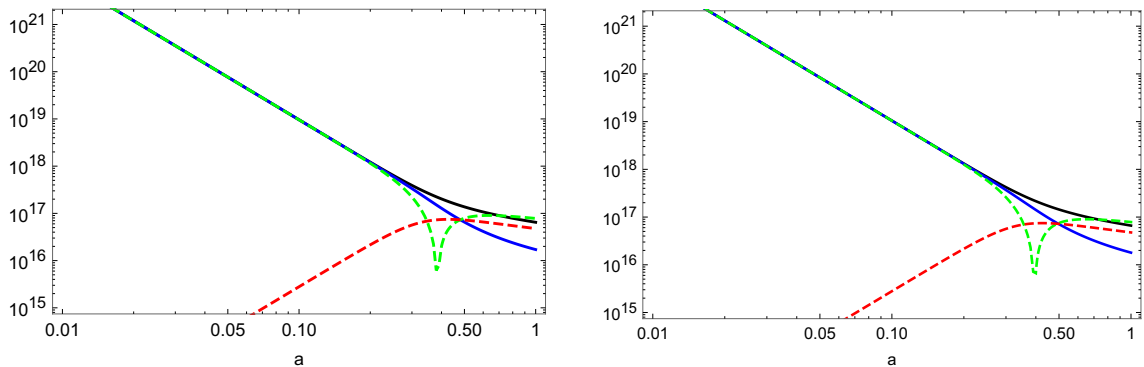


Figure 5.2: (*Left panel.*) Absolute values of the energy density, pressure and energy conditions for model 2. The black line corresponds to the energy density, the dashed red one corresponds to the pressure, the blue one corresponds to the WEC and the dashed green one to the SEC. (*Right panel.*) Same as before, but for model 3.

5.2 Lessons from the *umami* Chaplygin fluid

In this section we have introduced a new phenomenological cosmological fluid with a non-linear equation of state such that could be able to unify a dark matter cosmological behaviour with a dark energy one. We have considered three different possible contributions of such a fluid to the cosmic pie, namely: replacing only a dark energy fluid; replacing both a dark energy and a dark matter fluid; replacing both a dark energy and the total matter contribution, i.e., dark and baryonic matter. After having compared these three scenarios with a large set of cosmological data available

nowadays (geometrical probes), we have obtained some remarkable results we want to emphasize here. First of all we have found that our results are in agreement with the constraints given by *Planck* 2018. Secondly, for models 2 and 3, which contain a unified dark fluid and a unified baryonic-dark matter-dark energy fluid, the results obtained for the parameters \tilde{A} and w are completely beyond the values expected for a model with a non-unified equation of state. All this shows that this kind of unified models can properly mimic the background phenomenology even though being different from the standard cosmological Λ CDM model. Bayesian Evidence comparison shows a small but positive preference for such models. Thirdly, and not less important, although having a higher error, the mean values obtained for H_0 in models 2 and 3 are slightly higher than the one obtained from *Planck*, and, as a consequence, closer to its local measurements. Even if this result can not be taken as conclusive, we find interesting the observed tendency to solve the H_0 tension plaguing observational cosmology today. All the observed features give us information about attractive directions to follow in the search of alternative models to Λ CDM.

Chapter 6

Conclusions

We could describe the goal of this thesis as the analysis of viable descriptions of the late time universe through the study of its evolution from very different perspectives. Taking the cosmological constant as the reference model in a GR setting, we have investigated various alternatives. On the one hand, we have tackled the question of the late time expansion of the universe from the dark energy approach, where the main ingredient is a fluid which usually is understood as a generalization of the cosmological constant term. This dark fluid can adopt an innumerable quantity of descriptions and we have focused on a specific approach consisting on a parameterization that has been constructed phenomenologically. It does not only involve the effects dark energy may have (i.e. late acceleration) but also the effects which would correspond to dark matter (concretely in the form of dust). On the other hand, we have studied the possibility of the late time universe being described by extended theories of gravity. The huge variety of theories within this field may take completely different approaches, however, all of them must touch at some point GR, at least as a limit, in order for these theories to be able to reproduce the phenomenology which is well described by GR (e.g. solar system constraints). Within the modified gravity zoo we have centered our work on the so-called $f(R)$ theories. One part of the work consists on proposing and analyzing an observational cosmologist friendly approach where we translate the functions of the Ricci scalar into functions of the redshift. In another part of the work we study a natural alternative analog to $f(R)$ theories in which the Ricci scalar is replaced by the non-metricity giving rise to a new kind of models, i.e. $f(Q)$ theories. Finally, and also within the field of $f(R)$, we study another extension which includes a non-minimal coupling and try to find solutions assuming different cosmological scenarios.

Despite the differences between the theoretical approaches we have mentioned, we have used a common tool/ingredient to study the validity of our models: observational tests. We want to emphasize that a needed (but not sufficient) feature for a model to

be considered as a possible scenario is that it has to be able to reproduce the actual observational constraints. In this thesis, concretely, we have performed background observational analyses in order to constrain the different background cosmological parameters. We have used a variety of observational probes which we have been updated in each of the works. We will now describe in more detail the results obtained in each chapter.

We dedicate chapter 2 to $f(z)$ gravity. Here, after introducing different ways to study $f(R)$ theories we explain the approach we have followed, i.e. the redshift representation $f(z)$. The interest of this description relies on the manner cosmological probes provide the data. As our final aim is to check if a model's predictions satisfy current observations, we have found useful to provide this z -formalism to study $f(R)$ theories. In order to do that we propose some models within this approach ensuring that their phenomenology satisfies some basic limits settled by a significant class of dark energy models, i.e. matter domination at high redshift and constant behaviour at low redshift. At the end we have provided eight polynomial models on z which include different powers of $(1+z)$. Once we have performed the observational test using different probes we have found that the models which contain smaller powers of $(1+z)$ (but no constant term) perform in a similar way to the model corresponding to Λ CDM. Although no significant preferability has been observed, it has been shown that this approach may offer a new way of analyzing theories in an observer friendly way.

In chapter 3 we investigate $f(Q)$ theories of gravity using the approach described in the previous chapter. As we are starting from a different action we obtain different equations as well as different trends on $f(z)$ when looking at the low and high redshift limits. Here we have proposed seven polynomial models and, in the observational test, we have included Quasars and Gamma Ray Bursts data arriving to a conclusion which is similar to the previous one: small-order terms are preferred (in absence of constant term) and are compatible with current observations.

In chapter 4 we analyze a natural extension of $f(R)$ which includes a non-minimal coupling between R and the matter lagrangian. We find this proposal specially interesting "as well as tricky" due to the two $f(R)$ functions that appear in the action. After computing the background dynamics and assuming a Λ CDM expansion we have solved the Friedmann equation for various different scenarios, obtaining solutions that mimic a Λ CDM expansion but which do not include a cosmological constant. The inclusion of a coupling term allows to afford this and, as we have obtained in the

cosmographic analysis, it can be interpreted as playing the role of dark energy due to how it varied when we vary the value of Ω_Λ .

Finally, in chapter 5 we explore a dark fluid model which belongs to the family of the unified dark energy models, more specifically, the Chaplygin models. We construct a quite exotic equation of state which corresponds to a fluid whose behaviour evolves from a dust behaviour to a dark energy one. In fact we explore this fluid to adopt different roles and study three different scenarios described by three different Friedmann equations. We end up with an observational analysis where we obtain the values of the cosmological parameters for each case resulting in a high preference of two of the scenarios: one where the fluid acts as dark matter and dark energy and other where the fluid acts as total matter and dark energy. Moreover, an important result of this work is that the mean values that have been obtained for H_0 lie between Planck's prediction and local measurements, relaxing the existing tension around this quantity.

To sum up this general overview and to conclude, we can say that with this thesis we have paved a bit the way within the study of the late time universe adding some new techniques and information about extended theories of gravity and dark energy models. These results, although not providing a definitive answer to any of the hot questions in Cosmology, could serve as building blocks to continue learning about the universe.

Bibliography

- [1] M. García, *Introducción a La Historia de La Cosmología*. Unidad Didáctica. UNED, 2009.
- [2] A. Einstein, *Zur Elektrodynamik bewegter Körper [On the electrodynamics of moving bodies]*, *Annalen Phys.* **17** (1905) 891–921.
- [3] H. S. Leavitt and E. C. Pickering, *Periods of 25 Variable Stars in the Small Magellanic Cloud*, *Harvard Obs. Circ.* **173** (1912) 1–3.
- [4] H. Sawyer Hogg, *A third catalogue of variable stars in globular clusters comprising 2119 entries.*, *Publications of the David Dunlap Observatory* **3** (1973) 6.
- [5] V. Slipher, *Spectroscopic Observations of Nebulae*, *Popular Astronomy* **23** (1915) 21.
- [6] E. Hubble, *Extragalactic nebulae*, *Astrophys. J.* **64** (1926) 321–369.
- [7] E. Hubble, *A relation between distance and radial velocity among extra-galactic nebulae*, *Proc. Nat. Acad. Sci.* **15** (1929) 168–173.
- [8] E. Hubble and M. L. Humason, *The Velocity-Distance Relation among Extra-Galactic Nebulae*, *Astrophys. J.* **74** (1931) 43–80.
- [9] A. Friedmann, *Über die Krümmung des Raumes*, *Zeitschrift für Physik A* **10** (1922) 377–386. 0939–7922.
- [10] G. Lemaitre, *A Homogeneous Universe of Constant Mass and Growing Radius Accounting for the Radial Velocity of Extragalactic Nebulae*, *Annales Soc. Sci. Bruxelles A* **47** (1927) 49–59. [Gen. Rel. Grav.45,no.8,1635(2013)].

- [11] G. H. J. E. Lemaitre, *The gravitational field in a fluid sphere of uniform invariant density according to the theory of relativity ; Note on de Sitter Universe ; Note on the theory of pulsating stars*, Massachusetts Institute of Technology. Dept. Of Physics. (1927).
- [12] R. Alpher, H. Bethe, and G. Gamow, *The origin of chemical elements*, *Phys. Rev.* **73** (1948) 803–804.
- [13] G. Gamow, *The Origin of Elements and the Separation of Galaxies*, *Phys. Rev.* **74** (1948), no. 4 505–506.
- [14] R. A. Alpher and R. C. Herman, *On the Relative Abundance of the Elements*, *Phys. Rev.* **74** (1948), no. 12 1737–1742.
- [15] R. A. Alpher and R. Herman, *Evolution of the Universe*, *Nature* **162** (1948), no. 4124 774–775.
- [16] G. Gamow, *The Evolution of the Universe*, *Nature* **162** (1948), no. 4122 680–682.
- [17] **Supernova Search Team** Collaboration, A. G. Riess et al., *Observational evidence from supernovae for an accelerating universe and a cosmological constant*, *Astron. J.* **116** (1998) 1009–1038.
- [18] **Supernova Cosmology Project** Collaboration, S. Perlmutter et al., *Measurements of Omega and Lambda from 42 high redshift supernovae*, *Astrophys. J.* **517** (1999) 565–586.
- [19] W. de Sitter, *Einstein's theory of gravitation and its astronomical consequences*, *Monthly Notices of the Royal Astronomical Society* **76** (1916) 699–728.
- [20] W. de Sitter, *On Einstein's theory of gravitation and its astronomical consequences. Second paper*, *Monthly Notices of the Royal Astronomical Society* **77** (1916) 155–184.
- [21] W. de Sitter, *On Einstein's Theory of Gravitation and its Astronomical Consequences. Third Paper.*, *Monthly Notices of the Royal Astronomical Society* **78** (1917), no. 1 3–28.

- [22] W. de Sitter, *On the relativity of inertia. Remarks concerning Einstein's latest hypothesis*, *Koninklijke Nederlandse Akademie van Wetenschappen Proceedings Series B Physical Sciences* **19** (1917) 1217–1225.
- [23] A. H. Guth, *The Inflationary Universe: A Possible Solution to the Horizon and Flatness Problems*, *Phys. Rev.* **D23** (1981) 347–356.
- [24] A. Starobinsky, *A new type of isotropic cosmological models without singularity*, *Physics Letters B* **91** (1980), no. 1 99 – 102.
- [25] A. D. Linde, *The inflationary universe*, *Rept.Prog.Phys.* **47** (1984) 925–986.
- [26] A. Albrecht and P. J. Steinhardt, *Cosmology for Grand Unified Theories with Radiatively Induced Symmetry Breaking*, *Phys. Rev. Lett.* **48** (1982) 1220–1223.
- [27] V. C. Rubin and J. Ford, W.Kent, *Rotation of the Andromeda Nebula from a Spectroscopic Survey of Emission Regions*, *Astrophys. J.* **159** (1970) 379–403.
- [28] F. Zwicky, *Die Rotverschiebung von extragalaktischen Nebeln*, *Helv. Phys. Acta* **6** (1933) 110–127.
- [29] F. Zwicky, *Republication of: The redshift of extragalactic nebulae*, *General Relativity and Gravitation* **41** (2009), no. 1 207–224.
- [30] A. A. Penzias and R. W. Wilson, *A Measurement of Excess Antenna Temperature at 4080 Mc/s.*, *The Astrophysical Journal* **142** (1965) 419–421.
- [31] P. J. E. Peebles and J. T. Yu, *Primeval adiabatic perturbation in an expanding universe*, *Astrophys. J.* **162** (1970) 815–836.
- [32] P. Peebles, *Large scale background temperature and mass fluctuations due to scale invariant primeval perturbations*, *Astrophys. J. Lett.* **263** (1982) L1–L5.
- [33] K. Gebhardt et al., *A Relationship between nuclear black hole mass and galaxy velocity dispersion*, *Astrophys. J. Lett.* **539** (2000) L13.
- [34] L. Ferrarese and D. Merritt, *A Fundamental relation between supermassive black holes and their host galaxies*, *Astrophys. J. Lett.* **539** (2000) L9.
- [35] **HST** Collaboration, W. Freedman et al., *Final results from the Hubble Space Telescope key project to measure the Hubble constant*, *Astrophys. J.* **553** (2001) 47–72.

- [36] **SDSS** Collaboration, D. J. Eisenstein et al., *Detection of the Baryon Acoustic Peak in the Large-Scale Correlation Function of SDSS Luminous Red Galaxies*, *Astrophys. J.* **633** (2005) 560–574.
- [37] I. Zehavi, Z. Zheng, D. H. Weinberg, M. R. Blanton, N. A. Bahcall, A. A. Berlind, J. Brinkmann, J. A. Frieman, J. E. Gunn, R. H. Lupton, and et al., *Galaxy Clustering in the Completed SDSS Redshift Survey: The Dependence on Color and Luminosity*, *The Astrophysical Journal* **736** (2011), no. 1 59.
- [38] G. F. Smoot, *COBE observations and results*, *AIP Conf. Proc.* **476** (1999), no. 1 1–10.
- [39] C. L. Bennett, D. Larson, J. L. Weiland, N. Jarosik, G. Hinshaw, N. Odegard, K. M. Smith, R. S. Hill, B. Gold, M. Halpern, and et al., *Nine-Year Wilkinson Microwave Anisotropy Probe (WMAP) Observations: Final Maps and Results*, *The Astrophysical Journal Supplement Series* **208** (2013), no. 2 20.
- [40] **Planck** Collaboration, P. A. R. Ade et al., *Planck 2015 results. XIII. Cosmological parameters*, *Astron. Astrophys.* **594** (2016) A13.
- [41] **Planck** Collaboration, N. Aghanim et al., *Planck 2018 results. VI. Cosmological parameters*, 2018.
- [42] B. C. Barish and R. Weiss, *LIGO and the detection of gravitational waves.*, *Physics Today* **52** (1999), no. 10 44–50.
- [43] **LIGO Scientific, Virgo** Collaboration, B. Abbott et al., *Observation of Gravitational Waves from a Binary Black Hole Merger*, *Phys. Rev. Lett.* **116** (2016), no. 6 061102.
- [44] **LIGO Scientific, Virgo** Collaboration, B. Abbott et al., *GW170817: Observation of Gravitational Waves from a Binary Neutron Star Inspiral*, *Phys. Rev. Lett.* **119** (2017), no. 16 161101.
- [45] **Euclid** Collaboration, R. Scaramella et al., *Euclid space mission: a cosmological challenge for the next 15 years*, *IAU Symp.* **306** (2014) 375–378.
- [46] J. Green et al., *Wide-Field InfraRed Survey Telescope (WFIRST) Final Report*, 2012.
- [47] S. M. Carroll, *Lecture notes on general relativity*, 1997.

- [48] T. P. Sotiriou and V. Faraoni, *f(R) Theories Of Gravity*, *Rev. Mod. Phys.* **82** (2010) 451–497.
- [49] S. Weinberg, *Gravitation and cosmology: principles and applications of the general theory of relativity*. Wiley, 1972.
- [50] D. W. Hogg, *Distance measures in cosmology*, 1999.
- [51] E. Di Valentino, A. Melchiorri, and J. Silk, *Planck evidence for a closed Universe and a possible crisis for cosmology*, *Nat. Astron.* (2019).
- [52] D. Baumann, *TASI Lectures on Inflation*, 2009.
- [53] W. H. Kinney, *TASI Lectures on Inflation*, 2009.
- [54] J. M. Cline, *TASI Lectures on Early Universe Cosmology: Inflation, Baryogenesis and Dark Matter*, *PoS TASI2018* (2019) 001.
- [55] P.-H. Chavanis, *Cosmology with a stiff matter era*, *Phys. Rev. D* **92** (2015), no. 10 103004.
- [56] S. Dutta and R. J. Scherrer, *Big Bang nucleosynthesis with a stiff fluid*, *Phys. Rev. D* **82** (2010) 083501.
- [57] A. Galiakhmetov, *Stiff Fluid in Accelerated Universes with Torsion*, *Journal of Gravity* **2013** (2013).
- [58] **Supernova Search Team** Collaboration, A. G. Riess et al., *Observational evidence from supernovae for an accelerating universe and a cosmological constant*, *Astron. J.* **116** (1998) 1009–1038.
- [59] S. Perlmutter, *Supernovae, Dark Energy, and the Accelerating Universe*, *Physics Today* **56** (2003) 53.
- [60] C. Blake et al., *The WiggleZ Dark Energy Survey: Joint measurements of the expansion and growth history at $z < 1$* , *Mon. Not. Roy. Astron. Soc.* **425** (2012) 405–414.
- [61] D. Parkinson et al., *The WiggleZ Dark Energy Survey: Final data release and cosmological results*, *Phys. Rev.* **D86** (2012) 103518.

- [62] E. A. Kazin et al., *The WiggleZ Dark Energy Survey: improved distance measurements to $z = 1$ with reconstruction of the baryonic acoustic feature*, *Mon. Not. Roy. Astron. Soc.* **441** (2014), no. 4 3524–3542.
- [63] **SDSS-III** Collaboration, S. Alam et al., *The Eleventh and Twelfth Data Releases of the Sloan Digital Sky Survey: Final Data from SDSS-III*, *Astrophys. J. Suppl.* **219** (2015), no. 1 12.
- [64] F. Beutler, C. Blake, J. Koda, F. Marin, H.-J. Seo, A. J. Cuesta, and D. P. Schneider, *The BOSS–WiggleZ overlap region – I. Baryon acoustic oscillations*, *Mon. Not. Roy. Astron. Soc.* **455** (2016), no. 3 3230–3248.
- [65] **BOSS** Collaboration, S. Alam et al., *The clustering of galaxies in the completed SDSS-III Baryon Oscillation Spectroscopic Survey: cosmological analysis of the DR12 galaxy sample*, *Submitted to: Mon. Not. Roy. Astron. Soc.* (2016).
- [66] T. Tröster et al., *Cosmology from large-scale structure: Constraining Λ CDM with BOSS*, *Astron. Astrophys.* **633** (2020) L10.
- [67] **LIGO Scientific, Virgo** Collaboration, B. Abbott et al., *Observation of Gravitational Waves from a Binary Black Hole Merger*, *Phys. Rev. Lett.* **116** (2016), no. 6 061102.
- [68] **LIGO Scientific, Virgo, 1M2H, Dark Energy Camera GW-E, DES, DLT40, Las Cumbres Observatory, VINROUGE, MASTER** Collaboration, B. Abbott et al., *A gravitational-wave standard siren measurement of the Hubble constant*, *Nature* **551** (2017), no. 7678 85–88.
- [69] P. Bull et al., *Beyond Λ CDM: Problems, solutions, and the road ahead*, *Phys. Dark Univ.* **12** (2016) 56–99.
- [70] R. H. Brandenberger, *The early universe and observational cosmology*, *Lecture Notes in Physics* (2004).
- [71] V. F. Mukhanov, H. Feldman, and R. H. Brandenberger, *Theory of cosmological perturbations. Part 1. Classical perturbations. Part 2. Quantum theory of perturbations. Part 3. Extensions*, *Phys. Rept.* **215** (1992) 203–333.
- [72] V. Mukhanov, *Physical Foundations of Cosmology*. Cambridge University Press, Oxford, 2005.

- [73] Y. Gong, *The growth factor parameterization and modified gravity*, *Phys. Rev. D* **78** (2008) 123010.
- [74] P. J. E. Peebles, *Principles of Physical Cosmology*. Princeton University Press, 1993.
- [75] E. Macaulay, I. K. Wehus, and H. K. Eriksen, *Lower Growth Rate from Recent Redshift Space Distortion Measurements than Expected from Planck*, *Phys. Rev. Lett.* **111** (2013), no. 16 161301.
- [76] N. MacCrann, J. Zuntz, S. Bridle, B. Jain, and M. R. Becker, *Cosmic Discordance: Are Planck CMB and CFHTLenS weak lensing measurements out of tune?*, *Mon. Not. Roy. Astron. Soc.* **451** (2015), no. 3 2877–2888.
- [77] R. A. Battye, T. Charnock, and A. Moss, *Tension between the power spectrum of density perturbations measured on large and small scales*, *Phys. Rev. D* **91** (2015), no. 10 103508.
- [78] S. Nesseris, G. Pantazis, and L. Perivolaropoulos, *Tension and constraints on modified gravity parametrizations of $G_{\text{eff}}(z)$ from growth rate and Planck data*, *Phys. Rev. D* **96** (2017), no. 2 023542.
- [79] H. Hildebrandt et al., *KiDS+VIKING-450: Cosmic shear tomography with optical and infrared data*, *Astron. Astrophys.* **633** (2020) A69.
- [80] A. Quelle and A. L. Maroto, *On the tension between growth rate and CMB data*, *Eur. Phys. J. C* **80** (2020), no. 5 369.
- [81] J. L. Bernal, L. Verde, and A. G. Riess, *The trouble with H_0* , *JCAP* **10** (2016) 019.
- [82] A. G. Riess et al., *Cepheid Calibrations of Modern Type Ia Supernovae: Implications for the Hubble Constant*, *Astrophys. J. Suppl.* **183** (2009) 109–141.
- [83] A. G. Riess et al., *A Redetermination of the Hubble Constant with the Hubble Space Telescope from a Differential Distance Ladder*, *Astrophys. J.* **699** (2009) 539–563.

- [84] A. G. Riess, S. Casertano, W. Yuan, L. M. Macri, and D. Scolnic, *Large Magellanic Cloud Cepheid Standards Provide a 1% Foundation for the Determination of the Hubble Constant and Stronger Evidence for Physics beyond Λ CDM*, *Astrophys. J.* **876** (2019), no. 1 85.
- [85] M. Reid, D. Pesce, and A. Riess, *An Improved Distance to NGC 4258 and its Implications for the Hubble Constant*, *Astrophys. J. Lett.* **886** (2019), no. 2 L27.
- [86] G. C.-F. Chen et al., *A SHARP view of H0LiCOW: H_0 from three time-delay gravitational lens systems with adaptive optics imaging*, *Mon. Not. Roy. Astron. Soc.* **490** (2019), no. 2 1743–1773.
- [87] K. C. Wong et al., *H0LiCOW XIII. A 2.4% measurement of H_0 from lensed quasars: 5.3σ tension between early and late-Universe probes*, 2019.
- [88] S. Suyu et al., *H0LiCOW – I. H_0 Lenses in COSMOGRAIL’s Wellspring: program overview*, *Mon. Not. Roy. Astron. Soc.* **468** (2017), no. 3 2590–2604.
- [89] J. Frieman, M. Turner, and D. Huterer, *Dark Energy and the Accelerating Universe*, *Ann. Rev. Astron. Astrophys.* **46** (2008) 385–432.
- [90] M. Li, X.-D. Li, S. Wang, and Y. Wang, *Dark Energy*, *Commun. Theor. Phys.* **56** (2011) 525–604.
- [91] A. R. Cooray and D. Huterer, *Gravitational lensing as a probe of quintessence*, *Astrophys. J. Lett.* **513** (1999) L95–L98.
- [92] G. Efstathiou, *Constraining the equation of state of the universe from distant type Ia supernovae and cosmic microwave background anisotropies*, *Mon. Not. Roy. Astron. Soc.* **310** (1999) 842–850.
- [93] P. Astier, *Can luminosity distance measurements probe the equation of state of dark energy*, *Phys. Lett. B* **500** (2001) 8–15.
- [94] M. Goliath, R. Amanullah, P. Astier, A. Goobar, and R. Pain, *Supernovae and the nature of the dark energy*, *Astron. Astrophys.* **380** (2001) 6–18.
- [95] M. Chevallier and D. Polarski, *Accelerating universes with scaling dark matter*, *Int. J. Mod. Phys. D* **10** (2001) 213–224.

- [96] E. V. Linder, *Exploring the expansion history of the universe*, *Phys. Rev. Lett.* **90** (2003) 091301.
- [97] J. Weller and A. Albrecht, *Future supernovae observations as a probe of dark energy*, *Phys. Rev.* **D65** (2002) 103512.
- [98] V. Sahni, T. D. Saini, A. A. Starobinsky, and U. Alam, *Statefinder: A New geometrical diagnostic of dark energy*, *JETP Lett.* **77** (2003) 201–206.
- [99] T. Padmanabhan and T. R. Choudhury, *A theoretician’s analysis of the supernova data and the limitations in determining the nature of dark energy*, *Mon. Not. Roy. Astron. Soc.* **344** (2003) 823–834.
- [100] C. Wetterich, *Phenomenological parameterization of quintessence*, *Phys. Lett.* **B594** (2004) 17–22.
- [101] H. K. Jassal, J. S. Bagla, and T. Padmanabhan, *WMAP constraints on low redshift evolution of dark energy*, *Mon. Not. Roy. Astron. Soc.* **356** (2005) L11–L16.
- [102] **WMAP** Collaboration, E. Komatsu et al., *Five-Year Wilkinson Microwave Anisotropy Probe (WMAP) Observations: Cosmological Interpretation*, *Astrophys. J. Suppl.* **180** (2009) 330–376.
- [103] Y. Wang, *Model-Independent Distance Measurements from Gamma-Ray Bursts and Constraints on Dark Energy*, *Phys. Rev.* **D78** (2008) 123532.
- [104] J.-Z. Ma and X. Zhang, *Probing the dynamics of dark energy with novel parametrizations*, *Phys. Lett.* **B699** (2011) 233–238.
- [105] E. M. Barboza, B. Santos, F. E. M. Costa, and J. S. Alcaniz, *Scalar field description of a parametric model of dark energy*, *Phys. Rev.* **D85** (2012) 107304.
- [106] I. Sendra and R. Lazkoz, *SN and BAO constraints on (new) polynomial dark energy parametrizations: current results and forecasts*, *Mon. Not. Roy. Astron. Soc.* **422** (2012) 776–793.
- [107] L. Amendola and S. Tsujikawa, *Dark Energy: Theory and Observations*, 2010.
- [108] M. Doran and G. Robbers, *Early dark energy cosmologies*, *JCAP* **0606** (2006) 026.

- [109] V. Pettorino, L. Amendola, and C. Wetterich, *How early is early dark energy?*, *Phys. Rev.* **D87** (2013) 083009.
- [110] T. Karwal and M. Kamionkowski, *Early dark energy, the Hubble-parameter tension, and the string axiverse*, *Phys. Rev.* **D94** (2016), no. 10 103523.
- [111] I. Zlatev, L. M. Wang, and P. J. Steinhardt, *Quintessence, cosmic coincidence, and the cosmological constant*, *Phys. Rev. Lett.* **82** (1999) 896–899.
- [112] B. Ratra and P. Peebles, *Cosmological Consequences of a Rolling Homogeneous Scalar Field*, *Phys. Rev. D* **37** (1988) 3406.
- [113] R. R. Caldwell, R. Dave, and P. J. Steinhardt, *Cosmological imprint of an energy component with general equation of state*, *Phys. Rev. Lett.* **80** (1998) 1582–1585.
- [114] S. Tsujikawa, *Quintessence: A Review*, *Class. Quant. Grav.* **30** (2013) 214003.
- [115] T. Chiba, A. De Felice, and S. Tsujikawa, *Observational constraints on quintessence: thawing, tracker, and scaling models*, *Phys. Rev. D* **87** (2013), no. 8 083505.
- [116] J.-B. Durrive, J. Ooba, K. Ichiki, and N. Sugiyama, *Updated observational constraints on quintessence dark energy models*, *Phys. Rev. D* **97** (2018), no. 4 043503.
- [117] C. Armendariz-Picon, V. F. Mukhanov, and P. J. Steinhardt, *A Dynamical solution to the problem of a small cosmological constant and late time cosmic acceleration*, *Phys. Rev. Lett.* **85** (2000) 4438–4441.
- [118] L. Amendola, G. Camargo Campos, and R. Rosenfeld, *Consequences of dark matter-dark energy interaction on cosmological parameters derived from SNIa data*, *Phys. Rev.* **D75** (2007) 083506.
- [119] R.-J. Yang and X. Ting, *Observational Constraints on Purely Kinetic k -Essence Dark Energy Models*, *Chinese Physics Letters* **26** (2009) 089501.
- [120] R.-J. Yang and Z. Shuang-Nan, *Theoretical Constraint on Purely Kinetic k -Essence*, *Chinese Physics Letters* **25** (2008) 344.
- [121] M. Malquarti, E. J. Copeland, A. R. Liddle, and M. Trodden, *A New view of k -essence*, *Phys. Rev. D* **67** (2003) 123503.

- [122] C. Deffayet, X. Gao, D. Steer, and G. Zahariade, *From k-essence to generalised Galileons*, *Phys. Rev. D* **84** (2011) 064039.
- [123] R. J. Scherrer, *Purely kinetic k-essence as unified dark matter*, *Phys. Rev. Lett.* **93** (2004) 011301.
- [124] E. Babichev, V. Mukhanov, and A. Vikman, *k-Essence, superluminal propagation, causality and emergent geometry*, *JHEP* **02** (2008) 101.
- [125] L. P. Chimento, *Extended tachyon field, Chaplygin gas and solvable k-essence cosmologies*, *Phys. Rev. D* **69** (2004) 123517.
- [126] R. de Putter and E. V. Linder, *Kinetic k-essence and Quintessence*, *Astropart. Phys.* **28** (2007) 263–272.
- [127] H. Stefancic, *Generalized phantom energy*, *Phys. Lett.* **B586** (2004) 5–10.
- [128] M. P. Dabrowski, T. Stachowiak, and M. Szydlowski, *Phantom cosmologies*, *Phys. Rev.* **D68** (2003) 103519.
- [129] P.-Y. Wang, C.-W. Chen, and P. Chen, *Confronting Phantom Dark Energy with Observations*, 2012.
- [130] H. Mohseni Sadjadi and M. Alimohammadi, *Transition from quintessence to phantom phase in quintom model*, *Phys. Rev.* **D74** (2006) 043506.
- [131] D. Huterer and A. Cooray, *Uncorrelated estimates of dark energy evolution*, *Phys. Rev. D* **71** (2005) 023506.
- [132] B. Feng, X.-L. Wang, and X.-M. Zhang, *Dark energy constraints from the cosmic age and supernova*, *Phys. Lett. B* **607** (2005) 35–41.
- [133] P. S. Corasaniti, M. Kunz, D. Parkinson, E. Copeland, and B. Bassett, *The Foundations of observing dark energy dynamics with the Wilkinson Microwave Anisotropy Probe*, *Phys. Rev. D* **70** (2004) 083006.
- [134] A. Upadhye, M. Ishak, and P. J. Steinhardt, *Dynamical dark energy: Current constraints and forecasts*, *Phys. Rev. D* **72** (2005) 063501.
- [135] **SDSS** Collaboration, U. Seljak et al., *Cosmological parameter analysis including SDSS Ly-alpha forest and galaxy bias: Constraints on the primordial spectrum of fluctuations, neutrino mass, and dark energy*, *Phys. Rev. D* **71** (2005) 103515.

- [136] X.-m. Zhang, *Interacting dark energy, 12th International Conference on Supersymmetry and Unification of Fundamental Interactions (SUSY 04)* (10, 2004) 73–85.
- [137] G.-B. Zhao, J.-Q. Xia, M. Li, B. Feng, and X. Zhang, *Perturbations of the quintom models of dark energy and the effects on observations*, *Phys. Rev. D* **72** (2005) 123515.
- [138] Z.-K. Guo, Y.-S. Piao, X.-M. Zhang, and Y.-Z. Zhang, *Cosmological evolution of a quintom model of dark energy*, *Phys. Lett. B* **608** (2005) 177–182.
- [139] R. R. Caldwell and M. Doran, *Dark-energy evolution across the cosmological-constant boundary*, *Phys. Rev. D* **72** (2005) 043527.
- [140] X.-F. Zhang, H. Li, Y.-S. Piao, and X.-M. Zhang, *Two-field models of dark energy with equation of state across -1*, *Mod. Phys. Lett. A* **21** (2006) 231–242.
- [141] H. Wei, R.-G. Cai, and D.-F. Zeng, *Hessence: A New view of quintom dark energy*, *Class. Quant. Grav.* **22** (2005) 3189–3202.
- [142] R.-G. Cai, H.-S. Zhang, and A. Wang, *Crossing $w=-1$ in Gauss-Bonnet brane world with induced gravity*, *Commun. Theor. Phys.* **44** (2005) 948.
- [143] A. A. Andrianov, F. Cannata, and A. Y. Kamenshchik, *Smooth dynamical crossing of the phantom divide line of a scalar field in simple cosmological models*, *Phys. Rev. D* **72** (2005) 043531.
- [144] H. Stefancic, *Dark energy transition between quintessence and phantom regimes - An Equation of state analysis*, *Phys. Rev. D* **71** (2005) 124036.
- [145] Xia, Jun-Qing and Feng, Bo and Zhang, Xin-Min, *Constraints on oscillating quintom from supernova, microwave background and galaxy clustering*, *Mod. Phys. Lett. A* **20** (2005) 2409–2416.
- [146] B. J. Li, M.-C. Chu, K. Cheung, and A. Tang, *Dark energy as a signature of extra dimensions*, 1, 2005.
- [147] R. Lazkoz and G. Leon, *Quintom cosmologies admitting either tracking or phantom attractors*, *Phys. Lett. B* **638** (2006) 303–309.
- [148] C. Gao, X. Chen, and Y.-G. Shen, *A Holographic Dark Energy Model from Ricci Scalar Curvature*, *Phys. Rev. D* **79** (2009) 043511.

- [149] A. G. Cohen, D. B. Kaplan, and A. E. Nelson, *Effective field theory, black holes, and the cosmological constant*, *Phys. Rev. Lett.* **82** (1999) 4971–4974.
- [150] K. Y. Kim, H. W. Lee, and Y. S. Myung, *On the Ricci dark energy model*, *Gen. Rel. Grav.* **43** (2011) 1095–1101.
- [151] S. del Campo, J. C. Fabris, R. Herrera, and W. Zimdahl, *Cosmology with Ricci dark energy*, *Phys. Rev. D* **87** (2013), no. 12 123002.
- [152] L. Xu, W. Li, and J. Lu, *Cosmic Constraint on Ricci Dark Energy Model*, *Mod. Phys. Lett. A* **24** (2009) 1355–1360.
- [153] M. Suwa and T. Nihei, *Observational constraints on the interacting Ricci dark energy model*, *Physical Review D* **81** (2010), no. 2.
- [154] M. Suwa, K. Kobayashi, and H. Oshima, *The interacting generalized Ricci dark energy model in non-flat universe*, *J. Mod. Phys.* **6** (2015) 327.
- [155] V. Salvatelli, A. Marchini, L. Lopez-Honorez, and O. Mena, *New constraints on Coupled Dark Energy from the Planck satellite experiment*, *Phys. Rev. D* **88** (2013), no. 2 023531.
- [156] W. Yang, H. Li, Y. Wu, and J. Lu, *Cosmological constraints on coupled dark energy*, *JCAP* **10** (2016) 007.
- [157] A. Yu. Kamenshchik, U. Moschella, and V. Pasquier, *An Alternative to quintessence*, *Phys. Lett.* **B511** (2001) 265–268.
- [158] B. Pourhassan and E. O. Kahya, *FRW cosmology with the extended Chaplygin gas*, *Adv. High Energy Phys.* **2014** (2014) 231452.
- [159] J. Colistete, Roberto, J. Fabris, and S. Goncalves, *Bayesian statistics and parameter constraints on the generalized Chaplygin gas model using SNe Ia data*, *Int. J. Mod. Phys. D* **14** (2005) 775–796.
- [160] J. Colistete, Roberto, J. Fabris, S. Goncalves, and P. de Souza, *Bayesian analysis of the Chaplygin gas and cosmological constant models using the SNe Ia data*, *Int. J. Mod. Phys. D* **13** (2004) 669–694.
- [161] K. Liao, Y. Pan, and Z.-H. Zhu, *Observational constraints on the new generalized Chaplygin gas model*, *Research in Astronomy and Astrophysics* **13** (2013), no. 2 159–169.

- [162] B. C. Paul, P. Thakur, and A. Beesham, *Constraints on modified Chaplygin gas from large scale structure*, 2016.
- [163] D. Panigrahi, B. Paul, and S. Chatterjee, *Constraining Modified Chaplygin gas parameters*, *Grav. Cosmol.* **21** (2015) 83.
- [164] A. Hernandez-Almada, J. Magana, M. A. Garcia-Aspeitia, and V. Motta, *Cosmological constraints on alternative model to Chaplygin fluid revisited*, *Eur. Phys. J.* **C79** (2019), no. 1 12.
- [165] J. Lu, L. Xu, Y. Wu, and M. Liu, *Combined constraints on modified Chaplygin gas model from cosmological observed data: Markov Chain Monte Carlo approach*, *General Relativity and Gravitation* **43** (2010), no. 3 819–832.
- [166] V. K. Oikonomou, *Generalized logarithmic equation of state in classical and loop quantum cosmology dark energy–dark matter coupled systems*, *Annals Phys.* **409** (2019) 167934.
- [167] J. Bertheaud, J. Pasquet, T. Schücker, and A. Tilquin, *On a quadratic equation of state and a universe mildly bouncing above the Planck temperature*, 2018.
- [168] G. P. Singh and B. K. Bishi, *Bianchi type-I Universe with Cosmological constant and quadratic equation of state in $f(R, T)$ modified gravity*, *Adv. High Energy Phys.* **2015** (2015) 816826.
- [169] S. Chen, G. W. Gibbons, and Y. Yang, *Explicit Integration of Friedmann’s Equation with Nonlinear Equations of State*, *JCAP* **1505** (2015), no. 05 020.
- [170] S. Capozziello, V. Cardone, E. Elizalde, S. Nojiri, and S. Odintsov, *Observational constraints on dark energy with generalized equations of state*, *Phys. Rev. D* **73** (2006) 043512.
- [171] K. N. Ananda and M. Bruni, *Cosmo-dynamics and dark energy with non-linear equation of state: a quadratic model*, *Phys. Rev.* **D74** (2006) 023523.
- [172] J. Dutta, S. Chakraborty, and M. Ansari, *Non linear equation of state and effective phantom divide in brane models*, *Int. J. Theor. Phys.* **49** (2010) 2680–2690.

- [173] G. Sharov, *Observational constraints on cosmological models with Chaplygin gas and quadratic equation of state*, *JCAP* **06** (2016) 023.
- [174] X. Li and A. Shafieloo, *Generalised Emergent Dark Energy Model: Confronting Λ and PEDE*, 2020.
- [175] A. Hernández-Almada, G. Leon, J. Magaña, M. A. García-Aspeitia, and V. Motta, *Generalized Emergent Dark Energy: observational Hubble data constraints and stability analysis*, 2020.
- [176] H. Weyl, *Gravitation und Elektrizitaet*, *Sitzungsberichte der preuß.Akademie d. Wissenschaften*, **30** (1918).
- [177] A. Eddington, *The Mathematical Theory of Relativity*. Cambridge University Press, 1924.
- [178] V. A. A. Sanghai and T. Clifton, *Parameterized Post-Newtonian Cosmology*, *Class. Quant. Grav.* **34** (2017), no. 6 065003.
- [179] P. Jordan, *Schwerkraft und Weltall: Grundlagen d. theoret. Kosmologie. Mit 13 Abb.* Die Wissenschaft. Vieweg, 1955.
- [180] Y. Fujii and K.-i. Maeda, *The Scalar-Tensor Theory of Gravitation*. Cambridge Monographs on Mathematical Physics. Cambridge University Press, 2003.
- [181] P. G. Bergmann, *Comments on the scalar tensor theory*, *Int. J. Theor. Phys.* **1** (1968) 25–36.
- [182] J. Nordtvedt, Kenneth, *Post-Newtonian Metric for a General Class of Scalar-Tensor Gravitational Theories and Observational Consequences.*, *apj* **161** (1970) 1059.
- [183] C. Brans and R. H. Dicke, *Mach's principle and a relativistic theory of gravitation*, *Phys. Rev.* **124** (1961) 925–935. [,142(1961)].
- [184] R. Nagata, T. Chiba, and N. Sugiyama, *WMAP constraints on scalar- tensor cosmology and the variation of the gravitational constant*, *Phys. Rev. D* **69** (2004) 083512.

- [185] V. Acquaviva, C. Baccigalupi, S. M. Leach, A. R. Liddle, and F. Perrotta, *Structure formation constraints on the Jordan-Brans-Dicke theory*, *Phys. Rev. D* **71** (2005) 104025.
- [186] F. Wu and X. Chen, *Cosmic microwave background with Brans-Dicke gravity II: constraints with the WMAP and SDSS data*, *Phys. Rev. D* **82** (2010) 083003.
- [187] K. Arai, M. Hashimoto, and T. Fukui, *Primordial nucleosynthesis in the Brans-Dicke theory with a variable cosmological term*, *Astronomy and Astrophysics* **179** (1987) 17–22.
- [188] J. Casas, J. García-Bellido, and M. Quirós, *Updating nucleosynthesis bounds on Jordan-Brans-Dicke theories of gravity*, *Physics Letters B* **278** (1992), no. 1-2 94–96.
- [189] T. Damour and C. Gundlach, *Nucleosynthesis constraints on an extended Jordan-Brans-Dicke theory*, *Physical review D: Particles and fields* **43** (1991) 3873–3877.
- [190] A. Serna, R. Dominguez-Tenreiro, and G. Yepes, *Primordial Nucleosynthesis Bounds on the Brans-Dicke Theory*, *The Astrophysical Journal* **391** (1992) 433.
- [191] G. W. Horndeski, *Second-order scalar-tensor field equations in a four-dimensional space*, *Int. J. Theor. Phys.* **10** (1974) 363–384.
- [192] C. Charmousis, E. J. Copeland, A. Padilla, and P. M. Saffin, *General second order scalar-tensor theory, self tuning, and the Fab Four*, *Phys. Rev. Lett.* **108** (2012) 051101.
- [193] T. Kobayashi, M. Yamaguchi, and J. Yokoyama, *Generalized G-inflation: Inflation with the most general second-order field equations*, *Prog. Theor. Phys.* **126** (2011) 511–529.
- [194] A. Barreira, B. Li, C. M. Baugh, and S. Pascoli, *Linear perturbations in Galileon gravity models*, *Phys. Rev. D* **86** (2012) 124016.
- [195] J. Khoury and A. Weltman, *Chameleon fields: Awaiting surprises for tests of gravity in space*, *Phys. Rev. Lett.* **93** (2004) 171104.

- [196] J. Khoury and A. Weltman, *Chameleon cosmology*, *Phys. Rev. D* **69** (2004) 044026.
- [197] C. M. Will and J. Nordtvedt, Kenneth, *Conservation Laws and Preferred Frames in Relativistic Gravity. I. Preferred-Frame Theories and an Extended PPN Formalism*, *Astrophysical Journal* **177** (1972) 757.
- [198] J. Nordtvedt, Kenneth and C. M. Will, *Conservation Laws and Preferred Frames in Relativistic Gravity. II. Experimental Evidence to Rule Out Preferred-Frame Theories of Gravity*, *apj* **177** (1972) 775.
- [199] T. Jacobson, *Einstein-aether gravity: A Status report*, *PoS QG-PH* (2007) 020.
- [200] S. Kanno and J. Soda, *Lorentz Violating Inflation*, *Phys. Rev. D* **74** (2006) 063505.
- [201] E. A. Lim, *Can we see Lorentz-violating vector fields in the CMB?*, *Phys. Rev. D* **71** (2005) 063504.
- [202] T. Zlosnik, P. Ferreira, and G. Starkman, *Growth of structure in theories with a dynamical preferred frame*, *Phys. Rev. D* **77** (2008) 084010.
- [203] A. Halle and H. Zhao, *Perturbations In A Non-Uniform Dark Energy Fluid: Equations Reveal Effects of Modified Gravity and Dark Matter*, *Astrophys. J. Suppl.* **177** (2008) 1.
- [204] J. Zuntz, T. Zlosnik, F. Bourliot, P. Ferreira, and G. Starkman, *Vector field models of modified gravity and the dark sector*, *Phys. Rev. D* **81** (2010) 104015.
- [205] J. Magueijo, *Bimetric varying speed of light theories and primordial fluctuations*, *Phys. Rev. D* **79** (2009) 043525.
- [206] J. Moffat, *Bimetric gravity theory, varying speed of light and the dimming of supernovae*, *Int. J. Mod. Phys. D* **12** (2003) 281–298.
- [207] N. Rosen, *A bi-metric theory of gravitation*, *General Relativity and Gravitation* **4** (1973), no. 6 435–447.
- [208] I. T. Drummond, *Bimetric gravity and [dark matter]*, *Phys. Rev. D* **63** (2001) 043503.

- [209] C. de Rham and G. Gabadadze, *Generalization of the Fierz-Pauli Action*, *Phys. Rev. D* **82** (2010) 044020.
- [210] C. de Rham, *Massive Gravity*, *Living Rev. Rel.* **17** (2014) 7.
- [211] Y. Akrami, T. S. Koivisto, D. F. Mota, and M. Sandstad, *Bimetric gravity doubly coupled to matter: theory and cosmological implications*, *JCAP* **10** (2013) 046.
- [212] F. Koennig, Y. Akrami, L. Amendola, M. Motta, and A. R. Solomon, *Stable and unstable cosmological models in bimetric massive gravity*, *Phys. Rev. D* **90** (2014) 124014.
- [213] T. Damour, I. I. Kogan, and A. Papazoglou, *Nonlinear bigravity and cosmic acceleration*, *Phys. Rev. D* **66** (2002) 104025.
- [214] M. Banados, *Eddington-Born-Infeld action for dark matter and dark energy*, *Phys. Rev. D* **77** (2008) 123534.
- [215] M. Banados, A. Gomberoff, D. C. Rodrigues, and C. Skordis, *A Note on bigravity and dark matter*, *Phys. Rev. D* **79** (2009) 063515.
- [216] M. Banados, P. Ferreira, and C. Skordis, *Eddington-Born-Infeld gravity and the large scale structure of the Universe*, *Phys. Rev. D* **79** (2009) 063511.
- [217] A. Schmidt-May and M. von Strauss, *Recent developments in bimetric theory*, *J. Phys. A* **49** (2016), no. 18 183001.
- [218] C. Skordis, *The tensor-vector-scalar theory and its cosmology*, *Classical and Quantum Gravity* **26** (2009), no. 14 143001.
- [219] D. Lovelock, *The Einstein Tensor and Its Generalizations*, *Journal of Mathematical Physics* **12** (1971), no. 3 498–501.
- [220] D. Lovelock, *The Four-Dimensionality of Space and the Einstein Tensor*, *Journal of Mathematical Physics* **13** (1972), no. 6 874–876.
- [221] S. Nojiri and S. D. Odintsov, *Introduction to modified gravity and gravitational alternative for dark energy*, *eConf C0602061* (2006) 06. [Int. J. Geom. Meth. Mod. Phys.4,115(2007)].

- [222] H.-J. Schmidt, *Fourth order gravity: Equations, history, and applications to cosmology*, *eConf* **C0602061** (2006) 12.
- [223] T. P. Sotiriou and V. Faraoni, *f(R) Theories Of Gravity*, *Rev. Mod. Phys.* **82** (2010) 451–497.
- [224] A. De Felice and S. Tsujikawa, *f(R) theories*, *Living Rev. Rel.* **13** (2010) 3.
- [225] S. Capozziello and M. De Laurentis, *Extended Theories of Gravity*, *Phys. Rept.* **509** (2011) 167–321.
- [226] T. Clifton, P. G. Ferreira, A. Padilla, and C. Skordis, *Modified Gravity and Cosmology*, *Phys. Rept.* **513** (2012) 1–189.
- [227] T. Clifton and J. D. Barrow, *The Power of General Relativity*, *Phys. Rev. D* **72** (2005), no. 10 103005. [Erratum: *Phys.Rev.D* 90, 029902 (2014)].
- [228] A. W. Brookfield, C. van de Bruck, and L. M. Hall, *Viability of f(R) Theories with Additional Powers of Curvature*, *Phys. Rev. D* **74** (2006) 064028.
- [229] G. Lambiase and G. Scarpetta, *Baryogenesis in f(R): Theories of Gravity*, *Phys. Rev. D* **74** (2006) 087504.
- [230] J. D. Evans, L. M. Hall, and P. Caillol, *Standard Cosmological Evolution in a Wide Range of f(R) Models*, *Phys. Rev. D* **77** (2008) 083514.
- [231] S. Capozziello, V. F. Cardone, and A. Troisi, *Reconciling dark energy models with f(R) theories*, *Phys. Rev.* **D71** (2005) 043503.
- [232] T. Multamaki and I. Vilja, *Cosmological expansion and the uniqueness of gravitational action*, *Phys. Rev. D* **73** (2006) 024018.
- [233] S. Capozziello, S. Nojiri, S. Odintsov, and A. Troisi, *Cosmological viability of f(R)-gravity as an ideal fluid and its compatibility with a matter dominated phase*, *Phys. Lett. B* **639** (2006) 135–143.
- [234] A. de la Cruz-Dombriz and A. Dobado, *A f(R) gravity without cosmological constant*, *Phys. Rev. D* **74** (2006) 087501.
- [235] S. Carloni, R. Goswami, and P. K. Dunsby, *A new approach to reconstruction methods in f(R) gravity*, *Class. Quant. Grav.* **29** (2012) 135012.

- [236] S. Fay, S. Nesseris, and L. Perivolaropoulos, *Can $f(R)$ Modified Gravity Theories Mimic a Λ CDM Cosmology?*, *Phys. Rev. D* **76** (2007) 063504.
- [237] S. Nojiri and S. D. Odintsov, *Modified gravity as an alternative for Λ -CDM cosmology*, *J. Phys. A* **40** (2007) 6725–6732.
- [238] S. Ferraro, F. Schmidt, and W. Hu, *Cluster Abundance in $f(R)$ Gravity Models*, *Phys. Rev. D* **83** (2011) 063503.
- [239] K. Ananda, S. Carloni, and P. K. Dunsby, *A detailed analysis of structure growth in $f(R)$ theories of gravity*, *Class. Quant. Grav.* **26** (2009) 235018.
- [240] K. N. Ananda, S. Carloni, and P. K. Dunsby, *A characteristic signature of fourth order gravity*, *Springer Proc. Phys.* **137** (2011) 165–172.
- [241] F. Schmidt, A. Vikhlinin, and W. Hu, *Cluster Constraints on $f(R)$ Gravity*, *Phys. Rev. D* **80** (2009) 083505.
- [242] C.-G. Park, J.-c. Hwang, and H. Noh, *Constraints on a $f(R)$ gravity dark energy model with early scaling evolution*, *JCAP* **09** (2011) 038.
- [243] A. Nicolis, R. Rattazzi, and E. Trincherini, *The Galileon as a local modification of gravity*, *Phys. Rev.* **D79** (2009) 064036.
- [244] N. Arkani-Hamed, H.-C. Cheng, M. A. Luty, and S. Mukohyama, *Ghost condensation and a consistent infrared modification of gravity*, *JHEP* **05** (2004) 074.
- [245] G. Dvali, G. Gabadadze, and M. Porrati, *4-D gravity on a brane in 5-D Minkowski space*, *Phys. Lett. B* **485** (2000) 208–214.
- [246] C. Deffayet, S. Deser, and G. Esposito-Farese, *Generalized Galileons: All scalar models whose curved background extensions maintain second-order field equations and stress-tensors*, *Phys. Rev. D* **80** (2009) 064015.
- [247] C. Deffayet, G. Esposito-Farese, and A. Vikman, *Covariant Galileon*, *Phys. Rev.* **D79** (2009) 084003.
- [248] N. Chow and J. Khoury, *Galileon Cosmology*, *Phys. Rev. D* **80** (2009) 024037.
- [249] D. F. Mota, M. Sandstad, and T. Zlosnik, *Cosmology of the selfaccelerating third order Galileon*, *JHEP* **12** (2010) 051.

- [250] R. Gannouji and M. Sami, *Galileon gravity and its relevance to late time cosmic acceleration*, *Phys. Rev. D* **82** (2010) 024011.
- [251] A. Ali, R. Gannouji, and M. Sami, *Modified gravity a la Galileon: Late time cosmic acceleration and observational constraints*, *Phys. Rev. D* **82** (2010) 103015.
- [252] A. De Felice and S. Tsujikawa, *Cosmology of a covariant Galileon field*, *Phys. Rev. Lett.* **105** (2010) 111301.
- [253] S. Nesseris, A. De Felice, and S. Tsujikawa, *Observational constraints on Galileon cosmology*, *Phys. Rev. D* **82** (2010) 124054.
- [254] A. De Felice, R. Kase, and S. Tsujikawa, *Matter perturbations in Galileon cosmology*, *Phys. Rev. D* **83** (2011) 043515.
- [255] T. Clifton, P. G. Ferreira, A. Padilla, and C. Skordis, *Modified Gravity and Cosmology*, *Phys. Rept.* **513** (2012) 1–189.
- [256] C. de Rham and A. J. Tolley, *Mimicking Lambda with a spin-two ghost condensate*, *JCAP* **07** (2006) 004.
- [257] V. Kiselev, *Ghost condensate model of flat rotation curves*, 2004.
- [258] N. Frusciante and F. Pace, *Growth of structures and spherical collapse in the Galileon Ghost Condensate model*, 2020.
- [259] G. Nordstrom, *On the possibility of unifying the electromagnetic and the gravitational fields*, 1914.
- [260] T. Kaluza, *Zum Unitätsproblem der Physik*, *Sitzungsberichte der Königlich Preußischen Akademie der Wissenschaften (Berlin)* (1921) 966–972.
- [261] O. Klein, *Quantentheorie und fünfdimensionale Relativitätstheorie*, 1926.
- [262] O. Klein, *The Atomicity of Electricity as a Quantum Theory Law*, 1926.
- [263] K. Akama, *An Early Proposal of 'Brane World'*, *Lect. Notes Phys.* **176** (1982) 267–271.
- [264] V. Rubakov and M. Shaposhnikov, *Do We Live Inside a Domain Wall?*, *Phys. Lett. B* **125** (1983) 136–138.

- [265] N. Arkani-Hamed, S. Dimopoulos, and G. Dvali, *Phenomenology, astrophysics and cosmology of theories with submillimeter dimensions and TeV scale quantum gravity*, *Phys. Rev. D* **59** (1999) 086004.
- [266] I. Antoniadis, N. Arkani-Hamed, S. Dimopoulos, and G. Dvali, *New dimensions at a millimeter to a Fermi and superstrings at a TeV*, *Phys. Lett. B* **436** (1998) 257–263.
- [267] N. Arkani-Hamed, S. Dimopoulos, and G. Dvali, *The Hierarchy problem and new dimensions at a millimeter*, *Phys. Lett. B* **429** (1998) 263–272.
- [268] J. H. Schwarz, *Superstring Theory*, *Phys. Rept.* **89** (1982) 223–322.
- [269] C. Rovelli, *Loop quantum gravity*, *Living Rev. Rel.* **1** (1998) 1.
- [270] T. P. Sotiriou, V. Faraoni, and S. Liberati, *Theory of gravitation theories: A No-progress report*, *Int. J. Mod. Phys. D* **17** (2008) 399–423.
- [271] S. Tsujikawa, *Dark energy: investigation and modeling*, .
- [272] S. Tsujikawa, *Modified gravity models of dark energy*, *Lect. Notes Phys.* **800** (2010) 99–145.
- [273] S. Capozziello, M. De Laurentis, and V. Faraoni, *A Bird’s eye view of $f(R)$ -gravity*, *Open Astron. J.* **3** (2010) 49.
- [274] A. Joyce, L. Lombriser, and F. Schmidt, *Dark Energy Versus Modified Gravity*, *Ann. Rev. Nucl. Part. Sci.* **66** (2016) 95–122.
- [275] G. Gubitosi, F. Piazza, and F. Vernizzi, *The Effective Field Theory of Dark Energy*, *JCAP* **02** (2013) 032.
- [276] B. Hu, M. Raveri, N. Frusciante, and A. Silvestri, *EFTCAMB/EFTCosmoMC: Numerical Notes v3.0*, 2014.
- [277] L. Pogosian and A. Silvestri, *What can cosmology tell us about gravity? Constraining Horndeski gravity with Σ and μ* , *Phys. Rev. D* **94** (2016), no. 10 104014.
- [278] N. Frusciante and L. Perenon, *Effective Field Theory of Dark Energy: a Review*, 2019.

- [279] E. Berti et al., *Testing General Relativity with Present and Future Astrophysical Observations*, *Class. Quant. Grav.* **32** (2015) 243001.
- [280] T. Clifton, P. G. Ferreira, A. Padilla, and C. Skordis, *Modified Gravity and Cosmology*, *Phys. Rept.* **513** (2012) 1–189.
- [281] S. Capozziello, T. Harko, T. S. Koivisto, F. S. N. Lobo, and G. J. Olmo, *Hybrid metric-Palatini gravity*, *Universe* **1** (2015), no. 2 199–238.
- [282] S. Capozziello and M. Francaviglia, *Extended Theories of Gravity and their Cosmological and Astrophysical Applications*, *Gen. Rel. Grav.* **40** (2008) 357–420.
- [283] S. Capozziello, T. Harko, T. S. Koivisto, F. S. N. Lobo, and G. J. Olmo, *Hybrid metric-Palatini gravity*, *Universe* **1** (2015), no. 2 199–238.
- [284] A. A. Starobinsky, *Disappearing cosmological constant in $f(R)$ gravity*, *JETP Lett.* **86** (2007) 157–163.
- [285] W. Hu and I. Sawicki, *Models of $f(R)$ Cosmic Acceleration that Evade Solar-System Tests*, *Phys. Rev.* **D76** (2007) 064004.
- [286] S. A. Appleby and R. A. Battye, *Do consistent $F(R)$ models mimic General Relativity plus Λ ?*, *Phys. Lett.* **B654** (2007) 7–12.
- [287] S. Nojiri and S. D. Odintsov, *Newton law corrections and instabilities in $f(R)$ gravity with the effective cosmological constant epoch*, *Phys. Lett.* **B652** (2007) 343–348.
- [288] S. Nojiri and S. D. Odintsov, *Unifying inflation with LambdaCDM epoch in modified $f(R)$ gravity consistent with Solar System tests*, *Phys. Lett.* **B657** (2007) 238–245.
- [289] S. Tsujikawa, *Observational signatures of $f(R)$ dark energy models that satisfy cosmological and local gravity constraints*, *Phys. Rev.* **D77** (2008) 023507.
- [290] **Planck** Collaboration, Y. Akrami et al., *Planck 2018 results. X. Constraints on inflation*, 2018.
- [291] S. Capozziello, V. F. Cardone, S. Carloni, and A. Troisi, *Curvature quintessence matched with observational data*, *Int. J. Mod. Phys.* **D12** (2003) 1969–1982.

- [292] S. Capozziello, V. F. Cardone, and M. Francaviglia, *f(R) Theories of gravity in Palatini approach matched with observations*, *Gen. Rel. Grav.* **38** (2006) 711–734.
- [293] S. Capozziello, V. F. Cardone, and V. Salzano, *Cosmography of f(R) gravity*, *Phys. Rev.* **D78** (2008) 063504.
- [294] M. Bouhmadi-López, S. Capozziello, and V. F. Cardone, *Cosmography of f(R) - brane cosmology*, *Phys. Rev.* **D82** (2010) 103526.
- [295] M. Cataneo, D. Rapetti, F. Schmidt, A. B. Mantz, S. W. Allen, D. E. Applegate, P. L. Kelly, A. von der Linden, and R. G. Morris, *New constraints on f(R) gravity from clusters of galaxies*, *Phys. Rev.* **D92** (2015), no. 4 044009.
- [296] S. Basilakos, S. Nesseris, and L. Perivolaropoulos, *Observational constraints on viable f(R) parametrizations with geometrical and dynamical probes*, *Phys. Rev.* **D87** (2013), no. 12 123529.
- [297] A. Dev, D. Jain, S. Jhingan, S. Nojiri, M. Sami, and I. Thongkool, *Delicate f(R) gravity models with disappearing cosmological constant and observational constraints on the model parameters*, *Phys. Rev.* **D78** (2008) 083515.
- [298] R. C. Nunes, S. Pan, E. N. Saridakis, and E. M. C. Abreu, *New observational constraints on f(R) gravity from cosmic chronometers*, *JCAP* **1701** (2017), no. 01 005.
- [299] S. Capozziello, V. F. Cardone, S. Carloni, and A. Troisi, *Can higher order curvature theories explain rotation curves of galaxies?*, *Phys. Lett.* **A326** (2004) 292–296.
- [300] S. Capozziello, V. F. Cardone, and A. Troisi, *Dark energy and dark matter as curvature effects*, *JCAP* **0608** (2006) 001.
- [301] S. Capozziello, V. F. Cardone, and A. Troisi, *Low surface brightness galaxies rotation curves in the low energy limit of r**n gravity: no need for dark matter?*, *Mon. Not. Roy. Astron. Soc.* **375** (2007) 1423–1440.
- [302] S. Capozziello, V. F. Cardone, and A. Troisi, *Gravitational lensing in fourth order gravity*, *Phys. Rev.* **D73** (2006) 104019.

- [303] S. Capozziello, E. De Filippis, and V. Salzano, *Modelling clusters of galaxies by $f(R)$ -gravity*, *Mon. Not. Roy. Astron. Soc.* **394** (2009) 947–959.
- [304] S. Capozziello and V. Salzano, *Cosmography and large scale structure by $f(R)$ gravity: new results*, *Adv. Astron.* **2009** (2009) 217420.
- [305] W.-T. Lin, J.-A. Gu, and P. Chen, *Cosmological and Solar-System Tests of $f(R)$ Modified Gravity*, *Int. J. Mod. Phys.* **D20** (2011) 1357–1362.
- [306] H. Oyaizu, *Non-linear evolution of $f(R)$ cosmologies I: methodology*, *Phys. Rev.* **D78** (2008) 123523.
- [307] H. Oyaizu, M. Lima, and W. Hu, *Nonlinear evolution of $f(R)$ cosmologies. 2. Power spectrum*, *Phys. Rev.* **D78** (2008) 123524.
- [308] F. Schmidt, M. V. Lima, H. Oyaizu, and W. Hu, *Non-linear Evolution of $f(R)$ Cosmologies III: Halo Statistics*, *Phys. Rev.* **D79** (2009) 083518.
- [309] G.-B. Zhao, B. Li, and K. Koyama, *N -body Simulations for $f(R)$ Gravity using a Self-adaptive Particle-Mesh Code*, *Phys. Rev.* **D83** (2011) 044007.
- [310] B. Li, W. A. Hellwing, K. Koyama, G.-B. Zhao, E. Jennings, and C. M. Baugh, *The nonlinear matter and velocity power spectra in $f(R)$ gravity*, *Mon. Not. Roy. Astron. Soc.* **428** (2013) 743–755.
- [311] C. Arnold, E. Puchwein, and V. Springel, *Scaling relations and mass bias in hydrodynamical $f(R)$ gravity simulations of galaxy clusters*, *Mon. Not. Roy. Astron. Soc.* **440** (2014), no. 1 833–842.
- [312] C. Arnold, E. Puchwein, and V. Springel, *The Lyman α forest in $f(R)$ modified gravity*, *Mon. Not. Roy. Astron. Soc.* **448** (2015), no. 3 2275–2283.
- [313] S. Capozziello, S. Nojiri, S. Odintsov, and A. Troisi, *Cosmological viability of $f(R)$ -gravity as an ideal fluid and its compatibility with a matter dominated phase*, *Phys. Lett. B* **639** (2006) 135–143.
- [314] L. Amendola, R. Gannouji, D. Polarski, and S. Tsujikawa, *Conditions for the cosmological viability of $f(R)$ dark energy models*, *Phys. Rev. D* **75** (2007) 083504.
- [315] A. W. Brookfield, C. van de Bruck, and L. M. Hall, *Viability of $f(R)$ Theories with Additional Powers of Curvature*, *Phys. Rev. D* **74** (2006) 064028.

- [316] S. Capozziello, V. F. Cardone, and A. Troisi, *Reconciling dark energy models with $f(R)$ theories*, *Phys. Rev. D* **71** (2005) 043503.
- [317] A. de la Cruz-Dombriz and A. Dobado, *A $f(R)$ gravity without cosmological constant*, *Phys. Rev. D* **74** (2006) 087501.
- [318] V. Faraoni, *Solar System experiments do not yet veto modified gravity models*, *Phys. Rev. D* **74** (2006) 023529.
- [319] G. Cognola and S. Zerbini, *Homogeneous cosmologies in generalized modified gravity*, *Int. J. Theor. Phys.* **47** (2008) 3186–3200.
- [320] G. Cognola, M. Gastaldi, and S. Zerbini, *On the stability of a class of modified gravitational models*, *Int. J. Theor. Phys.* **47** (2008) 898–910.
- [321] T. P. Sotiriou, *Modified Actions for Gravity: Theory and Phenomenology*. PhD thesis, SISSA, Trieste, 2007.
- [322] A. De Felice, M. Hindmarsh, and M. Trodden, *Ghosts, Instabilities, and Superluminal Propagation in Modified Gravity Models*, *JCAP* **08** (2006) 005.
- [323] G. Calcagni, B. de Carlos, and A. De Felice, *Ghost conditions for Gauss-Bonnet cosmologies*, *Nucl. Phys. B* **752** (2006) 404–438.
- [324] A. Nunez and S. Solganik, *The Content of $f(R)$ gravity*, 2004.
- [325] D. Comelli, *Born-Infeld type gravity*, *Phys. Rev. D* **72** (2005) 064018.
- [326] I. Navarro and K. Van Acoleyen, *Consistent long distance modification of gravity from inverse powers of the curvature*, *JCAP* **03** (2006) 008.
- [327] V. Faraoni, *$f(R)$ gravity: Successes and challenges*, in *18th SIGRAV Conference*, 2008.
- [328] A. V. Frolov, *A Singularity Problem with $f(R)$ Dark Energy*, *Phys. Rev. Lett.* **101** (2008) 061103.
- [329] T. Kobayashi and K.-i. Maeda, *Relativistic stars in $f(R)$ gravity, and absence thereof*, *Phys. Rev. D* **78** (2008) 064019.
- [330] J. Dossett, B. Hu, and D. Parkinson, *Constraining models of $f(R)$ gravity with Planck and WiggleZ power spectrum data*, *JCAP* **03** (2014) 046.

- [331] S. Capozziello, K. F. Dialektopoulos, and O. Luongo, *Maximum turnaround radius in $f(R)$ gravity*, *Int. J. Mod. Phys. D* **28** (2018), no. 03 1950058.
- [332] S. Capozziello, M. Faizal, M. Hameeda, B. Pourhassan, V. Salzano, and S. Upadhyay, *Clustering of Galaxies with $f(R)$ gravity*, *Mon. Not. Roy. Astron. Soc.* **474** (2018), no. 2 2430–2443.
- [333] N. Straumann, *Problems with Modified Theories of Gravity, as Alternatives to Dark Energy*, *Einstein Stud.* **14** (2018) 243–259.
- [334] S. Nojiri and S. D. Odintsov, *Dark energy, inflation and dark matter from modified $F(R)$ gravity*, *TSPU Bulletin* **N8(110)** (2011) 7–19.
- [335] O. Bertolami, C. G. Böhmer, T. Harko, and F. S. N. Lobo, *Extra force in $f(R)$ modified theories of gravity*, *Phys. Rev.* **D75** (2007) 104016.
- [336] M. P. L. P. Ramos and J. Páramos, *Baryogenesis in Nonminimally Coupled $f(R)$ Theories*, *Phys. Rev.* **D96** (2017), no. 10 104024.
- [337] C. Gomes, J. G. Rosa, and O. Bertolami, *Inflation in non-minimal matter-curvature coupling theories*, *JCAP* **1706** (2017), no. 06 021.
- [338] O. Bertolami, F. S. N. Lobo, and J. Paramos, *Non-minimum coupling of perfect fluids to curvature*, *Phys. Rev.* **D78** (2008) 064036.
- [339] O. Bertolami and J. Paramos, *Mimicking dark matter through a non-minimal gravitational coupling with matter*, *JCAP* **1003** (2010) 009.
- [340] O. Bertolami and J. Paramos, *Mimicking dark matter through a non-minimal gravitational coupling with matter*, *JCAP* **03** (2010) 009.
- [341] A. Silva and J. Páramos, *Visible and Dark Matter Profiles in a Non-Minimally Coupled Model*, *Class. Quant. Grav.* **35** (2018), no. 2 025002.
- [342] O. Bertolami and J. Páramos, *Modified Friedmann Equation from Nonminimally Coupled Theories of Gravity*, *Phys. Rev.* **D89** (2014) 044012.
- [343] O. Bertolami, P. Frazao, and J. Paramos, *Accelerated expansion from a non-minimal gravitational coupling to matter*, *Phys. Rev.* **D81** (2010) 104046.
- [344] R. Ribeiro and J. Páramos, *Dynamical analysis of nonminimal coupled theories*, *Phys. Rev.* **D90** (2014), no. 12 124065.

- [345] O. Bertolami, P. Frazão, and J. Páramos, *Cosmological perturbations in theories with non-minimal coupling between curvature and matter*, *JCAP* **1305** (2013) 029.
- [346] S. Nesseris, *Matter density perturbations in modified gravity models with arbitrary coupling between matter and geometry*, *Phys. Rev.* **D79** (2009) 044015.
- [347] O. Bertolami, C. Gomes, and F. S. N. Lobo, *Gravitational waves in theories with a non-minimal curvature-matter coupling*, *Eur. Phys. J.* **C78** (2018), no. 4 303.
- [348] S. D. Odintsov and V. K. Oikonomou, *Unification of Inflation with Dark Energy in $f(R)$ Gravity and Axion Dark Matter*, *Phys. Rev.* **D99** (2019), no. 10 104070.
- [349] F. W. Hehl, J. D. McCrea, E. W. Mielke, and Y. Ne'eman, *Metric affine gauge theory of gravity: Field equations, Noether identities, world spinors, and breaking of dilation invariance*, *Phys. Rept.* **258** (1995) 1–171.
- [350] T. Ortin, *Gravity and Strings*. Cambridge Monographs on Mathematical Physics. Cambridge University Press, 2nd ed. ed., 7, 2015.
- [351] J. B. Jiménez, L. Heisenberg, and T. S. Koivisto, *The Geometrical Trinity of Gravity*, *Universe* **5** (2019), no. 7 173.
- [352] R. Aldrovandi and J. G. Pereira, *Teleparallel Gravity: An Introduction*, vol. 173. Springer, 2013.
- [353] J. M. Nester and H.-J. Yo, *Symmetric teleparallel general relativity*, *Chin. J. Phys.* **37** (1999) 113.
- [354] R. Ferraro and F. Fiorini, *On Born-Infeld Gravity in Weitzenböck spacetime*, *Phys. Rev.* **D78** (2008) 124019.
- [355] E. V. Linder, *Einstein's Other Gravity and the Acceleration of the Universe*, *Phys. Rev.* **D81** (2010) 127301. [Erratum: *Phys. Rev.*D82,109902(2010)].
- [356] Y.-F. Cai, S. Capozziello, M. De Laurentis, and E. N. Saridakis, *$f(T)$ teleparallel gravity and cosmology*, *Rept. Prog. Phys.* **79** (2016), no. 10 106901.

- [357] C.-Q. Geng, C.-C. Lee, E. N. Saridakis, and Y.-P. Wu, “Teleparallel” dark energy, *Phys. Lett.* **B704** (2011) 384–387.
- [358] L. Jarv and A. Toporensky, *General relativity as an attractor for scalar-torsion cosmology*, *Phys. Rev.* **D93** (2016), no. 2 024051.
- [359] J. B. Jiménez, L. Heisenberg, and T. Koivisto, *Coincident General Relativity*, *Phys. Rev.* **D98** (2018), no. 4 044048.
- [360] A. Conroy and T. Koivisto, *The spectrum of symmetric teleparallel gravity*, *Eur. Phys. J.* **C78** (2018), no. 11 923.
- [361] L. Järv, M. Rünkla, M. Saal, and O. Vilson, *Nonmetricity formulation of general relativity and its scalar-tensor extension*, *Phys. Rev.* **D97** (2018), no. 12 124025.
- [362] W. L. Freedman, C. D. Wilson, and B. F. Madore, *New Cepheid Distances to Nearby Galaxies Based on BVRI CCD Photometry. II. The Local Group Galaxy M33*, *Astrophysical Journal* **372** (1991) 455.
- [363] W. L. Freedman, B. F. Madore, S. L. Hawley, I. K. Horowitz, J. Mould, M. Navarrete, and S. Sallmen, *New Cepheid Distances to Nearby Galaxies Based on BVRI CCD Photometry. III. NGC 300*, *Astrophysical Journal* **396** (Sept., 1992) 80.
- [364] L. Szabados, *Pulsating stars – plethora of variables and observational tasks*, 2014.
- [365] D. Turner, *The Progenitors of Classical Cepheid Variables*, *Journal of the Royal Astronomical Society of Canada* **90** (1996).
- [366] B. F. Madore and W. L. Freedman, *The Cepheid distance scale*, *Publ. Astron. Soc. Pac.* **103** (1991) 933–957.
- [367] N. R. Tanvir, *Cepheid Standard Candles*, 1998.
- [368] A. Sandage and G. A. Tammann, *Absolute Magnitude Calibrations of Population I and II Cepheids and Other Pulsating Variables in the Instability Strip of the Hertzsprung-Russell Diagram*, *Annual Review of Astronomy and Astrophysics* **44** (2006), no. 1 93–140.

- [369] A. Sandage, *Current Problems in the Extragalactic Distance Scale*, *Astrophys. J.* **127** (1958) 513–526.
- [370] A. Saha, F. Thim, G. Tammann, B. Reindl, and A. Sandage, *Cepheid distances to sne ia host galaxies based on a revised photometric zero-point of the hst-wfpc2 and new p-l relations and metallicity corrections*, *Astrophys. J. Suppl.* **165** (2006) 108–137.
- [371] B. F. Madore and W. L. Freedman, *The Cepheid distance scale*, *Publ. Astron. Soc. Pac.* **103** (1991) 933–957.
- [372] M. Turatto, *Classification of supernovae*, *Lect. Notes Phys.* **598** (2003) 21.
- [373] Y. Kang, Y.-W. Lee, Y.-L. Kim, C. Chung, and C. H. Ree, *Early-type Host Galaxies of Type Ia Supernovae. II. Evidence for Luminosity Evolution in Supernova Cosmology*, 2019.
- [374] K. J. Shen, S. Toonen, and O. Graur, *The Evolution of the Type Ia Supernova Luminosity Function*, *Astrophys. J. Lett.* **851** (2017), no. 2 L50.
- [375] D. Howell et al., *Type Ia supernova science 2010-2020*, 2009.
- [376] D. Branch, S. Perlmutter, E. Baron, and P. Nugent, *Coping with type Ia supernova 'evolution' when probing the nature of the dark energy*, 2001.
- [377] M. Hamuy, J. Maza, M. M. Phillips, N. B. Suntzeff, M. Wischnjewsky, R. C. Smith, R. Antezana, L. A. Wells, L. E. Gonzalez, P. Gigoux, M. Navarrete, F. Barrientos, R. Lamontagne, M. della Valle, J. E. Elias, A. C. Phillips, S. C. Odewahn, J. A. Baldwin, A. R. Walker, T. Williams, C. R. Sturch, F. K. Baganoff, B. C. Chaboyer, R. A. Schommer, H. Tirado, M. Hernandez, P. Ugarte, P. Guhathakurta, S. B. Howell, P. Szkody, P. C. Schmidtke, and J. Roth, *The 1990 Calan/Tololo Supernova Search*, *Astrophysics Journal* **106** (1993) 2392.
- [378] M. M. Phillips, *The Absolute Magnitudes of Type IA Supernovae*, *Astrophysical Journal Letters* **413** (1993) L105.
- [379] **Supernova Cosmology Project** Collaboration, S. Perlmutter et al.
- [380] P. J. Brown et al., *The Absolute Magnitudes of Type Ia Supernovae in the Ultraviolet*, *Astrophys. J.* **721** (2010) 1608–1626.

- [381] **Supernova Cosmology Project** Collaboration, S. Perlmutter et al., *Scheduled Discoveries of 7+ High-Redshift Supernovae: First Cosmology Results and Bounds on $q(0)$* , in *NATO Advanced Study Institute Thermonuclear Supernovae Conference*, 1998.
- [382] **Supernova Cosmology Project** Collaboration, G. Goldhaber et al., *Observation of cosmological time dilation using Type Ia supernovae as clocks*, in *NATO Advanced Study Institute Thermonuclear Supernovae Conference*, 1998.
- [383] **Supernova Cosmology Project** Collaboration, G. Goldhaber et al., *Timescale stretch parameterization of Type Ia supernova B-band light curves*, *Astrophys. J.* **558** (2001) 359–368.
- [384] A. G. Riess, W. H. Press, and R. P. Kirshner, *Using SN-Ia light curve shapes to measure the Hubble constant*, *Astrophys. J. Lett.* **438** (1995) L17–20.
- [385] A. G. Riess, W. H. Press, and R. P. Kirshner, *A Precise distance indicator: Type Ia supernova multicolor light curve shapes*, *Astrophys. J.* **473** (1996) 88.
- [386] G. Goldhaber and D. B. Cline, *The Acceleration of the Expansion of the Universe: A Brief Early History of the Supernova Cosmology Project (SCP)*, *AIP Conference Proceedings* (2009).
- [387] S. Jha, A. G. Riess, and R. P. Kirshner, *Improved Distances to Type Ia Supernovae with Multicolor Light Curve Shapes: MLCS2k2*, .
- [388] M. Feast and R. Catchpole, *The Cepheid period-luminosity zero-point from HIPPARCOS trigonometrical parallaxes*, *Mon. Not. Roy. Astron. Soc.* **286** (1997) L1–L5.
- [389] F. van Leeuwen, M. W. Feast, P. A. Whitelock, and C. D. Laney, *Cepheid Parallaxes and the Hubble Constant*, *Mon. Not. Roy. Astron. Soc.* **379** (2007) 723–737.
- [390] **SNLS** Collaboration, E. Y. Hsiao, A. J. Conley, D. Howell, M. Sullivan, C. Pritchett, R. Carlberg, P. Nugent, and M. Phillips, *K-corrections and spectral templates of Type Ia supernovae*, *Astrophys. J.* **663** (2007) 1187–1200.
- [391] D. Branch and G. Tammann, *Type Ia Supernovae as standard candles*, *Ann. Rev. Astron. Astrophys.* **30** (1992) 359–389.

- [392] A. G. Riess, W. H. Press, and R. P. Kirshner, *A Precise distance indicator: Type Ia supernova multicolor light curve shapes*, *Astrophys. J.* **473** (1996) 88.
- [393] D. M. Scolnic et al., *The Complete Light-curve Sample of Spectroscopically Confirmed SNe Ia from Pan-STARRS1 and Cosmological Constraints from the Combined Pantheon Sample*, *Astrophys. J.* **859** (2018), no. 2 101.
- [394] W. Hu and S. Dodelson, *Cosmic Microwave Background Anisotropies*, *Ann. Rev. Astron. Astrophys.* **40** (2002) 171–216.
- [395] W. Hu, *Lecture Notes on CMB Theory: From Nucleosynthesis to Recombination*, 2008.
- [396] S. Dodelson, *Modern Cosmology*. Academic Press, Amsterdam, 2003.
- [397] M. Bucher, *Physics of the cosmic microwave background anisotropy*, *Int. J. Mod. Phys. D* **24** (2015), no. 02 1530004.
- [398] R. Sachs, A. Wolfe, G. Ellis, J. Ehlers, and A. Krasinski, *Republication of: Perturbations of a cosmological model and angular variations of the microwave background (By R.K. Sachs and A.M. Wolfe)*, *General Relativity and Gravitation* **39** (2007) 1929–1961.
- [399] J. Silk, *Cosmic black body radiation and galaxy formation*, *Astrophys. J.* **151** (1968) 459–471.
- [400] W. Hu and M. J. White, *Acoustic signatures in the cosmic microwave background*, *Astrophys. J.* **471** (1996) 30–51.
- [401] A. Lewis and A. Challinor, *Weak gravitational lensing of the CMB Weak gravitational lensing of the CMB*, *Phys. Rept.* **429** (2006) 1–65.
- [402] Y. Wang and P. Mukherjee, *Observational Constraints on Dark Energy and Cosmic Curvature*, *Phys. Rev.* **D76** (2007) 103533.
- [403] **Planck** Collaboration, P. Ade et al., *Planck 2015 results. XIV. Dark energy and modified gravity*, *Astron. Astrophys.* **594** (2016) A14.
- [404] W. Hu and N. Sugiyama, *Small scale cosmological perturbations: An analytic approach*, *Astrophys. J.* **471** (1996) 542–570.

- [405] D. Fixsen, *The Temperature of the Cosmic Microwave Background*, *Astrophys. J.* **707** (2009) 916–920.
- [406] B. A. Bassett and R. Hlozek, *Baryon Acoustic Oscillations*, 2009.
- [407] D. J. Eisenstein, H.-j. Seo, and M. J. White, *On the Robustness of the Acoustic Scale in the Low-Redshift Clustering of Matter*, *Astrophys. J.* **664** (2007) 660–674.
- [408] D. J. Eisenstein and W. Hu, *Baryonic Features in the Matter Transfer Function*, *Astrophys. J.* **496** (1998), no. 2 605–614.
- [409] **SDSS** Collaboration, D. J. Eisenstein et al., *Detection of the Baryon Acoustic Peak in the Large-Scale Correlation Function of SDSS Luminous Red Galaxies*, *Astrophys. J.* **633** (2005) 560–574.
- [410] D. H. Weinberg, M. J. Mortonson, D. J. Eisenstein, C. Hirata, A. G. Riess, and E. Rozo, *Observational Probes of Cosmic Acceleration*, *Phys. Rept.* **530** (2013) 87–255.
- [411] M. Crocce and R. Scoccimarro, *Nonlinear Evolution of Baryon Acoustic Oscillations*, *Phys. Rev. D* **77** (2008) 023533.
- [412] N. Kaiser, *Clustering in real space and in redshift space*, *Mon. Not. Roy. Astron. Soc.* **227** (1987) 1–27.
- [413] M. Tegmark, M. R. Blanton, M. A. Strauss, F. Hoyle, D. Schlegel, R. Scoccimarro, M. S. Vogeley, D. H. Weinberg, I. Zehavi, A. Berlind, and et al., *The Three-Dimensional Power Spectrum of Galaxies from the Sloan Digital Sky Survey*, *The Astrophysical Journal* **606** (2004), no. 2 702–740.
- [414] S. D. Landy and A. S. Szalay, *Bias and Variance of Angular Correlation Functions*, *The Astrophysical Journal* **412** (1993) 64.
- [415] A. Hamilton, *Measuring Omega and the real correlation function from the redshift correlation function*, *Astrophys. J. Lett.* **385** (1992) L5–L8.
- [416] C.-H. Chuang and Y. Wang, *Measurements of $H(z)$ and $D_A(z)$ from the two-dimensional two-point correlation function of Sloan Digital Sky Survey luminous red galaxies*, *Monthly Notices of the Royal Astronomical Society* **426** (2012), no. 1 226–236.

- [417] C. Alcock and B. Paczynski, *An evolution free test for non-zero cosmological constant*, *Nature* **281** (1979) 358.
- [418] **SDSS** Collaboration, D. J. Eisenstein et al., *Average Spectra of Massive Galaxies in the SDSS*, *Astrophys. J.* **585** (2003) 694–713.
- [419] C. Blake and K. Glazebrook, *Probing dark energy using baryonic oscillations in the galaxy power spectrum as a cosmological ruler*, *Astrophys. J.* **594** (2003) 665–673.
- [420] **SDSS** Collaboration, D. J. Eisenstein et al., *Detection of the Baryon Acoustic Peak in the Large-Scale Correlation Function of SDSS Luminous Red Galaxies*, *Astrophys. J.* **633** (2005) 560–574.
- [421] **2dFGRS** Collaboration, S. Cole et al., *The 2dF Galaxy Redshift Survey: Power-spectrum analysis of the final dataset and cosmological implications*, *Mon. Not. Roy. Astron. Soc.* **362** (2005) 505–534.
- [422] A. Slosar et al., *Measurement of Baryon Acoustic Oscillations in the Lyman-alpha Forest Fluctuations in BOSS Data Release 9*, *JCAP* **04** (2013) 026.
- [423] C. Blake, S. Brough, W. Couch, K. Glazebrook, G. Poole, T. Davis, M. Drinkwater, R. Jurek, K. Pimbblet, M. Colless, R. Sharp, S. Croom, M. Pracy, D. Woods, B. Madore, C. Martin, and T. Wyder, *The WiggleZ Dark Energy Survey*, *Astronomy and Geophysics* **49** (2008), no. 5 5.19–5.24.
- [424] K. S. Dawson et al., *The SDSS-IV extended Baryon Oscillation Spectroscopic Survey: Overview and Early Data*, *Astron. J.* **151** (2016) 44.
- [425] R. Jimenez and A. Loeb, *Constraining Cosmological Parameters Based on Relative Galaxy Ages*, *The Astrophysical Journal* **573** (2002), no. 1 37–42.
- [426] M. Moresco, R. Jimenez, A. Cimatti, and L. Pozzetti, *Constraining the expansion rate of the Universe using low-redshift ellipticals as cosmic chronometers*, *JCAP* **03** (2011) 045.
- [427] D. Thomas, C. Maraston, R. Bender, and C. Mendes de Oliveira, *The Epochs of early-type galaxy formation as a function of environment*, *Astrophys. J.* **621** (2005) 673–694.

- [428] A. Cimatti et al., *GMASS Ultra-deep Spectroscopy of Galaxies at $1.4 < z < 2$. II. Superdense passive galaxies: how did they form and evolve?*, *Astron. Astrophys.* **482** (2008) 21–42.
- [429] D. Thomas, C. Maraston, K. Schawinski, M. Sarzi, and J. Silk, *Environment and self-regulation in galaxy formation*, *Monthly Notices of the Royal Astronomical Society* (2010).
- [430] L. Pozzetti, M. Bolzonella, E. Zucca, G. Zamorani, S. Lilly, A. Renzini, M. Moresco, M. Mignoli, P. Cassata, L. Tasca, and et al., *zCOSMOS – 10k-bright spectroscopic sample*, *Astronomy and Astrophysics* **523** (2010) A13.
- [431] M. Moresco et al., *Improved constraints on the expansion rate of the Universe up to $z \sim 1.1$ from the spectroscopic evolution of cosmic chronometers*, *JCAP* **08** (2012) 006.
- [432] J. Simon, L. Verde, and R. Jimenez, *Constraints on the redshift dependence of the dark energy potential*, *Phys. Rev. D* **71** (2005) 123001.
- [433] D. Stern, R. Jimenez, L. Verde, M. Kamionkowski, and S. Stanford, *Cosmic Chronometers: Constraining the Equation of State of Dark Energy. I: $H(z)$ Measurements*, *JCAP* **02** (2010) 008.
- [434] M. Moresco, *Raising the bar: new constraints on the Hubble parameter with cosmic chronometers at $z \sim 2$* , *Mon. Not. Roy. Astron. Soc.* **450** (2015), no. 1 L16–L20.
- [435] D. J. Mortlock, S. J. Warren, B. P. Venemans, M. Patel, P. C. Hewett, R. G. McMahon, C. Simpson, T. Theuns, E. A. González-Solares, A. Adamson, and et al., *A luminous quasar at a redshift of $z = 7.085$* , *Nature* **474** (2011), no. 7353 616–619.
- [436] G. A. Shields, *A Brief History of Active Galactic Nuclei*, *The Publications of the Astronomical Society of the Pacific* **111** (1999), no. 760 661–678.
- [437] T. A. Matthews and A. R. Sandage, *Optical Identification of 3C 48, 3C 196, and 3C 286 with Stellar Objects.*, *The Astrophysical Journal* **138** (1963) 30.
- [438] H. Tananbaum, Y. Avni, G. Branduardi, M. Elvis, G. Fabbiano, E. Feigelson, R. Giacconi, J. Henry, J. Pye, A. Soltan, et al., *X-ray studies of quasars with the Einstein Observatory*, *Astrophys. J.* **234** (1979) L9–L13.

- [439] G. Zamorani, J. Henry, T. Maccacaro, H. Tananbaum, A. Soltan, Y. Avni, J. Liebert, J. Stocke, P. Strittmatter, R. Weymann, et al., *X-ray studies of quasars with the Einstein Observatory. II*, *Astrophys. J.* **245** (1981) 357–374.
- [440] A. T. Steffen, I. Strateva, W. Brandt, D. Alexander, A. Koekemoer, B. Lehmer, D. Schneider, and C. Vignali, *The x-ray-to-optical properties of optically-selected active galaxies over wide luminosity and redshift ranges*, *Astron. J.* **131** (2006) 2826–2842.
- [441] G. Risaliti and E. Lusso, *A Hubble Diagram for Quasars*, *Astrophys. J.* **815** (2015) 33.
- [442] G. Risaliti and E. Lusso, *A Hubble Diagram for Quasars*, *Astrophys. J.* **815** (2015) 33.
- [443] D. Just, W. Brandt, O. Shemmer, A. Steffen, D. Schneider, G. Chartas, and G. Garmire, *The X-ray Properties of the Most-Luminous Quasars from the Sloan Digital Sky Survey*, *Astrophys. J.* **665** (2007) 1004–1022.
- [444] M. Young, M. Elvis, and G. Risaliti, *The Reddest DR3 SDSS/XMM-Newton Quasars*, *The Astrophysical Journal* **688** (2008), no. 1 128–147.
- [445] D. Grupe, S. Komossa, K. M. Leighly, and K. L. Page, *VizieR Online Data Catalog: The simultaneous optical-to-X-ray SED of AGNs (Grupe+, 2010)*, *VizieR Online Data Catalog* (2010) J/ApJS/187/64.
- [446] F. Vagnetti, S. Turriziani, D. Trevese, and M. Antonucci, *VizieR Online Data Catalog: X-ray/UV ratio of 2XMM AGN (Vagnetti+, 2010)*, *VizieR Online Data Catalog* (2010) J/A+A/519/A17.
- [447] A. Cucchiara, A. J. Levan, D. B. Fox, N. R. Tanvir, T. N. Ukwatta, E. Berger, T. Krühler, A. K. Yoldaş, X. F. Wu, K. Toma, and et al., *A Photometric Redshift of $z \sim 9.4$ for GRB 090429B*, *The Astrophysical Journal* **736** (2011), no. 1 7.
- [448] T. Krühler et al., *GRB hosts through cosmic time - VLT/X-Shooter emission-line spectroscopy of 96 γ -ray-burst-selected galaxies at $0.1 < z < 3.6$* , *Astron. Astrophys.* **581** (2015) A125.

- [449] R. Salvaterra, M. D. Valle, S. Campana, G. Chincarini, S. Covino, P. D’Avanzo, A. Fernández-Soto, C. Guidorzi, F. Mannucci, R. Margutti, and et al., *GRB 090423 at a redshift of $z \sim 8.1$* , *Nature* **461** (2009), no. 7268 1258–1260.
- [450] N. Tanvir et al., *A gamma-ray burst at a redshift of $z \sim 8.2$* , *Nature* **461** (2009) 1254–1257.
- [451] F. Wang, Z. Dai, and E. Liang, *Gamma-ray Burst Cosmology*, *New Astron. Rev.* **67** (2015) 1–17.
- [452] P. Meszaros, *Gamma-Ray Bursts*, *Rept. Prog. Phys.* **69** (2006) 2259–2322.
- [453] S. Woosley and A. Heger, *The Progenitor stars of gamma-ray bursts*, *Astrophys. J.* **637** (2006) 914–921.
- [454] D. Q. Lamb and D. E. Reichart, *Gamma-Ray Bursts as a Probe of the Very High Redshift Universe*, *The Astrophysical Journal* **536** (2000), no. 1 1–18.
- [455] B. E. Schaefer, *The Hubble Diagram to Redshift > 6 from 69 Gamma-Ray Bursts*, *Astrophys. J.* **660** (2007) 16–46.
- [456] V. Cardone, S. Capozziello, and M. Dainotti, *An updated Gamma Ray Bursts Hubble diagram*, *Mon. Not. Roy. Astron. Soc.* **400** (2009), no. 2 775–790.
- [457] Y. Kodama, D. Yonetoku, T. Murakami, S. Tanabe, R. Tsutsui, and T. Nakamura, *Gamma-Ray Bursts in $1.8 < z < 5.6$ Suggest that the Time Variation of the Dark Energy is Small*, *Mon. Not. Roy. Astron. Soc.* **391** (2008) 1.
- [458] D. Yonetoku, T. Murakami, T. Nakamura, R. Yamazaki, A. Inoue, and K. Ioka, *Gamma-ray burst formation rates inferred from the spectral peak energy-peak luminosity relation*, *Astrophys. J.* **609** (2004) 935.
- [459] G. Ghirlanda, G. Ghisellini, and C. Firmani, *Gamma Ray Bursts as standard candles to constrain the cosmological parameters*, *New J. Phys.* **8** (2006) 123.
- [460] R. Trotta, *Bayesian Methods in Cosmology*, 2017.
- [461] G. D’Agostini, *Probability and Measurement Uncertainty in Physics - a Bayesian Primer*, 1995.

- [462] I. ISO and B. OIML, *Guide to the Expression of Uncertainty in Measurement*, Geneva, Switzerland **122** (1995).
- [463] D. G. Denison, C. C. Holmes, B. K. Mallick, and A. F. Smith, *Bayesian methods for nonlinear classification and regression*, vol. 386. John Wiley and Sons, 2002.
- [464] L. Verde, *A practical guide to Basic Statistical Techniques for Data Analysis in Cosmology*, 12, 2007.
- [465] **SNLS** Collaboration, A. Conley et al., *Supernova Constraints and Systematic Uncertainties from the First 3 Years of the Supernova Legacy Survey*, *Astrophys. J. Suppl.* **192** (2011) 1.
- [466] **SDSS** Collaboration, M. Betoule et al., *Improved cosmological constraints from a joint analysis of the SDSS-II and SNLS supernova samples*, *Astron. Astrophys.* **568** (2014) A22.
- [467] **BOSS** Collaboration, S. Alam et al., *The clustering of galaxies in the completed SDSS-III Baryon Oscillation Spectroscopic Survey: cosmological analysis of the DR12 galaxy sample*, *Mon. Not. Roy. Astron. Soc.* **470** (2017), no. 3 2617–2652.
- [468] M. Ata et al., *The clustering of the SDSS-IV extended Baryon Oscillation Spectroscopic Survey DR14 quasar sample: first measurement of baryon acoustic oscillations between redshift 0.8 and 2.2*, *Mon. Not. Roy. Astron. Soc.* **473** (2018), no. 4 4773–4794.
- [469] **BOSS** Collaboration, A. Font-Ribera et al., *Quasar-Lyman α Forest Cross-Correlation from BOSS DR11 : Baryon Acoustic Oscillations*, *JCAP* **1405** (2014) 027.
- [470] Y. Wang and M. Dai, *Exploring uncertainties in dark energy constraints using current observational data with Planck 2015 distance priors*, *Phys. Rev. D* **94** (2016), no. 8 083521.
- [471] J. Liu and H. Wei, *Cosmological models and gamma-ray bursts calibrated by using Padé method*, *Gen. Rel. Grav.* **47** (2015), no. 11 141.
- [472] B. A. Berg, *Introduction to Markov Chain Monte Carlo Simulations and their Statistical Analysis*, 2004.

- [473] D. J. C. MacKay, *Information Theory, Inference, and Learning Algorithms*, *IEEE Transactions on Information Theory* **50** (2003) 2544–2545.
- [474] W. K. Hastings, *Monte Carlo sampling methods using Markov chains and their applications*, *Biometrika* **57** (1970), no. 1 97–109.
- [475] A. E. Raftery, *Bayesian Model Selection in Social Research*, *Sociological Methodology* **25** (1995) 111–163.
- [476] A. Gelman and D. B. Rubin, *Inference from iterative simulation using multiple sequences*, *Statist. Sci.* **7** (1992), no. 4 457–472.
- [477] J. Dunkley, M. Bucher, P. G. Ferreira, K. Moodley, and C. Skordis, *Fast and reliable mcmc for cosmological parameter estimation*, *Mon. Not. Roy. Astron. Soc.* **356** (2005) 925–936.
- [478] S. Nesseris and J. Garcia-Bellido, *Is the Jeffreys’ scale a reliable tool for Bayesian model comparison in cosmology?*, *JCAP* **1308** (2013) 036.
- [479] P. Mukherjee, D. Parkinson, and A. R. Liddle, *A nested sampling algorithm for cosmological model selection*, *Astrophys. J.* **638** (2006) L51–L54.
- [480] H. Jeffreys, *The theory of probability*, vol. 4 of *Oxford Classic Texts in the Physical Sciences*. Oxford University Press, The address, 3 ed., 1998.
- [481] P. K. S. Dunsby, E. Elizalde, R. Goswami, S. Odintsov, and D. S. Gomez, *On the LCDM Universe in $f(R)$ gravity*, *Phys. Rev.* **D82** (2010) 023519.
- [482] de la Cruz-Dombriz, P. K. S. Dunsby, S. Kandhai, and D. Sáez-Gómez, *Theoretical and observational constraints of viable $f(R)$ theories of gravity*, *Phys. Rev.* **D93** (2016), no. 8 084016.
- [483] S. Capozziello, O. Farooq, O. Luongo, and B. Ratra, *Cosmographic bounds on the cosmological deceleration-acceleration transition redshift in $f(\mathfrak{R})$ gravity*, *Phys. Rev.* **D90** (2014), no. 4 044016.
- [484] S. Nojiri, S. D. Odintsov, and D. Saez-Gomez, *Cosmological reconstruction of realistic modified $F(R)$ gravities*, *Phys. Lett.* **B681** (2009) 74–80.
- [485] de la Cruz-Dombriz, P. K. S. Dunsby, S. Kandhai, and D. Sáez-Gómez, *Theoretical and observational constraints of viable $f(R)$ theories of gravity*, *Phys. Rev.* **D93** (2016), no. 8 084016.

- [486] S. Capozziello, S. Nojiri, and S. D. Odintsov, *Dark energy: The Equation of state description versus scalar-tensor or modified gravity*, *Phys. Lett.* **B634** (2006) 93–100.
- [487] **Planck** Collaboration, P. A. R. Ade et al., *Planck 2015 results. XIII. Cosmological parameters*, *Astron. Astrophys.* **594** (2016) A13.
- [488] Y.-Y. Xu and X. Zhang, *Comparison of dark energy models after Planck 2015*, *Eur. Phys. J.* **C76** (2016), no. 11 588.
- [489] G. R. Dvali, G. Gabadadze, and M. Porrati, *4-D gravity on a brane in 5-D Minkowski space*, *Phys. Lett.* **B485** (2000) 208–214.
- [490] C. Deffayet, G. Dvali, and G. Gabadadze, *Accelerated universe from gravity leaking to extra dimensions*, *Phys. Rev. D* **65** (2002) 044023.
- [491] M. Bouhmadi-Lopez, *Self-accelerating the normal DGP branch*, *JCAP* **11** (2009) 011.
- [492] **SDSS** Collaboration, M. Betoule et al., *Improved cosmological constraints from a joint analysis of the SDSS-II and SNLS supernova samples*, *Astron. Astrophys.* **568** (2014) A22.
- [493] A. Einstein *Sitzungsber. Preuss. Akad. Wiss.* **217** (1928).
- [494] R. Lazkoz, M. Ortiz-Banos, and V. Salzano, *$f(R)$ gravity modifications: from the action to the data*, *Eur. Phys. J.* **C78** (2018), no. 3 213.
- [495] T. Harko, T. S. Koivisto, F. S. N. Lobo, G. J. Olmo, and D. Rubiera-Garcia, *Coupling matter in modified Q gravity*, *Phys. Rev.* **D98** (2018), no. 8 084043.
- [496] P. K. S. Dunsby, E. Elizalde, R. Goswami, S. Odintsov, and D. S. Gomez, *On the Λ CDM Universe in $f(R)$ gravity*, *Phys. Rev.* **D82** (2010) 023519.
- [497] J.-h. He and B. Wang, *Revisiting $f(R)$ gravity models that reproduce Λ CDM expansion*, *Phys. Rev. D* **87** (2013), no. 2 023508.
- [498] M. Abramowitz and I. A. Stegun, *Handbook of Mathematical Functions with Formulas, Graphs, and Mathematical Tables*. Dover, New York, ninth dover printing, tenth gpo printing ed., 1964.

- [499] A. A. Starobinsky, *A new type of isotropic cosmological models without singularity*, *Physics Letters B* **91** (1980) 99–102.
- [500] E. A. Milne, *World-Structure and the Expansion of the Universe. Mit 6 Abbildungen.*, *Nature* **130** (1932) 9–10.
- [501] M. Visser, *Cosmography: Cosmology without the Einstein equations*, *Gen. Rel. Grav.* **37** (2005) 1541–1548.
- [502] C. Cattoen and M. Visser, *The Hubble series: Convergence properties and redshift variables*, *Class. Quant. Grav.* **24** (2007) 5985–5998.
- [503] C. Cattoen and M. Visser, *Cosmographic Hubble fits to the supernova data*, *Phys. Rev.* **D78** (2008) 063501.
- [504] S. Capozziello, R. Lazkoz, and V. Salzano, *Comprehensive cosmographic analysis by Markov Chain Method*, *Phys. Rev.* **D84** (2011) 124061.
- [505] J.-Q. Xia, V. Vitagliano, S. Liberati, and M. Viel, *Cosmography beyond standard candles and rulers*, *Phys. Rev.* **D85** (2012) 043520.
- [506] J. Morais, M. Bouhmadi-López, and S. Capozziello, *Can $f(R)$ gravity contribute to (dark) radiation?*, *JCAP* **1509** (2015), no. 09 041.
- [507] M. P. Dabrowski, *Are singularities the limits of cosmology?*, pp. 101–118. 7, 2014.
- [508] A. G. Riess et al., *A 2.4% Determination of the Local Value of the Hubble Constant*, *Astrophys. J.* **826** (2016), no. 1 56.
- [509] **Planck** Collaboration, N. Aghanim et al., *Planck intermediate results. XLVI. Reduction of large-scale systematic effects in HFI polarization maps and estimation of the reionization optical depth*, *Astron. Astrophys.* **596** (2016) A107.
- [510] S. M. Carroll, M. Hoffman, and M. Trodden, *Can the dark energy equation-of-state parameter w be less than -1 ?*, *Phys. Rev. D* **68** (2003) 023509.